Chemosphere

Biodiesel production from waste cooking oils – Application of green chemistry principles to the multi-objective optimisation of alkaline transesterification

--Manuscript Draft--

Manuscript Number:	CHEM141343R4
Article Type:	VSI:Environment and Sustainable Practices
Section/Category:	Environmental Chemistry
Keywords:	biodiesel, multi-objective optimisation, green chemistry, transesterification, waste cooking oils, response surface methodology.
Corresponding Author:	Catia Giovanna Lopresto University of Calabria Rende, Calabria ITALY
First Author:	Catia Giovanna Lopresto
Order of Authors:	Catia Giovanna Lopresto
	Rosy Paletta
	Antonio Scarpello
	Vincenza Calabrò
Abstract:	In the present work, alkaline transesterification converted waste household cooking oil into biodiesel, a renewable alternative to fossil fuels. After characterising oil and choosing the independent variables of the reaction (methanol-to-oil molar ratio, catalyst concentration, temperature, and stirring), three dependent variables were selected to analyse biodiesel production globally, considering technical, energetic and environmental aspects. Therefore, biodiesel yield, energy intensity, and green chemistry balance were chosen as responses. This work considered four normalised green metrics with the best values close to 100% to calculate the green chemistry balance and the “greenness” of the reaction, providing a comprehensive view of the sustainability of biodiesel production. After obtaining an experimental plan using a central composite design, the process responses under different operating conditions were assessed. The optimal conditions were obtained by response surface methodology and optimisation tools in both a single-criterion approach for each response and a multi-objective approach. Moreover, the analysis of variance was performed to determine the significance of quadratic models and the effects of independent factors on each response. When the three responses were simultaneously optimised, the results showed a maximum ester yield of 83.3%, minimum energy intensity of 10.2 MJ/kg, and maximum green chemistry balance of 81.4% at methanol to oil molar ratio of 3, KOH catalyst concentration of 1.3 wt%, temperature of 50.7 °C and stirring of 350 rpm. Nevertheless, different results were obtained when a single performance criterion was used, indicating the importance of a global multi-objective approach to the process involving green chemistry principles and process performance optimisation.
Opposed Reviewers:	

Dear Editor,

My colleagues Rosy Paletta, Antonio Scarpello, Vincenza Calabrò, and I would like to express our sincere gratitude for your consideration of our paper. We would be honoured if you could review our work on applying a novel approach of green chemistry principles to optimise biodiesel production from waste cooking oils (WCO) via alkaline transesterification. Unlike most works in the literature, our paper did not consider biodiesel yield as the only dependent variable. Indeed, the highest yield does not guarantee the greenest process. Still, it is essential to use the principles of so-called green chemistry and green engineering to ensure the sustainability of a process or product and promote the transition from a linear economy to a circular economy. Therefore, this paper aimed to optimise the operating conditions of converting household waste cooking oils into biodiesel by response surface methodology applied to a central composite design-derived experimental plan. Although this topic has been widely investigated in the literature, the results reported are not unique, given the substantial heterogeneity of the raw material. Moreover, very little attention has been paid to a broader vision of the process, which considers the biodiesel yield, energy aspects, and environmental sustainability. Therefore, we chose a multi-objective approach to investigate the alkali-catalyzed transesterification from WCO. The effect of the temperature, the methanol to oil molar ratio, the catalyst amount, and the stirring on the WCO transesterification were investigated. Yields, energy consumption, and green metrics were experimentally obtained, and quadratic models related each studied response to the four factors. The significance of the factors and models was determined by analysis of variance (ANOVA) with the Minitab 18 software tool. Finally, the operating conditions were analysed by RSM, and the multi-objective optimisation was compared with single-objective optimisation. We found that the optimal conditions varied significantly when each response was used as a single performance criterion and were further different from optimised conditions in a multi-objective approach. The simultaneous optimisation of all reaction responses – but the same is proper for any process – has proved necessary to have an overall idea of the conditions to be optimised.

Currently, this topic is of immense importance. It is being financed by two research projects (ComESto, Community Energy Storage: Aggregated Management of Energy Storage Systems in Power Cloud, project code ARS01_01259 - CUP: H56C18000150005; Tech4You, Technologies to reduce energy consumption and save biodiversity) in which we are involved at University of Calabria, Italy.

We hope our proposed paper will interest your journal and readers. It concerns a global approach to optimising biofuel production.

Sincerely,

Catia Giovanna Lopresto, on behalf of all authors

Highlights

- Transesterification of WCO was studied by single- and multi-objective optimization.
- Yield Y, energy EI and green chemistry balance GCB were simultaneously optimized.
- Simultaneously optimized responses were 83.3% (Y), 10.2 MJ/kg (EI), 81.4% (GCB).
- The effect of operating conditions was evaluated by RSM and ANOVA analysis.
- Optimized conditions were MeOH/oil molar ratio 3, KOH 1.3 wt%, 50.7 °C and 350 rpm.

Declaration of interests

☒The authors declare that they have no known competing financial interests or personal relationships that could have appeared to influence the work reported in this paper.

☐The authors declare the following financial interests/personal relationships which may be considered as potential competing interests:

Biodiesel production from waste cooking oils – Application of green chemistry principles to the multi-objective optimisation of alkaline transesterification

Catia Giovanna Lopresto [1,*], Rosy Paletta [1], Antonio Scarpello [1] and Vincenza Calabrò [1]

[1] *Department of Computer Science, Modeling, Electronics and Systems Engineering (DIMES), University of Calabria, 87036 Rende (Italy).*

∗ *Corresponding author Email addresses: catialopresto@gmail.com; catiagiovanna.lopresto@unical.it*

Abstract

In the present work, alkaline transesterification converted waste household cooking oil into biodiesel, a renewable alternative to fossil fuels. After characterising oil and choosing the independent variables of the reaction (methanol-to-oil molar ratio, catalyst concentration, temperature, and stirring), three dependent variables were selected to analyse biodiesel production globally, considering technical, energetic and environmental aspects. Therefore, biodiesel yield, energy intensity, and green chemistry balance were chosen as responses. This work considered four normalised green metrics with the best values close to 100% to calculate the green chemistry balance and the "greenness" of the reaction, providing a comprehensive view of the sustainability of biodiesel production. After obtaining an experimental plan using a central composite design, the process responses under different operating conditions were assessed. The optimal conditions were obtained by response surface methodology and optimisation tools in both a single-criterion approach for each response and a multi-objective approach. Moreover, the analysis of variance was performed to determine the significance of quadratic models and the effects of independent factors on each response. When the three responses were simultaneously optimised, the results showed a maximum ester yield of 83.3%, minimum energy intensity of 10.2 MJ/kg, and maximum green chemistry balance of 81.4% at methanol to oil molar ratio of 3, KOH catalyst concentration of 1.3 wt%, temperature of 50.7

°C and stirring of 350 rpm. Nevertheless, different results were obtained when a single performance criterion was used, indicating the importance of a global multi-objective approach to the process involving green chemistry principles and process performance optimisation.

Author Contributions

CGL: conceptualization, data curation, methodology, validation, visualization, writing – original draft, writing – review & editing.

RP: formal analysis, software, validation.

AS: investigation, software.

VC: funding acquisition, project administration, resources, supervision, writing – review & editing.

Conflicts of interest

The authors have no conflict to declare.

Acknowledgements

The authors are very grateful to Dr. Vincenzo Mantino, Dr. Angela Fazio and ILSAP srl (Lamezia Terme, Italy) for their valuable support in the characterization analysis of WCO and biodiesel.

Funding

This work was financially supported by the Italian Ministry of University and Research (MUR) through the research project ComESto (Community Energy Storage: Aggregated Management of Energy Storage Systems in Power Cloud, project code ARS01_01259, CUP H56C18000150005) and by the Next Generation EU - Italian NRRP, Mission 4, Component 2, Investment 1.5, call for the creation and strengthening of “Innovation Ecosystems”, building “Territorial R&D Leaders” (Directorial Decree n. 2021/3277) by the research project Tech4You (Technologies for climate change adaptation and quality of life improvement, project code ECS 00000009, CUP H23C22000370006).

Graphical Abstract

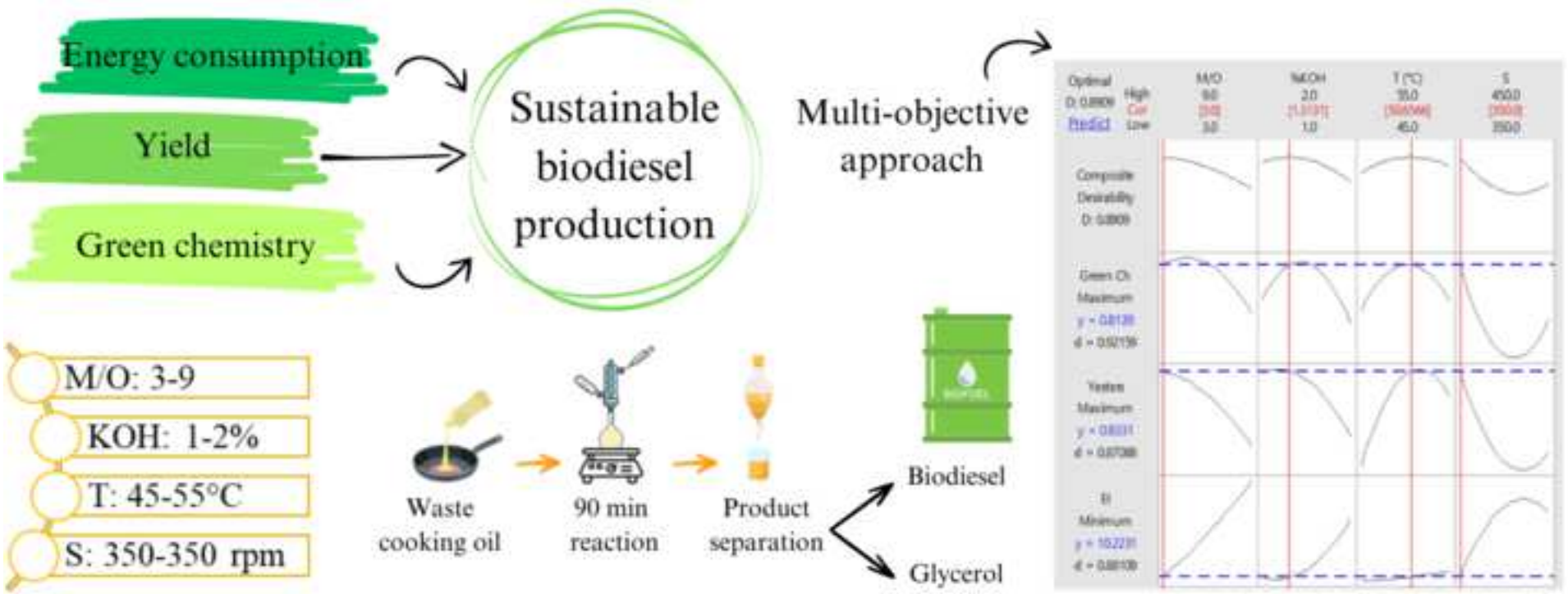

Comments:

Line # 55: Table 1. Advantages and disadvantages of different biodiesel production techniques.

Comment: Dilution, and Microemulsion does not produce biodiesel. These methods only lower the viscosity of the oil. Rectify the caption of the table

Thank you for your comment. We have corrected the caption of Table 1 to read: "Advantages and disadvantages of various techniques to reduce oil viscosity or produce biodiesel."

Comment: Some further details of Gas chromatography analysis need to be incorporated. It is mentioned that Chromatograms were studied using the ChromNav 2.0 software. Whether any internal standard was used. How were the peaks of methyl esters identified?

Thank you for your comment. We added the following information in Section 2.4: "Chromatograms were analysed using the ChromNav 2.0 software, and the peaks of esters, monoglycerides, diglycerides, and triglycerides were identified using methyl oleate, monoolein, diolein, and triolein as standards, respectively."

Biodiesel production from waste cooking oils – Application of green chemistry principles to the multi-objective optimisation of alkaline transesterification

Abstract

In the present work, alkaline transesterification converted waste household cooking oil into biodiesel, a renewable alternative to fossil fuels. After characterising oil and choosing the independent variables of the reaction (methanol-to-oil molar ratio, catalyst concentration, temperature, and stirring), three dependent variables were selected to analyse biodiesel production globally, considering technical, energetic and environmental aspects. Therefore, biodiesel yield, energy intensity, and green chemistry balance were chosen as responses. This work considered four normalised green metrics with the best values close to 100% to calculate the green chemistry balance and the "greenness" of the reaction, providing a comprehensive view of the sustainability of biodiesel production. After obtaining an experimental plan using a central composite design, the process responses under different operating conditions were assessed. The optimal conditions were obtained by response surface methodology and optimisation tools in both a single-criterion approach for each response and a multi-objective approach. Moreover, the analysis of variance was performed to determine the significance of quadratic models and the effects of independent factors on each response. When the three responses were simultaneously optimised, the results showed a maximum ester yield of 83.3%, minimum energy intensity of 10.2 MJ/kg, and maximum green chemistry balance of 81.4% at methanol to oil molar ratio of 3, KOH catalyst concentration of 1.3 wt%, temperature of 50.7 °C and stirring of 350 rpm. Nevertheless, different results were obtained when a single performance criterion was used, indicating the importance of a global multi-objective approach to the process involving green chemistry principles and process performance optimisation.

Keywords: biodiesel, multi-objective optimisation, green chemistry, transesterification, waste

cooking oils, response surface methodology.

1. Introduction

The ASTM (American Society for Testing and Materials) standard defines biodiesel as an apolar mixture of alkyl esters (usually Fatty Acid Methyl Esters, FAME) with long chains of fatty acids. Over the past few decades, biodiesel has gained significant attention for its versatility in applications such as a phase change material (De Paola and Lopresto, 2021) and a green solvent (Knot he and Razon, 2017), as well as innovative uses like plasticiser and lubricant. However, its most prominent application is as a green alternative to conventional petrodiesel. Biodiesel offers several advantages, including reduced pollutant emissions and particulate matter, mitigation of global warming impacts, enhanced countries' energy independence, and positive effects on agriculture (De Paola et al., 2021a). Despite these benefits, the widespread adoption of biodiesel is limited by its high production price, low feedstock availability, fluctuating oil prices, and inconsistent policy support (Suhara et al., 2024). Moreover, biodiesel production from waste sources has gained attention as a sustainable alternative to avoid the environmental consequences of dedicated feedstock cultivation, such as deforestation and biodiversity loss, often associated with expanding plantations like palm oil in tropical regions (Ali Ijaz Malik et al., 2024). Given their established collection and processing infrastructure, this highlights the potential of waste materials like waste cooking oil (WCO) and animal fats as economically viable feedstocks.

Oil can be diluted, micro-emulsified or chemically converted by many technologies from more traditional pyrolysis and transesterification to less conventional methods such as reactive distillation and supercritical conditions, microwaves, ultrasound, membrane, plasma, etc. The advantages and disadvantages of each technique are summarised in Table 1 (Abbaszaadeh et al., 2012; Babadi et al., 2022; Bashir et al., 2022; Singh et al., 2020; Zulqarnain et al., 2021).

Table 1. Advantages and disadvantages of various techniques to reduce oil viscosity or produce biodiesel.

Production technologies	Advantages	Disadvantages
Dilution	Simplicity of the process.	Carbon deposit in the engine cylinder, ineffective combustion.
Microemulsion	Simplicity of the process.	Less volatile and stable fuel, higher viscosity.
Pyrolysis	Simplicity of the process and low emissions.	High installation cost, high carbon residue, lower purity, high temperature clinker requirement.
Transesterification	Biodiesel properties comparable to fossil diesel, ease of scale-up for industrial scale.	Low conversion efficiency, non-reusability of the catalyst.
Catalytic distillation	Simple separation of products.	The use of solvents and reaction rate are dependent on catalyst recovery.
Reactive distillation	The possibility of processing raw materials with a high content of free fatty acids, simplicity of the process, lower requirement for methanol, and simple separation of products.	High energy demand and process conversion are influenced by catalyst efficiency.
Microwave-assisted transesterification	High reaction speeds, low heat losses, high yield, higher biodiesel purity, and simple product separation.	Process conversion is strongly influenced by catalyst activity, and it is difficult to scale up commercially due to uncontrolled heating.
Ultrasound-assisted transesterification	High reaction speeds and yields; reduced energy consumption, quantity of catalyst, production cost, separation time, reaction temperature and alcohol/oil ratio.	Higher catalyst demand, soap formation, high cost, difficult scale-up.
Plasma-assisted transesterification	Very low reaction times, non-dependency on the catalyst, and absence of soaps.	Difficult control of the reaction mechanism. High cost.
Electrolysis-assisted transesterification	Low temperature, short reaction times, and the presence of water increase the yield. The presence of free fatty acids and water does not cause problems, and it is low-cost.	Sensitivity to high pH. Need to monitor the conductivity of the electrolyte constantly.
Magnetic particle-assisted transesterification	Not limited by the disadvantages of filtration, lower pressure heat, efficient separation	Agglomeration of magnetic catalysts, preliminary coating of organic catalysts.
Transesterification with supercritical fluids	High reaction speed, high conversion efficiency, absence of catalysts, no problems in free fatty acids and water presence, and no pre-treatment required.	High energy, high cost, high temperatures (250-400 °C), and high pressure (40 MPa) are required. It is not easy to scale up to an industrial scale.
Transesterification with ionic liquids	High chemical and thermal stability, high catalytic activity, low or negligible vapour pressure and flammability, lower toxicity than organic solvents, a wide range of applications, liquids at room temperature, and possible recyclability.	High synthesis costs, limitations in large-scale applications, non-biodegradability, high viscosity, and inconvenient separation.
Transesterification with eutectic solvents	Simplicity of preparation, high purity, low cost, absence of reactivity with water and toxicity, biodegradability.	Formation of a complex liquid-liquid interface, uncertainty about stability after prolonged uses and over the entire life cycle of the process.
Biocatalytic transesterification	Eco-friendly process, simplified product separation, recyclability of biocatalysts, high product quality.	High initial cost, inhibition by glycerol, complex immobilisation techniques, lower reaction rates.

Various researchers have given more attention to transesterification for producing biodiesel, as it has several advantages, such as the employment of various feedstocks, production of biodiesel with good fuel properties, reduction of fuel viscosity, miscibility of the biodiesel with any

proportion of fossil fuel, cost-effectiveness, and high conversion efficiency (Dwivedi et al., 2022; Mandari and Devarai, 2022). Transesterification is the conversion of triglycerides into biodiesel using alcohols (typically methanol or ethanol), as shown in Figure 1.

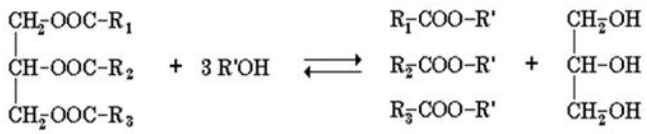

Figure 1. Transesterification of triglycerides with alcohol to produce biodiesel (methyl or ethyl–esters mixture) and glycerol (R1, R2, R3: long-chain fatty acids; R': short-chain carbon group).

Catalysts play a significant role in the transesterification process (Bohlouli and Mahdavian, 2021) and are classified as chemical (acid or alkali) and biological (enzymes) (Lopresto et al., 2019, 2015). The selection of any catalyst depends on the oil quality, quantity of FFA content in oil, operating conditions, catalyst activity required, cost, and availability (Mandari and Devarai, 2022). The chemical catalytic transesterification is industrially adopted and includes homogeneous or heterogeneous catalysis (Okechukwu et al., 2022). Homogeneous catalysts, distinguished in alkaline (such as potassium or sodium hydroxide) or acid (mainly sulfuric or phosphoric acid), are commonly used in commercialised biodiesel production as they possess high catalytic activity (Dwivedi et al., 2022). The alkaline reaction mechanism encompasses three distinct stages (refer to Figure 2). The initial stage involves an attack by the alcohol anion (alkoxide ion) on the carbonyl carbon atom of the triglyceride molecule, forming a tetrahedral intermediate. In the subsequent stage, the tetrahedral intermediate reacts with an alcohol, thereby regenerating the anion of the alcohol. The third and final stage entails the rearrangement of the tetrahedral intermediate produced during the second stage, which yields the fatty acid ester and a diglyceride.

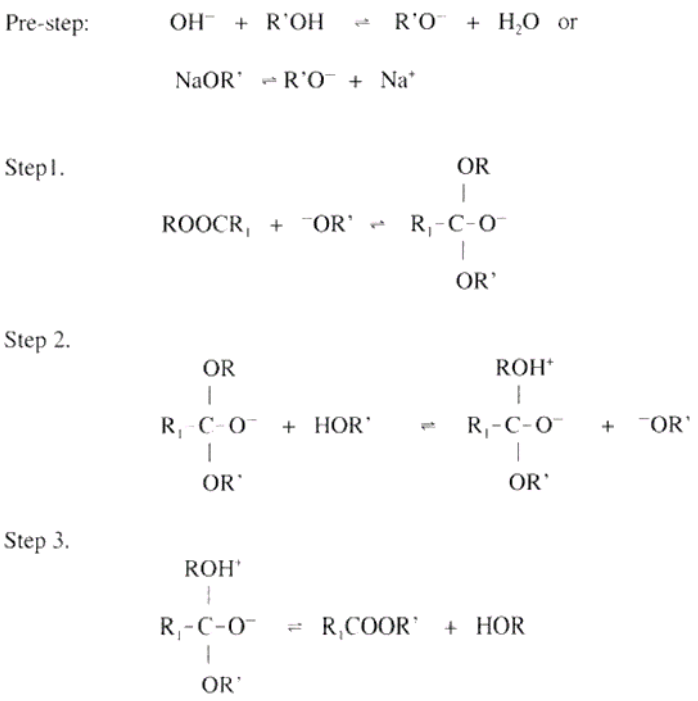

Figure 2. Alkaline transesterification mechanism of triglycerides.

Alkaline catalysts are usually used in the reaction due to their high availability, cost-effectiveness and lower corrosivity than acids. Moreover, they require moderate operating conditions, and the rate of base-catalysed reaction is about 4000 times higher than that of acid catalysis, with the same amount of catalyst used, which is why it is used more for industrial applications. Still, alkaline catalysis has technological limits related to the process's sensitivity to the reagents' purity and the presence of water in the starting oil, causing undesired hydrolysis and saponification reactions with consequent lower biodiesel yield and more difficult and expensive process downstream (Lopresto et al., 2025; Marchetti et al., 2007).

Acid-catalysed transesterification (Fig. 3) involves the protonation of the ester's carbonyl group, forming the carbocation (II). Following a nucleophilic attack by the alcohol, this produces the tetrahedral intermediate (III), which eliminates the alcohol to form the new ester (IV) and regenerate the catalyst H^+ (Pathak, 2015).

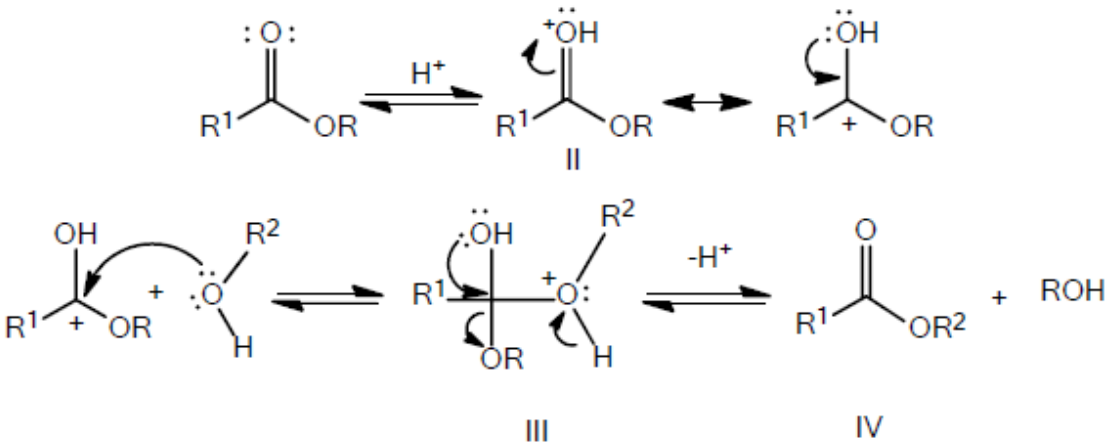

Figure 3. Acid transesterification mechanism of triglycerides.

Due to the low reaction rate, the higher temperature (55–80 °C) and the high alcohol/oil molar ratio required of 30:1, acid-catalysed transesterification has not gained the same attention as the alkaline process. Among the negative aspects, the corrosion of equipment, valves, and pipes in contact with the reaction mixture is added, resulting in a request for more constructive measures. However, acid catalysts do not give rise to the unwanted saponification reaction in the presence of free fatty acid (FFA) and water in the starting oil. Therefore, it is advisable to use acid catalysis with oils containing a high FFA content, possibly at a preliminary reaction stage (Lopresto, 2024). Although conventional alkaline homogeneous transesterification quickly leads to high triglyceride conversions at fast reaction rates, energy demand is high for the post-treatments, and product purification and catalyst recovery processes are complex, aqueous quenching, wastewater and loss of catalysts (Tan et al., 2016). Such critical issues can be overcome with heterogeneous catalysis, both basic (basic zeolites, alkaline earth metal oxides, hydrotalcites) and acidic (ZrO_2, cation-exchange resins, solid heteropoly acids, zeolites). They have high activity, high selectivity, reusability, easy separation from the products, and water tolerance properties (Ruhul et al., 2015). Moreover, they avoid soaps forming during the reaction and make the catalyst easily recoverable, but with possible leaching of active sites of the medium during the reaction and product contamination, catalyst deactivation, mass transfer limitation, lower yields

at higher reaction times and temperatures, low scalability, and high total costs (Gupta and Pal Singh, 2023; Mukhtar et al., 2022; Stoytcheva and Montero, 2011).

In order to decrease the cost of biodiesel product, some new oil feedstocks and catalysts have been developed such as basic ionic liquids (Zhang et al., 2024a, 2024b; Zhang and Sun, 2023) and low-cost liquid lipases(Sun et al., 2021; Sun and Li, 2020). Moreover, transitioning from the current technology based on homogeneous alkaline catalysis to a new approach based on heterogeneous catalysts is a fundamental challenge for lower-cost biodiesel production (Farouk et al., 2024). However, it is not mature for commercial application and is still under development. Therefore, homogenous alkaline transesterification is the most commonly employed technique in industrial biodiesel production from WCO, an economically viable feedstock derived from household, restaurant, and food-processing residues (Lopresto et al., 2024). Three catalysts are usually used for alkaline-catalysed transesterification: sodium hydroxide (NaOH), potassium hydroxide (KOH) and sodium methoxide (CH_3ONa). Most of the studies show that the best properties of biodiesel were obtained by using KOH as a catalyst (Darnoko and Cheryan, 2000; Dorado et al., 2004; Encinar et al., 2005; Karmee and Chadha, 2005; Meher et al., 2006; Ugheoke et al., 2007). Besides, some studies show the best results as fuel using NaOH (Felizardo et al., 2006; Foon Cheng and Hock Chuah, 2004; Oliveira et al., 2005; Vicente et al., 2004). In another study, they exhibited similar trends in converting triglycerides to esters, reaching a similar value of ester content in the product. Still, the amount of NaOH used was smaller than that of KOH and CH_3ONa for the same mass feedstock oil. Nevertheless, after the reaction and product separation, the product mixture was separated into two liquid layers for KOH. In contrast, a mixture of glycerol and soap in a solid state was formed for NaOH and CH_3ONa. Since the lower solid phase could not flow out directly from the bottom of the separation unit, using KOH as a catalyst is undoubtedly more convenient and straightforward since the glycerol layer in liquid state can be removed easily by directly outflowing from the bottom of the separation unit. For

this reason, KOH is commonly used to produce biodiesel using waste cooking oil (Leung and Guo, 2006).

Firstly, this study aims to optimise the operating conditions for converting household WCO into biodiesel using Response Surface Methodology (RSM) applied to a Central Composite Design (CCD)-based experimental plan. Optimising the parameters affecting the transesterification process is critical to improve biodiesel production efficiency. RSM provides the statistical framework for analysing experimental data collected using designs like CCD, by generating a response surface model. This mathematical relationship describes how input variables influence the response variable. CCD combines factorial and axial points, allowing for efficient exploration of the RSM with fewer experimental runs and helping estimate the nonlinearity of dependent variables, maximising information from experimental results. By using fewer runs, CCD helps reduce the overall cost and time associated with experimentation. The combination of CCD and RSM allows for identifying optimal conditions, leading to improved process or product outcomes. Together, they minimise experimentation time and costs, enhance process understanding, and enable prediction of responses. Although the optimisation of biodiesel production from WCO has been extensively studied, the reported results vary significantly due to the heterogeneity of raw materials, as summarised in Table 2.

155 **Table 2**. Optimisation of batch homogeneous alkaline transesterification from WCO by RSM since 2014.

Alcohol	Temperature [°C]	Alcohol-to-oil molar ratio	Amount of catalyst [% wt]	Mixing intensity [rpm]	Reaction time [min]	Yield of biodiesel [%]	Ref.
Methanol	24.44	6.52:1	0.78 (NaOH)	499.67	19.99	100	(Bobadilla et al., 2017)
	40	6:1 (v/v)	2 (NaOH)	-	180	95.71	(Adekoya et al., 2015)
	40	9:1	1 (NaOH)	300	90	83.6	(García-Moreno et al., 2014)
	52.7	7.54:1	0.875 (KOH)	266	70.2	99	(El-Gendy et al., 2015)
	55	8:1	0.6 (KOH)	-	80	92.43	(Jeyakumar et al., 2019)
	55	60 (% vol)	0.5 (KOH)	1000	90	93.3	(Milano et al., 2018b)
	57.50	8.5:1	0.25 (KOH)	600	180	93	(Razzaq et al., 2020)
	60	5:1	0.75 (KOH)	-	80	92	(Dubey et al., 2020)
	60	7.2:1	1.27 (KOH)	300	60	83.94	(Tacias-Pascacio et al., 2019)
	60-62	9.51-10.67:1	0.86-1.24 (KOH)	400	70-80	97.7-98.5	(Ayoola et al., 2016)
	62	4.5:1	1.2 (KOH)	600	75	93	(Yatish et al., 2016)
	62.75	6.05:1	0.77 (KOH)	-	72.63	93.124	(Özgür, 2021)
	65	3:1	0.55 (KOH)	-	45	95.28	(Gumahin et al., 2019)
	65	7.5:1	1.4 (KOH)	500	60	99.38	(Hamze et al., 2015)
	65	9:1	0.72 (NaOH)	-	45	92.05	(Atapour et al., 2014)
	65	15:1	5 (KOH)	700	150	95.40	(Ahmad et al., 2023)
	65	0.15:1 (v/v)	0.75 (NaOH) (%w/v)	800-900	90	97	(Kiran and Hebbar, 2021)
	73.8	6.58:1	1.13 (NaOH)	824.45	74.02	95.92	(Najafi et al., 2018)
Methanol	-	59.6 (% v/v)	0.774 (KOH)	600	7.15	97.65	(Milano et al., 2018a)
(microwave-	-	10:1	1.05 (KOH)	350	3	94	(Bajwa et al., 2024)
assisted)	50	7:1	0.65 (KOH)	8 s ON/22 s OFF (pulse time)	9.6	96.55	(Sharma et al., 2019)
	75	6:1	1 (KOH)	600	1	93	(Selvaraj et al., 2019)
Methanol (+ novel solvent)	36.83	4:1	0.5 (KOH)	1000	10	94.83	(Bhonsle et al., 2022)
Methanol (ultrasound-assisted)	50	6:1	0.5 (KOH)	-	10	98	(Oza et al., 2021a, 2021b)
Methanol (ultrasound-assisted + co-solvent)	40	6:1	2 (KOH)	7 s ON/1 s OFF (pulse time)	-	98.5	(Bai et al., 2022)

Methanol (hydrodynamic cavitation)	55	12:1	14 (KOH) [g]	-	42.5	100	(Halwe et al., 2021)
Ethanol	60	6:1	1 (Na ethoxide)	600	180	96.5 (%FAEE in biodiesel)	(Ortega et al., 2021)
	60	12.9:1	1.62 (KOH)	200	60	89.75	(Danane et al., 2022)
	64.96	7.005:1	1.25 (NaOH)	592.18	88.02	95.53	(Najafi et al., 2018)
Ethanol (microwave-assisted)	70	-	1 (KOH)	-	200 s	97	(Thirugnanasambandham et al., 2017)

156

In literature, reaction time, alcohol type, alcohol-to-oil molar ratio, reaction temperature, catalyst amount, and mixing intensity were usually optimised by RSM to obtain the maximum biodiesel yield from WCO. Nevertheless, the highest yield does not guarantee the greenest process. Indeed, to ensure the sustainability of a process or product and promote the transition from a linear economy to a circular economy, it becomes essential to use the principles of so-called green chemistry and green engineering, which have been established in the last decades (Mulvihill et al., 2011). Therefore, addressing a more comprehensive optimisation approach involving green chemistry principles is necessary, considering consumed reagents, non-recovered solvents, and energy consumption. Despite this, very little attention has been paid to a broader vision of the process, which considers the biodiesel yield, energy aspects, and environmental sustainability (De et al., 2019; Outili et al., 2020; Patle et al., 2014). Therefore, we chose a multi-objective approach to investigate the alkali-catalysed transesterification from WCO. The effect of the temperature, the methanol-to-oil molar ratio, the catalyst amount, and the stirring on the WCO transesterification was investigated. Yields, energy consumption, and green metrics were experimentally obtained, and quadratic models related each studied response to the four factors. The significance of the factors and models was determined by analysis of variance (ANOVA) with the Minitab 18 software tool. Finally, the operating conditions were analysed by RSM, and the multi-objective optimisation was compared with single-objective optimisation.

2. Experimental

2.1 Chemicals

Honeywell provided acetone (>99.8%), acetonitrile (>99.9%), diethyl ether (99.8%), ethanol (>98%), and methanol (99.8%). VWR Chemicals supplied sodium hydroxide (99.2%) and potassium hydroxide (85.5%), and Fluka Chemika provided phenolphthalein (>99%).

2.2 Waste cooking oils

WCO is a very heterogeneous feedstock with various properties depending on the type of virgin

oil and frying procedure. The WCO used in this experiment was waste oil from domestic cooking operations with a mixture of olive oil, sunflower seed oil, and peanut oil, used for frying once or twice. Firstly, solid residues of foods in frying oil were removed by a first gross filtration with a steel cooking filter and a subsequent vacuum filtration. Then, the acidity and moisture were measured by titration. Specifically, the content of FFA was determined by acid-base titration according to EN 14104 (Özbay et al., 2008), with a titrant solution of NaOH 0.01 M, a 50:50 solution by volume of diethyl ether and ethanol (to which oil is added), and phenolphthalein as an indicator. In detail, 2 g of oil and 1 g of phenolphthalein per 100 ml of solvent were solubilised, and the titrant solution was added to the point of toning with the appearance of a pink colour. Acidity (A), the amount of sodium hydroxide neutralising the fatty acids contained in one gram of sample, was obtained by Equation 1 or 2.

$$A\ (\%) = \frac{C_{NaOH} * V_{NaOH} * MW_{OA}}{1000 * m_{sample}} * 100 \quad (1)$$

$$A\ (\frac{\text{mg KOH}}{\text{g sample}}) = \frac{C_{KOH} * V_{KOH} * MW_{KOH}}{m_{sample}} \quad (2)$$

where C [mmol/mL] was the concentration of NaOH or KOH in the titrant solution, V [mL] was the volume of the titrant solution added up to the point of colour change, MW_{OA} was the molecular weight [mg/mmol] of oleic acid (OA) used as a reference, MW_{KOH} was the molecular weight [mg/mmol] of potassium hydroxide (KOH) equal to 56.1, and m [g] was the mass of the oil sample used for the titration.

The presence of water was measured by a coulometric titration in the MKC-501 Karl Fischer Moisture Titrator (Coulometric) from Kyoto Electronics (KEM). After a pre-titration (injecting 5 mL of catholyte into the inner burette and 150 mL of anolyte into the titration cell), a sample of oil is injected into the titration cell. Then, electrolysis begins, and titration is carried out. In the Karl Fisher titration, the iodine is generated by electrolysis of an iodide contained in the solvent loaded into the titration cell, to which the sample for analysis is added after weighing.

The electrolytic process and the subsequent quantitative measurement of iodine, generated stoichiometrically as a function of the water content in the sample, are made possible by an electrolytic cell and a double electrode of Pt. Finally, the detected moisture and titrated water amounts are displayed.

The fatty acid composition of the WCO determines the characteristics of the oils and, therefore, of the obtained biodiesel. The fatty acids of the glycerides present in the oil were converted into the respective methyl esters by esterification. A Clarus 500 gas chromatograph (GC) with the N9316354 Elite-FFAP Capillary Column (30 m x 0.32 mm I.D. x 0.25 µm) from PerkinElmer was used to evaluate the content of the esters and methyl esters of fatty acids using the UNI EN 14103 method. The mean molecular weight of the oil (MW_{oil}) was calculated according to the fatty acid analysis by Equation 3 (Atapour et al., 2014):

$$MW_{oil} = 3 \cdot \sum(MW_i \cdot x_i) \quad (3)$$

where MW_i and x_i are molecular weight and mass fraction of the i^{th} fatty acid, respectively.

2.3 Experimental plan

Based on the literature (De Paola et al., 2021a; Issariyakul and Dalai, 2012; Pisarello et al., 2018), four operating parameters were chosen to vary to evaluate the effect on biodiesel yield, energy consumption, and process greenness. The four independent variables were methanol/oil molar ratio M/O (3; 6; 9), KOH content (1%; 1.5%; 2%), temperature T (45 °C; 50 °C; 55 °C) and stirring S (350 rpm; 400 rpm; 450 rpm). An experimental plan (Table 3) has been developed based on a Central Composite Design (CCD) through the Minitab 18 software tool.

Table 3. An experimental plan was developed using the Minitab® software tool.

Run Order	M/O	%KOH	T (°C)	S (rpm)
1	9	2	55	450
2	9	1	55	450
3	6	1.5	50	400
4	9	1	55	350
5	3	1	55	450
6	9	1	45	450
7	3	1	45	350
8	9	1	45	350

9	9	2	45	450
10	3	2	45	350
11	3	2	55	350
12	3	2	45	450
13	3	1	45	450
14	3	1	55	350
15	9	2	45	350
16	3	2	55	450
17	6	1.5	50	400
18	9	2	55	350
19	6	1.5	45	400
20	6	1.5	50	350
21	6	1.5	50	400
22	6	1.5	50	400
23	6	1.5	50	450
24	6	2	50	400
25	3	1.5	50	400
26	6	1.5	55	400
27	6	1	50	400
28	9	1.5	50	400

2.4 Reaction

The reaction tests were carried out in batch mode in a system consisting of a magnetic heating plate, a glass three-necked round-bottom flask, and a condensation column connected to a Crioterm thermostat bath set to a cooling water temperature of 20 °C for the refrigerant action of the condenser in a closed loop. The flask acted as a reactor and was equipped with three necks: a side neck was intended for the insertion of a thermocouple for measuring the temperature; the other lateral neck was used for the insertion of reagents and the sampling of the reaction mixture to be analysed; the third, finally, was the upper one, used for connection with a six-bubble condenser for the recovery of methanol evaporated during the reaction, which was then condensed and made to fall back into the reaction mixture (Fig. 4). The stirring was guaranteed by a magnet placed in rotation by the magnetic action of the heating plate on which the flask was placed.

Figure 4. Batch reaction system.

The oil was preheated inside the flask until the reaction temperature was reached. According to Table 3, the stirring speed (350-450 rpm) and temperature (45-55 °C) values varied in each test. Then, the solution formed by methanol and potassium hydroxide, previously prepared, was added to the oil. Each reaction test was conducted for 90 minutes. Samples of the reaction mixture were taken at predefined times and stored in the freezer at -20 °C until analysis. The concentrations of triglycerides and esters in reaction mixture were analysed by High-Performance Liquid Chromatography (HPLC), model Jasco 4000, column Adsorbosphere HS C18 (Alltech, 250 mm x 4.6 mm x 5 μm), mobile phase acetone/acetonitrile 70:30 v/v, flux 1 mL/min, injection loop 20 μL, pump mode Single Pressure Gradient, detector RI, analysis time 40 min. This is a common method for separating esters, monoglycerides, diglycerides, and triglycerides, which have different retention times. Chromatograms were analysed using the ChromNav 2.0 software, and the peaks of esters, monoglycerides, diglycerides, and triglycerides were identified using methyl oleate, monoolein, diolein, and triolein as standards, respectively.

2.5 Product separation and biodiesel washing

After the reaction, each reaction mixture was transferred for 24 h to a separating funnel to separate esters and glycerol into two distinct layers due to their different densities. After the separation, the masses of the biodiesel and glycerol phases were measured. Then, crude biodiesel was repeatedly washed with 30%v/v of distilled water. This step was crucial to removing excess glycerol, methanol or potassium hydroxide. Initial washing caused the water to turn murky; thus, it was left to settle for an hour and was centrifuged at 4000 rpm for 10 minutes. The washed biodiesel was then extracted from the biodiesel–water mixture. The washing process was repeated until the water became clear. The pure biodiesel was extracted and stored in a conical flask.

The yield of crude biodiesel is defined in Equation 4 (Kerras et al., 2018):

$$Y_{\text{crude biodiesel}} = \frac{\text{mass of crude biodiesel (g)}}{\text{mass of oil (g)}} \quad (4)$$

where "mass of crude biodiesel" is the mass of the ester phase after the separation from the glycerol phase; "mass of oil" is the mass of oil used as a reagent.

The yield of esters after 90 minutes considers the mass percentage of esters in crude biodiesel based on HPLC analyses (Equation 5).

$$Y_{\text{esters}} = Y_{\text{crude biodiesel}} \cdot \%\text{esters}_{\text{HPLC}}/100 \quad (5)$$

where $Y_{\text{crude biodiesel}}$ is defined in Equation 4.

2.6 Analysis of crude biodiesel

The progress of the reaction mixture's refractive index was found to be correlated with the oil's conversion into biodiesel (Zabala et al., 2014). This analysis, carried out on biodiesel after its separation from glycerol by a portable digital refractometer (Hanna Instruments), allows for the online monitoring of the reaction progress and data acquisition in a relatively simple, reliable, and cost-effective manner (Tubino et al., 2014).

Moreover, crude biodiesel was analysed using the Turbiscan® instrument for 15 minutes at 25

°C, with scans every minute to assess its stability and the possible phenomena of phase separation and destabilisation. Turbiscan® is based on multiple light scattering and used to detect up to 200 times more rapidly than the human eye destabilisation phenomena, such as sedimentation, coalescence, flocculation, and creaming, providing guidance on the stability of the solution analysed (De Paola et al., 2021b, 2016; Maria Gabriela De Paola et al., 2017; M. G. De Paola et al., 2017). Graphs show the trends of backscattering and transmission in ordinate and the cell's height in abscissa. The first profile is displayed in blue, and the last one is in red. Graphs are usually in reference mode, so the first profile is subtracted from all other profiles to optimise variations.

Finally, biodiesel was characterised as follows. The presence of water was measured by MKC-501 Karl Fischer Moisture Titrator (Coulometric) from Kyoto Electronics (KEM). The iodine value (IV) is the mass of iodine absorbed by the sample under the conditions specified in international standard EN 14111. The iodine value of biodiesel was evaluated by dissolving a biodiesel sample in the solvent (50:50 by weight of cyclohexane and acetic acid) and adding the Wijs reagent containing iodine mono-chlorinate to acetic acid. After a certain period, a solution of potassium iodide and water was added, proceeding with the titration of the iodine released with a sodium thiosulphate solution until the blue stain appeared in the titrated solution. The impact of sulphur and phosphorus on engine integrity and catalyst life is crucial to our research. We measured this using the optical emission spectrometer Optima 7000 DV (PerkinElmer), equipped with a Polyscience NO772035 chiller and a FIAC EwispireVS204 compressor, to provide valuable insights for the field of renewable energy. The cold filter plugging point (CFPP) serves as a crucial index, indicating the temperature at which a standard test filter starts clogging due to the formation of a gel or crystal under specified test conditions. This measurement, determined with dedicated equipment (New Lab 200), is a key factor in assessing biodiesel quality. Esters and methyl esters of fatty acids were measured using the UNI EN 14103 method

by Clarus 500 gas chromatograph (GC) with the N9316354 Elite-FFAP Capillary Column (30 m x 0.32 mm I.D. x 0.25 µm) from PerkinElmer.

2.7 Energy consumption measurement

As part of our comprehensive study, we measured the reaction system's energy consumption. The magnetic heating plate and the cooling system were connected to a power meter (branded Maxcio, model PM01, maximum power 3680 W) to assess the energy absorbed by the reaction system, recorded at 15-minute intervals. These data were crucial in determining the energy intensity (EI) and the energy consumed after 90 minutes per mass of the desired product, biodiesel (Equation 6) (Calvo-Flores, 2009).

$$\text{EI}\ [\text{MJ/kg}] = \frac{\text{total energy}}{\text{mass of desired product}} \quad (6)$$

2.8 Green metrics evaluation

Green chemistry is the design of chemical products and processes that reduce or eliminate the use and generation of hazardous substances throughout their lifecycles (design, manufacture, use, and end of life) according to 12 principles (Anastas and Warner, 1998). To apply and evaluate these principles objectively, several crucial parameters – known as green metrics – have been defined to determine biodiesel production's sustainability and environmental impact and assess the best solution between alternatives. Six green mass-based metrics were evaluated in this work: environmental factor (E factor, Eq. 7), atom economy (AE, Eq. 8), atom efficiency (AEff, Eq. 9), process mass intensity (PMI, Eq. 10), process mass productivity (PMP, Eq. 11), reaction mass efficiency (RME, Eq. 12), stoichiometric factor (FSt, Eq. 13) (Calvo-Flores, 2009; Dicks and Hent, 2015; Lapkin and Constable, 2009; Sheldon, 2018).

$$\text{E factor} = \frac{\sum m_{\text{waste}}}{m_{\text{desired product}}} \quad (7)$$

$$AE = \frac{n_{desired\ product} MW_{desired\ product}}{\sum n_{reagents} MW_{reagents}} \quad (8)$$

$$AEff = AE \cdot Y_{reaction} \quad (9)$$

$$PMI = \frac{\sum m_{reagents}}{m_{desired\ product}} = E\ factor + 1 \quad (10)$$

$$PMP = \frac{1}{PMI} \cdot 100 \quad (11)$$

$$RME = \frac{m_{desired\ product}}{\sum m_{reagents}} = \frac{1}{1+E\ factor} \quad (12)$$

$$FSt = 1 + \frac{\sum m_{reagents\ in\ excess}}{\sum m_{stoichiometric\ reagents}} \quad (13)$$

In our case, the desired product is biodiesel. The waste comprises by-products (glycerol) and non-reacted reagents, oil and methanol. The reagent in excess is methanol.

All green metrics are normalised to have a value between 0 and 1, corresponding to the worst and ideal situations. The E factor is the only parameter for which the optimal situation is 0 and the worst situation is 1. Therefore, to unify the impact of all the used parameters, a new environmental factor is defined by complementing 1 as in Equation 14 (Naveenkumar and Baskar, 2021).

$$E' = 1 - E\ factor \quad (14)$$

Moreover, the stoichiometric factor is 1 when reagents are in stoichiometric proportions; otherwise, it is higher than 1. A new stoichiometric factor is defined as

$$FSt' = \frac{1}{FSt} \quad (15)$$

The green chemistry balance estimates the reaction's greenness, which is the mean value of four normalised green metrics (E', AEff, PMP, FSt'). The best value is close to 1 (or 100%).

A graphical representation of the results in an Excel radar chart evidenced the reaction's green

346 character.

347 ***2.9 Statistical analysis***

348 Statistical analysis was performed by the Minitab 18 software tool.

349 The one-way analysis of variance (ANOVA) was performed with a significance level of 0.05 to
350 assess which parameters and combinations of these most affect each response (yield of reaction,
351 energy consumption, green chemistry balance). A full quadratic model (Equation 16) was
352 generated by setting the following parameters: factors = 4, replicates = 1, α = 1, cube points =
353 16, centre points in cube = 2; axial points = 8, centre points in axial = 2 ("All statistics for Create
354 Response Surface Design (Central Composite)," 2023). It correlated each studied response with
355 the four factors as follows:

356 $$R = a_0 + \sum_{i=1}^{4} a_i X_i + \sum_{i=1}^{4} a_{ii} {X_i}^2 + \sum_{i=1}^{4} \sum_{j=1}^{4} a_{ij} X_i X_j \quad (16)$$

357 where R is the response, a_o is the intercept term, a_i are the linear coefficients, a_{ii} are the quadratic
358 coefficients, a_{ij} are the interactive coefficients, X_1 is M/O, X_2 is %KOH, X_3 is T and X_4 is S.

359 A probability (p-test) [50] confirmed the significant condition with a Pareto graph, together with
360 a Fisher test (F-test) evaluating the significance of the model and its factors in the ANOVA. The
361 Pareto Chart of the standardised effects allows identifying the most statistically significant
362 factors and their combination with each response. The red line indicates which effects are
363 statistically significant.

364 The values of p-test, F-test, total degrees of freedom (DF), adjusted sum of squares (Adj SS) and
365 adjusted mean squares (Adj MS) were provided by the Minitab 18 software.

366 Then, residual plots confirm the validity of the experimental tests, as described below. *Normal*
367 *Probability Plot* identifies deviations from normality and any anomaly in the values from the
368 experimental tests. *Versus Fits* shows an analysis of the residuals, i.e., the difference between the

value obtained from the experimental values and the estimate through a regression analysis. The *histogram* is the diagram of the residual values *vs* the frequency and evaluates whether the variance follows the normal distribution. *Versus Order* presents the values of the residuals on the ordinates and the order in which the data were collected on the abscissas.

In addition, the factors or combinations of them that most influence the process and their optimal values were obtained by RSM (Myers et al., 2016) and contour diagrams, two-dimensional diagrams in which different colours indicate the response to different factors.

Finally, a multi-objective optimisation was performed considering the effects of temperature, molar alcohol to oil ratio, stirring, and catalyst amount on biodiesel yield, green chemistry balance, and energy consumption.

3. Results and discussion

3.1 Waste cooking oils

Homogeneous alkaline transesterification is usually recommended for WCO with free fatty acid content below 0.5% in anhydrous conditions. Based on the measured low free fatty acid content of the WCO (<0.5%) and not detected water, a homogeneous alkaline transesterification was pursued for biodiesel synthesis without any pre-treatment. The GC results are given in Table 4.

Table 4. Fatty acid composition and esters produced of waste cooking oil (GC analysis).

Fatty acid	%
Myristic (C14:0)	0.1
Palmitic (C16:0)	10.4
Palmitoleic (C16:1)	0.7
Stearic (C18:0)	3.0
Oleic (C18:1)	57.7
Linoleic (C18:2)	25.0
Linolenic (C18:3)	0.6
Arachidic (C20:0)	0.5
Eicosenic (C20:1)	0.5
Behenic (C22:0)	0.8
Erucic (C22:1)	0.1
Lignoceric (C24:0)	0.4
Nervonic (C24:1)	0.1

Esters C14-C24	95.4
Total esters	96.7
Total saturated fatty acids	15.2

The primary fatty acids are oleic, linoleic, and palmitic, with prevalent oleic acid as expected in olive oil (Blekas et al., 2006). The amount of esterifiable fatty acids exceeds 95%, consistent with domestic WCO characterisation. Domestic frying is usually carried out for a few minutes and a maximum of 2-3 reuses, so oil degradation is limited. The molecular weight of WCO was estimated at 838 g/mol.

3.2 Reaction

The 28 experiments proposed by the CCD (Table 3) were performed following the above experimental protocol. The percentage of esters and triglycerides in relation to the total mass of glycerides and esters after 90 minutes of reaction is given in Table 5. The lowest percentage of esters was obtained in test 15 at the lowest values of stirring (350 rpm) and temperature (45 °C) but at the highest value of catalyst quantity (2%) and molar methanol/oil ratio (9). The highest percentage of esters was obtained in test 4 with the lowest values of stirring (350 rpm) and catalyst quantity (1%) and the highest values of temperature (55 °C) and methanol/oil ratio (9). The effect of each variable on biodiesel yield is well-known and optimised in literature. Although the stoichiometric methanol-to-oil ratio (M/O) is 3:1, the reversible transesterification requires methanol excess to be effective towards the ester production by shifting the equilibrium to the expected product. A M/O value below 5:1 is insufficient and gives low yields. Most literature finds the optimum molar ratio between 5:1 and 7:1. A further increase of the molar ratio to 9:1 or 12:1 is often associated with a decrease in the biodiesel yield, probably because of the catalyst deactivation by the excess methanol. Moreover, an unnecessary excess of methanol complicates the separation between biodiesel and glycerol after the reaction (Hoque et al., 2011). In contrast, some researchers (see Table 2) considered an optimal M/O ratio higher than 6:1, up to 15:1. This depends on the interactions with other operating conditions. As regards the catalyst concentration, its increase leads to higher biodiesel production. Still, the biodiesel yield declines

significantly when the catalyst concentration becomes higher than a particular value due to the formation of fatty acid salts (soap) (Hoque et al., 2011; Leung and Guo, 2006). As evident in Table 2, most optimal values are in the range 0.5-1.5%wt when KOH is used as an alkaline catalyst, but lower (e.g. 0.25%) (Razzaq et al., 2020) and higher (e.g. 5%) (Ahmad et al., 2023) values were found as optimal. Transesterification can occur at different temperatures ranging from ambient temperature to a temperature close to the boiling point of methanol (68 °C at atmospheric pressure). A higher reaction temperature generally speeds up the reaction and increases the biodiesel yield in a shorter reaction period due to the reduction in the viscosity of oils (Hoque et al., 2011). However, some studies observed that an increase in reaction temperature beyond the optimal level of 55-60 °C led to decreased biodiesel yield: higher reaction temperature accelerated the saponification of the triglycerides and increased volatility and miscibility (Abbah et al., 2016; Leung and Guo, 2006). Finally, the reaction rate of transesterification increases with increasing mixing degree (Leung and Guo, 2006). On the other hand, a higher stirring speed favours the formation of soap (Mathiyazhagan and Ganapathi, 2011).

Therefore, each operating condition influences the biodiesel yield in different ways. The different results found in this manuscript and the literature depend on how the levels of the investigated variables interact.

3.3 Separation of biodiesel and glycerol

After a few minutes, the separation between the upper phase, consisting essentially of biodiesel (golden coloured), and the lower phase, composed mainly of glycerol (dark brown), was already evident (Fig. 5).

Figure 5. The reaction mixture is separated in a funnel. The yellow upper phase consists of crude esters, and the brownish lower phase consists of crude glycerol.

After the separation, the crude biodiesel was extracted and transferred to another conical flask. Then, the yields of crude biodiesel and esters were calculated and shown in Table 5. The highest yield was reached in test 4 at 55 °C, 350 rpm, with a M/O of 9 and 1% of catalyst. The maximum yield in esters was 89.43% (compared to the initial oil mass) in Test 4. As reported in Table 2, this value is lower than some reported data in the literature (Ayoola et al., 2016; El-Gendy et al., 2015; Hamze et al., 2015), but it is higher than other optimised results (García-Moreno et al., 2014; Tacias-Pascacio et al., 2019). The GC analysis revealed that the total fraction of oil that could be esterified is 96.7%. Then, the actual yield of esters compared to the effectively convertible oil is 92.5%. This value is in accordance with most previous findings, with optimised yields typically in the range of 92-95% (see Table 2). The variation in biodiesel yield for different fat/oil sources could be mainly due to the variation of FFA and water contents in various types of oils. This difference in FFA content causes the catalyst to react differently towards the oils (Verma and Sharma, 2016).

3.4 Analysis of biodiesel

Biodiesel was characterised by refractometry. Fig. 6 shows the Brix degrees of crude esters, measured by a digital refractometer, for all experimental tests.

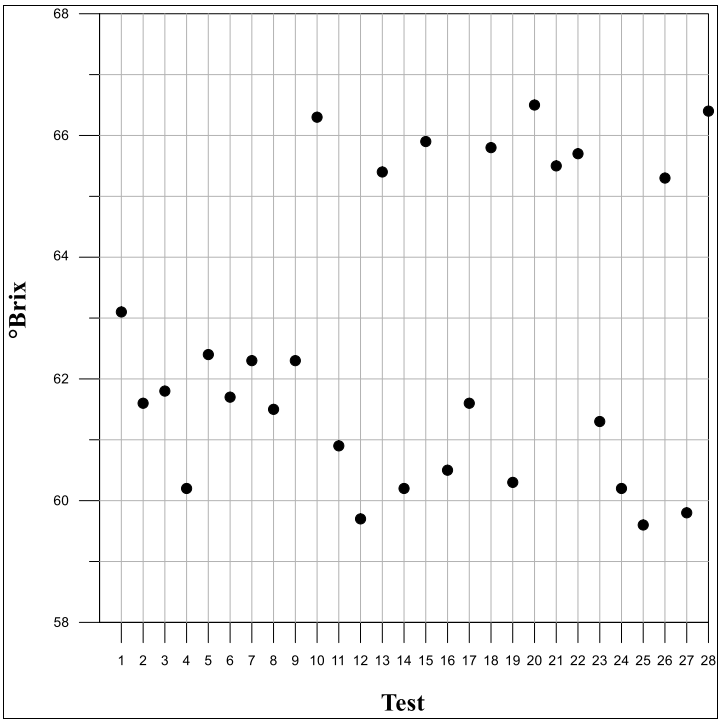

Figure 6. Brix degrees of crude esters after a 90-minute reaction and separation in a funnel.

The minimum value of °Brix of esters is about 60, corresponding to a refractive index (nD) of 1.44, corresponding to conversion values of waste oil greater or equal to 85% (Zabala et al., 2014). This result is following previous literature (Kerras et al., 2018). In addition, when the Brix value was higher than 65 (tests 10, 13, 15, 18, 20, 21, 22, 26, 28), the corresponding refractive index was 1.45, in turn corresponding to low conversions and yields (<85%).

Moreover, Turbiscan analysis was functional in analysing the product stability and comparing sedimentation and centrifugation to separate reaction products.

Centrifugation leads to a clear separation between the phases, and the biodiesel phase is clear and relatively stable, as evident from the analyses by Turbiscan (Fig. 7a).

After product separation by decanting in a separating funnel, the biodiesel sample was unstable and turbid after 60 minutes (Fig. 7b) but clear and stable after 24 hours (Fig. 7c), with a transmittance profile comparable to that obtained after centrifugation. This confirms the literature on waiting about a day for efficient decantation.

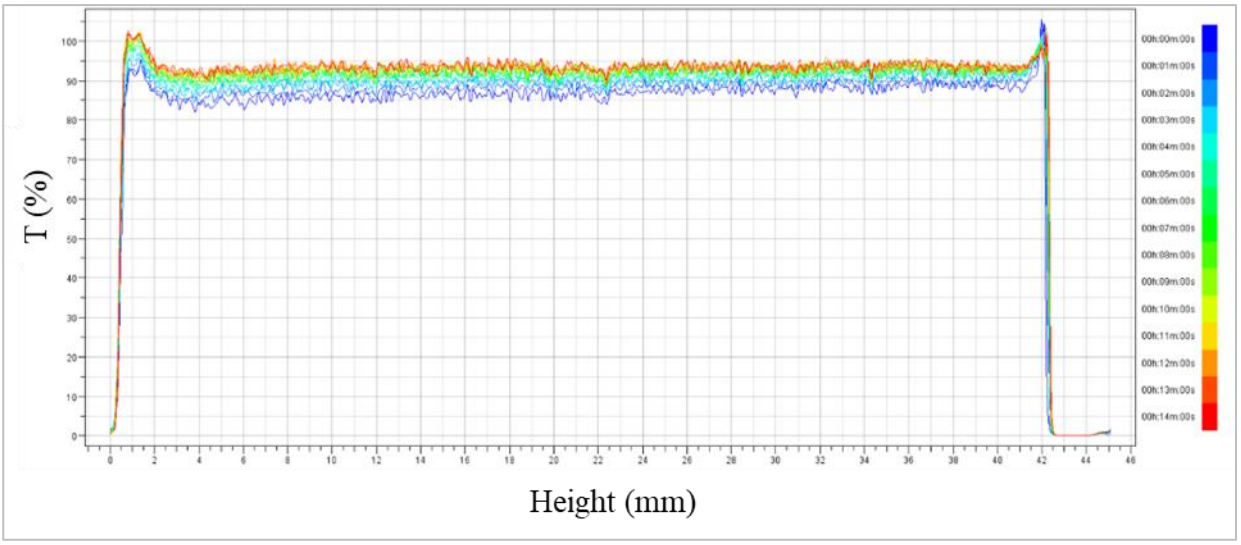

(a)

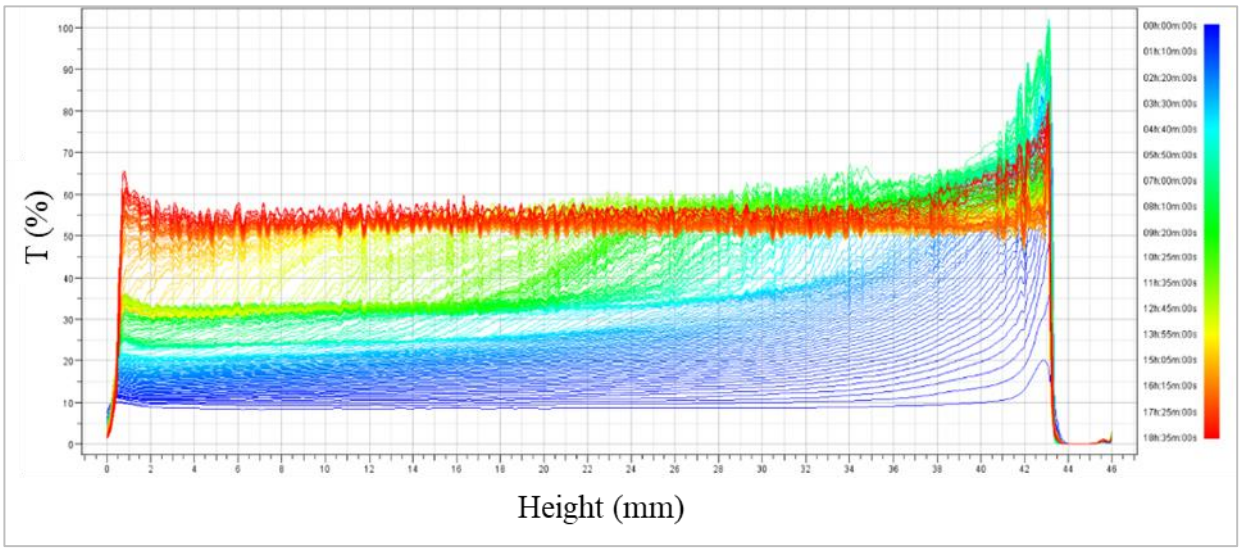

(b)

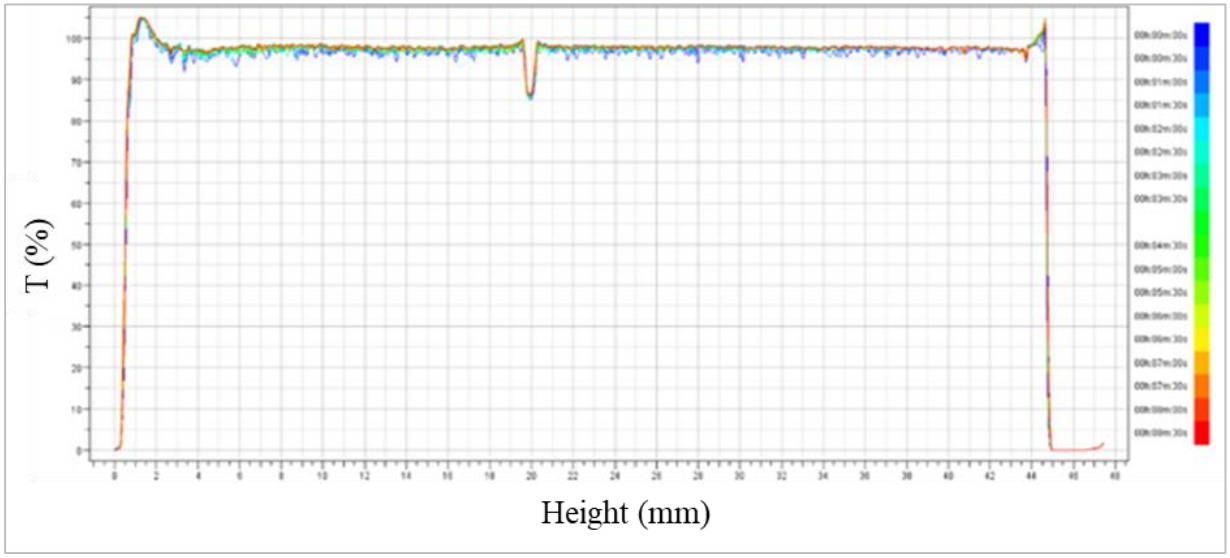

(c)

Figure 7. Transmittance profiles by Turbiscan for a biodiesel sample after separation from glycerol by centrifugation (a); after 60 minutes of separation from glycerol by sedimentation in a separating funnel (b); after 24 hours of separation from glycerol by sedimentation in a separating funnel (c).

Finally, biodiesel was characterised for water content, iodine value, sulphur and phosphorus content, cold filter plugging point, and fatty acid composition.

The sulphur content of a fuel affects engine wear and deposit formation. It must not exceed 10 ppm for EN 14214, with two standard values, S15 and S500, for ASTM D6751. The S15 sulphur content standard allows a maximum of 15 ppm, whereas the S500 sulphur content standard permits a maximum of 500 ppm. When animal fats and waste vegetable oils are utilised for biodiesel production, the sulphur content is likely higher due to sulphur-containing compounds such as proteins (Alptekin et al., 2014). Nevertheless, no sulphur traces were detected in this study.

Furthermore, no soaps, water, or traces of phosphorus were found in the biodiesel samples.

As the iodine value depends solely on the source of the vegetable oil, the biodiesel esters derived from the same oil should exhibit similar iodine values. Conversely, the iodine value ought to remain unaffected by the conversion process and, therefore, should not vary with the yield of esters. The iodine value of the produced methyl esters was approximately 96, consistent with literature that shows values ranging from 73.2 to 99.4 for WCO-derived biodiesel. It aligns with the biodiesel fuel standard within the limits set by legislation, which stipulates a maximum permissible iodine value of 120. Therefore, the biodiesel produced exhibited a low tendency for oxidation.

The CFPP characterises a fuel's cold-flow operability, as it directly influences its utility, particularly in cold climate conditions. Biodiesel has a CFPP value of -4 °C, rendering it suitable for temperate winter climates, in line with existing literature and compliant with standard EN 14214, which sets limits at 4 °C in summer and 1 °C in winter (Yıldızhan et al., 2017).

The composition of fatty acids in biodiesel can indicate significant fuel properties, particularly the cetane number, which is determined by the fatty acids' structure, chain length, and bonding (Kolakoti et al., 2021). Since the transesterification reaction does not affect the fatty acid composition (Alptekin et al., 2014), the fatty acid profile of biodiesel was the same as that of the oil (Table 4) and other biodiesel derived from WCO. For instance, Park et al. produced biodiesel containing 64.9% methyl oleate and 20.1% methyl palmitate, values that are very close to those obtained in this study, which were 57.7% and 25.0%, respectively (Park et al., 2019). The low amount of saturated esters (15.1%) confirms the good low-temperature characteristic of biodiesel, which does not tend to solidify during the winter in temperate climate regions.

3.5 Energy consumption

Figure 8a shows the cumulative power and energy the reaction system consumed after 90 minutes. It is immediately clear that the condition at which the highest yields of crude biodiesel and esters are obtained (test 4) is also the most energy-consuming. Nevertheless, it is not necessary to wait for all tests for 90 minutes to consider the achievement of the reaction equilibrium. Therefore, the power and energy values consumed until the moment the concentration of esters can be regarded as constant (an increase of less than 2 percentage points after 15 minutes) are reported in Fig. 8b.

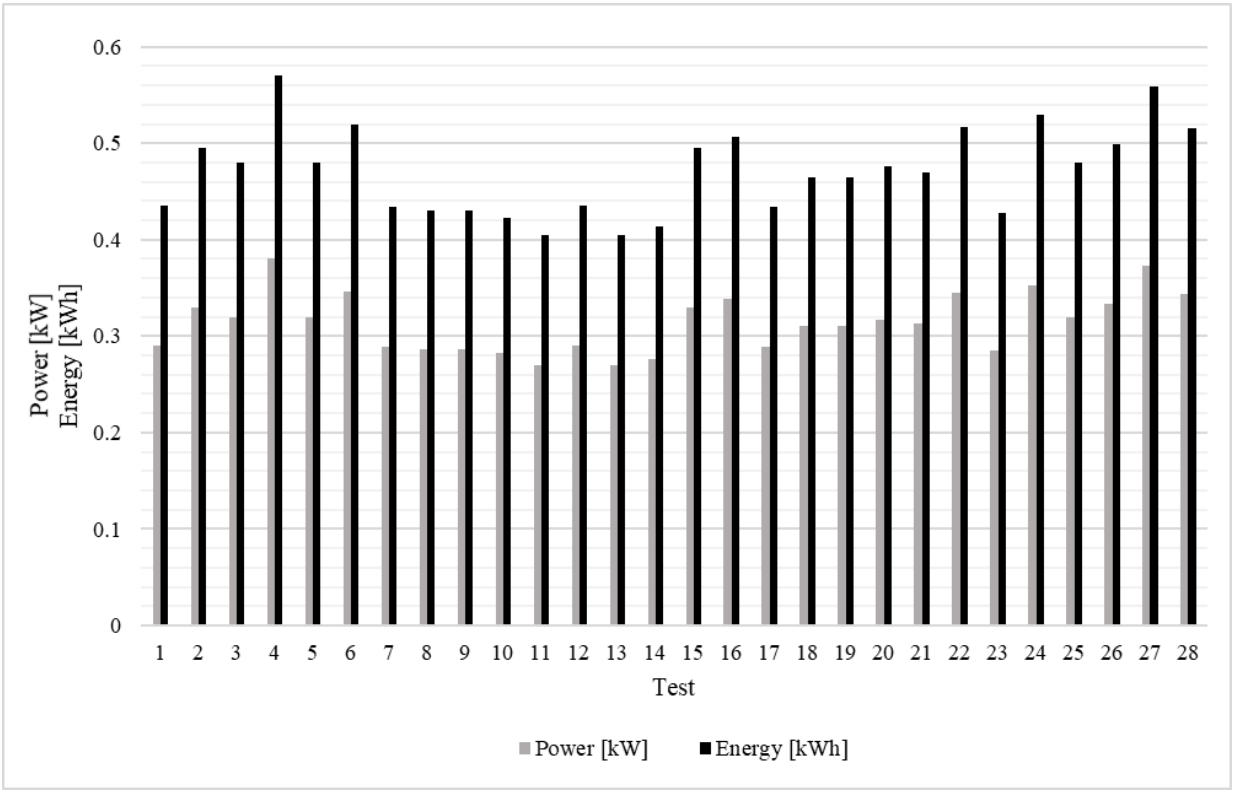

515

516 **(a)**

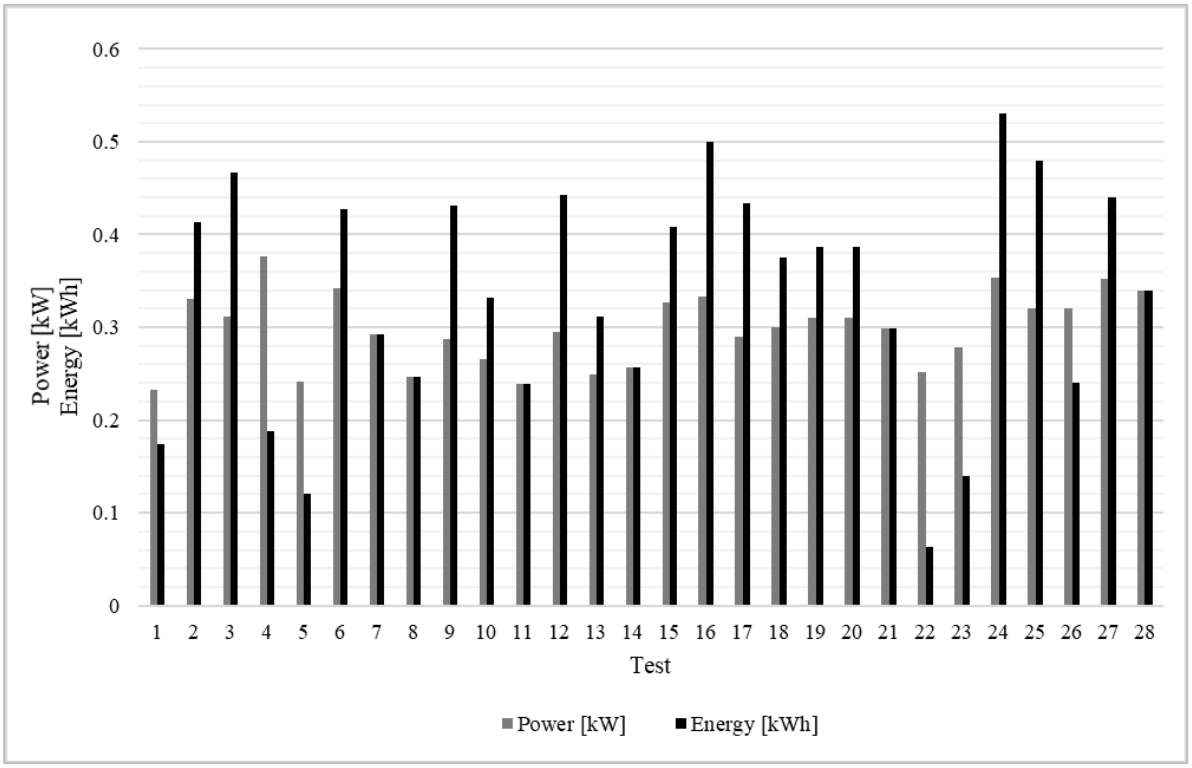

517

518 **(b)**

519 **Figure 8**. Power and energy consumed by the reaction equipment after 90 minutes (a); after
520 achieving reaction equilibrium (increase in ester concentration of less than 2 percentage points

after 15 minutes) (b).

Table 5 reports the energy intensity values for all tests. The EI values of the transesterification reaction are acceptable for a laboratory scale and are also consistent with the 37.13 MJ/kg value estimated by several industrial processes to obtain biodiesel (Marchetti et al., 2007).

3.6 Green metrics evaluation

Green metrics and green chemistry balance are summarised in Table 5 for each test.

The values of RME and PMI (and PMP, in turn) are closely related to the E factor. At the same time, atom efficiency and atom economy depend on the molecular weights of reagents, products, and yield. Energy intensity depends on the mass of biodiesel obtained and the energy absorbed.

The closer the E factor is to 0, the more virtuous the process will be, with fewer undesired products. Although it has an average value of 0.36, the parameter varies from a minimum of 0.21 in Test 23 to a maximum of 0.57 in Test 15, with a value of 0.27 in Test 4, where optimal process conditions were demonstrated. It can be observed that the optimal condition from the point of view of the yield does not correspond to the optimal condition from the point of view of the E factor and, in general, of the eco-sustainability.

The atom economy is 0.92 for all tests because the molecular weights of products and reagents are always the same when using the same reaction.

The atom efficiency considers the actual reaction yield. Therefore, the minimum atom efficiency is calculated in the test where the minimum yield of esters was observed (Test 15). At the same time, its maximum value corresponds to Test 4, which shows the optimal conditions of the reaction and the maximum yield of crude biodiesel and esters.

The PMI value varies between a minimum of 1.21 in test 23 and a maximum of 1.57 in test 15, while the PMP value (which is the reciprocal of PMI·100 and the percentage form of RME) follows a reverse trend, with a minimum of 63.58% in test 15 and a maximum of 82.63% in test

545 23.

546 The stoichiometric factor is 1 with the stoichiometric M/O ratio and higher than 1 with excess
547 alcohol, as expected.

548 The highest green chemistry balance value, 83.11%, in test 23 corresponds to the minimum
549 energy intensity value, so test 23 has the most favourable conditions for green chemistry and
550 energy consumption. However, a non-optimal ester yield was achieved in test 23. The lowest
551 green chemistry balance, 61.21%, was achieved in test 15, where the minimum ester yield of
552 42% and high EI of 14.36 MJ/kg were also reached.

553 **Table 5**. Yield values, energy intensity, some green metrics (E factor, atom efficiency AEff,
554 process mass intensity PMI, reaction mass efficiency RME, stoichiometric factor FSt), and green
555 chemistry balance.

Test	$Y_{crude\ biodiesel}$ (%)	Y_{esters} (%)	*EI (MJ/kg)*	E factor (/)	AEff (/)	PMI (/)	RME (/)	FSt (/)	*Green chemistry balance (%)*
1	89.83	*85.57*	*9.76*	0.24	0.79	1.24	0.80	1.08	*81.73*
2	90.53	*87.04*	*13.89*	0.26	0.80	1.26	0.80	1.08	*81.56*
3	83.01	*78.18*	*13.50*	0.29	0.72	1.29	0.77	1.08	*78.09*
4	**91.98** ↑	***89.43*** ↑	*13.13*	0.27	0.82	1.27	0.79	1.16	*79.86*
5	85.99	*78.00*	*13.34*	0.30	0.72	1.30	0.77	1.08	*77.82*
6	85.98	*71.37*	***14.47*** ↑	0.36	0.66	1.36	0.74	1.08	*73.96*
7	90.10	*72.22*	*11.48*	0.35	0.66	1.35	0.74	1.08	*74.56*
8	83.73	*68.99*	*12.35*	0.42	0.63	1.42	0.71	1.08	*71.14*
9	89.97	*86.61*	*11.50*	0.25	0.80	1.25	0.80	1.08	*81.64*
10	83.13	*67.69*	*12.20*	0.31	0.62	1.31	0.76	1	*76.72*
11	90.89	*82.95*	*10.80*	0.33	0.76	1.33	0.75	1.16	*76.26*
12	89.41	*74.84*	*11.86*	0.41	0.69	1.41	0.71	1.16	*71.22*
13	**75.01** ↓	*50.43*	*12.02*	0.52	0.46	1.52	0.66	1	*64.97*
14	91.53	*75.42*	*10.88*	0.38	0.69	1.38	0.72	1.16	*72.32*
15	81.79	***42.01*** ↓	*14.36*	0.57	0.39	1.57	0.64	1	***61.21*** ↓
16	90.30	*66.79*	*13.27*	0.42	0.61	1.42	0.70	1.16	*68.97*
17	89.26	*85.47*	*11.59*	0.22	0.78	1.22	0.82	1.08	*82.67*
18	84.53	*45.08*	*13.22*	0.54	0.41	1.54	0.65	1	*62.90*
19	87.37	*78.18*	*10.81*	0.33	0.72	1.33	0.75	1.16	*75.04*
20	80.22	*73.81*	*11.84*	0.25	0.68	1.25	0.80	1	*80.85*
21	79.88	*61.29*	11.72	0.39	0.56	1.39	0.72	1	*72.26*
22	82.13	*48.06*	12.72	0.52	0.44	1.52	0.66	1	64.61
23	88.73	*85.25*	**9.65** ↓	0.21	0.78	1.21	0.83	1.08	**83.11** ↑
24	87.14	*67.99*	12.17	0.37	0.62	1.37	0.73	1.16	71.16
25	90.80	*73.26*	10.66	0.39	0.67	1.39	0.72	1.16	71.78
26	78.66	*53.94*	12.56	0.45	0.50	1.45	0.69	1	68.27
27	87.55	*72.73*	12.15	0.42	0.67	1.42	0.71	1.16	70.50
28	79.84	*70.42*	12.87	0.39	0.65	1.39	0.72	1	74.45

Fig. 9 below reports a global representation of the main green metrics calculated in this work and reported in percentage scale (E', Aeff, PMP, FSt'), energy intensity (EI, MJ/kg), and crude biodiesel yield (Y, %) for tests 4 and 15.

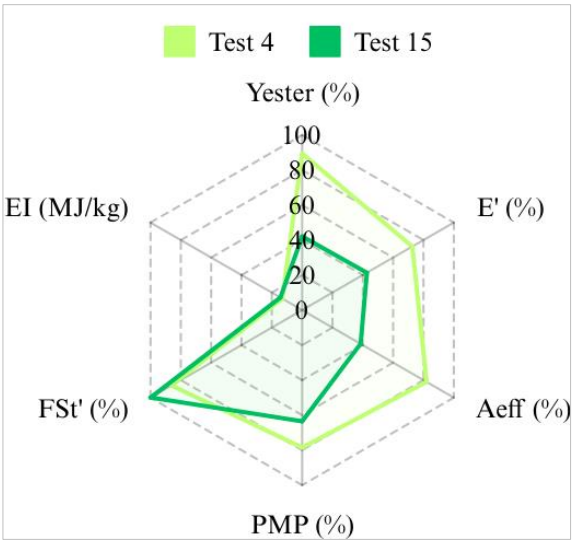

Figure 9. Radar chart of green metrics, energy intensity, and yield in tests 4 and 15.

3.7 Statistical analysis

Experimental results were analysed using the response surface model, a quadratic polynomial equation, and the Minitab 18 software tool for CCD data treatment. Analysis of variance (ANOVA) and regression were performed to evaluate the fitting model, the primary factors and interactions, and the significance of each studied response.

Effect on ester yield. The Minitab 18 software tool performed the one-way ANOVA to evaluate the influence of independent variables (M/O, %KOH, T, S) on ester yield as a response.

The analysis of the CCD design in uncoded units generated the following quadratic model averaged over blocks:

$$Y_{esters} = -2.62 - 0.117\,X_1 + 0.30\,X_2 + 0.341\,X_3 - 0.0265\,X_4 - 0.00207\,{X_1}^2 - 0.134\,{X_2}^2$$
$$- 0.00306\,{X_3}^2 + 0.000027\,{X_4}^2 - 0.037\,X_1\,X_2 + 0.00001\,X_1\,X_3$$
$$+ 0.000472\,X_1\,X_4 - 0.0144\,X_2\,X_3 + 0.00238\,X_2\,X_4 - 0.00002\,X_3\,X_4$$

where X_1 is M/O, X_2 is %KOH, X_3 is T and X_4 is S.

The F-test and p-value evaluated the significance of the model and its factors in the ANOVA (Table 6).

Table 6. Analysis of Variance for a yield of esters as a response.

Source	DF	Adj SS	Adj MS	F-Value	p-Value
Model	15	0.285589	0.019039	1.20	0.380
Blocks	1	0.016163	0.016163	1.02	0.333
Linear	4	0.054350	0.013588	0.86	0.517
M/O	1	0.000134	0.000134	0.01	0.928
%KOH	1	0.011807	0.011807	0.74	0.405
T (°C)	1	0.014953	0.014953	0.94	0.351
S	1	0.027456	0.027456	1.73	0.213
Square	4	0.028918	0.007229	0.46	0.767
M/O*M/O	1	0.000849	0.000849	0.05	0.821
%KOH*%KOH	1	0.002735	0.002735	0.17	0.685
T (°C)*T (°C)	1	0.014302	0.014302	0.90	0.361
S*S	1	0.011420	0.011420	0.72	0.413
2-Way Interaction	6	0.192144	0.032024	2.02	0.142
M/O*%KOH	1	0.034003	0.034003	2.14	0.169
M/O*T (°C)	1	0.000000	0.000000	0.00	0.998
M/O*S	1	0.080231	0.080231	5.05	0.044
%KOH*T (°C)	1	0.020765	0.020765	1.31	0.275
%KOH*S	1	0.056763	0.056763	3.58	0.083
T (°C)*S	1	0.000382	0.000382	0.02	0.879
Error	12	0.190459	0.015872		
Lack-of-Fit	10	0.179050	0.017905	3.14	0.266
Pure Error	2	0.011409	0.005704		
Total	27	0.476048			

DF: total degrees of freedom; Adj SS: adjusted sum of squares; Adj MS: adjusted mean squares; F-Value: Fisher test statistic; p-Value: probability value.

The F-value for certain variables and their combinations is lower than that for the Lack of Fit. Consequently, a partial lack of fit is associated with the quadratic model, suggesting that a more complex model should be adopted to adequately describe the experimental behaviour of the objective function in relation to specific quadratic combinations of variables. Indeed, at the 95% confidence level, the p-value of the quadratic model was higher than 0.05, indicating that it is not adequate to describe the process. With a p-value lower than 0.05, only the combination of M/O and stirring had a significant effect at the operating conditions tested, as confirmed by the Pareto graph (Fig. 10). Equilibrium conditions were probably reached after 90 minutes, and the impact of different initial operating conditions was not significant.

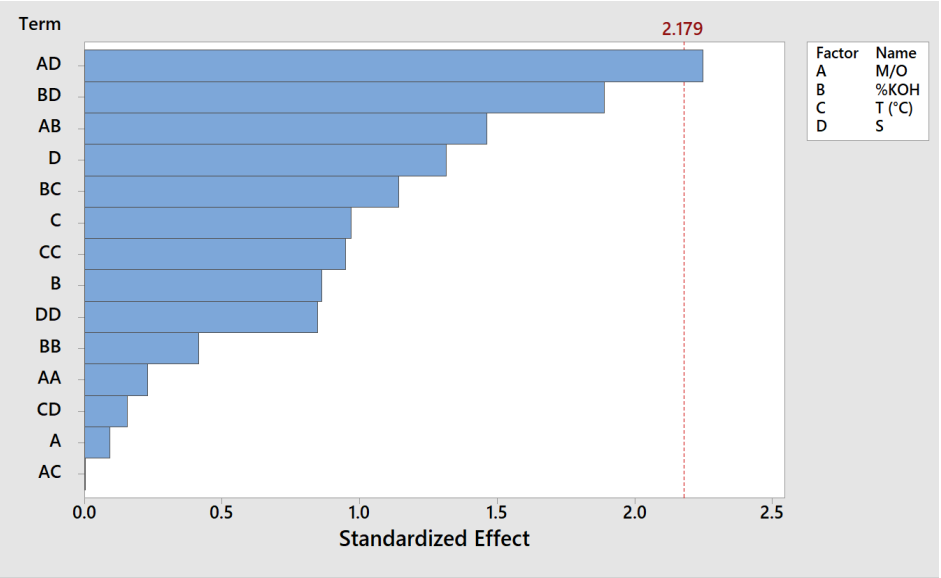

588

589 **Figure 10**. Pareto Chart of the standardised effects of single factors and their combinations on
590 esters yield (significance value: 0.05).

591 Fig. 11 shows a set of graphs confirming the validity of the experimental tests. Since the points

592 fluctuate around zero, there is no relation.

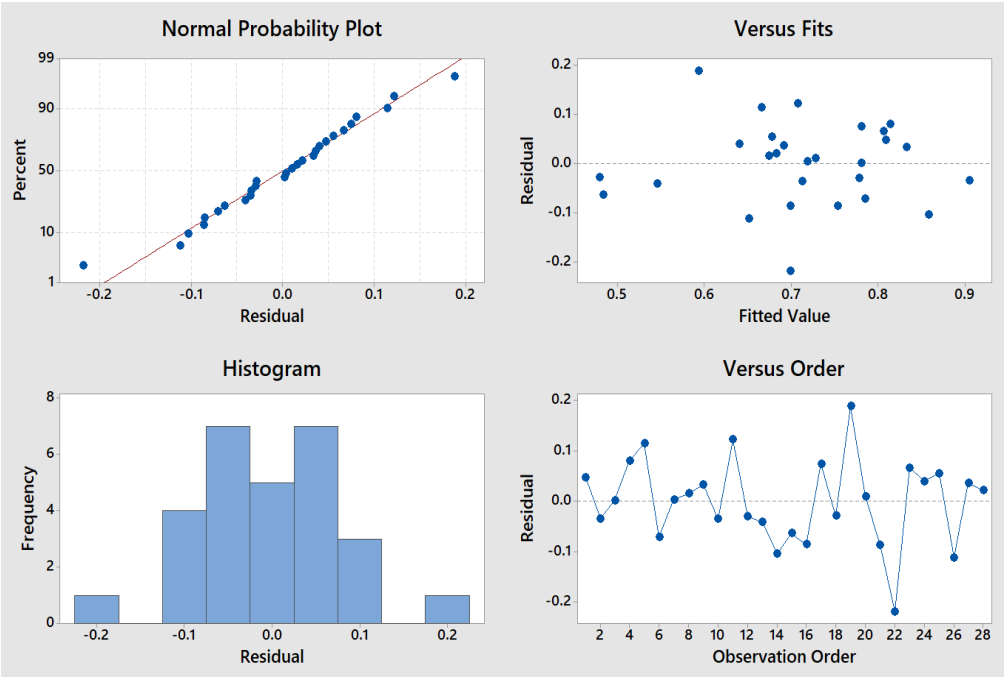

593

594 **Figure 11**. Residual plots for the statistical analysis with a yield of esters as a response.

595 The surface plots (Fig. 12a-f) show the influence of independent variables on the yield of esters

596 Y_{esters}. Combining M/O and stirring (Fig. 12c) allows obtaining higher yield values than other

combinations. In particular, a yield higher than 90% was attained with the combination of M/O=9 and S=450 rpm. Fig. 13a-f shows the contour diagrams of the different factors, confirming that the combination of the highest stirring and methanol/oil ratio gave the highest yield (dark green, Fig. 13c).

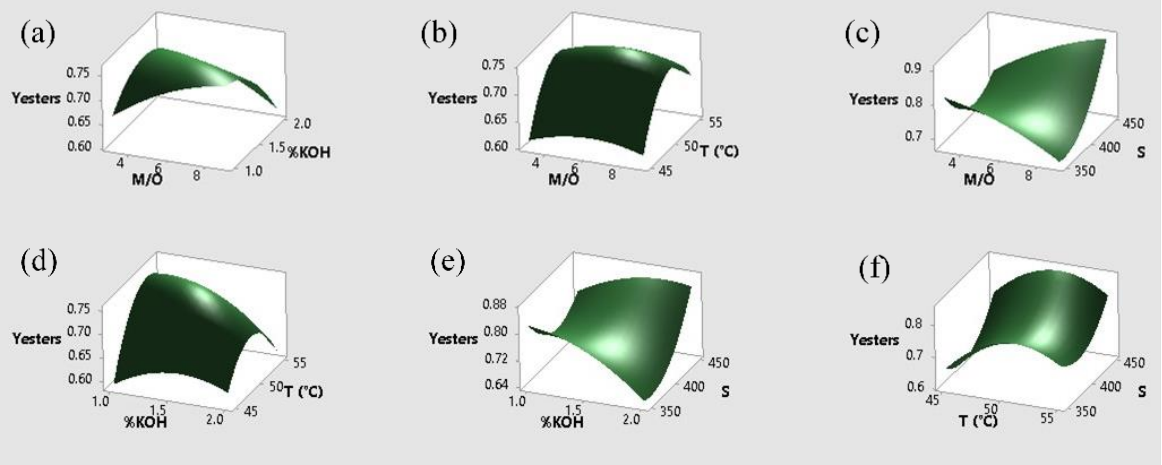

Figure 12. Surface plots of esters yields from alkaline transesterification of WCO at different combinations of operating conditions by RSM (hold values: M/O: 6; %KOH: 1.5; T: 50 °C; S: 400 rpm).

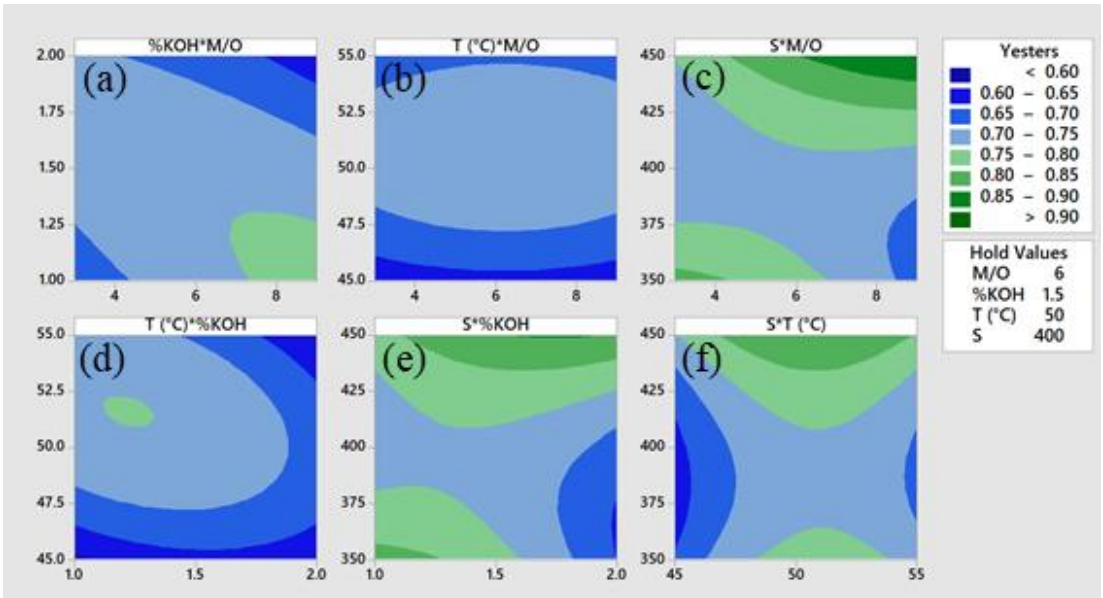

Figure 13. Contour plots of response surfaces for a yield of esters as a response.

Effect on energy intensity. The one-way ANOVA was performed to evaluate the influence of independent variables on energy intensity (EI) as a response.

The analysis of the CCD design in uncoded units generated the following quadratic model averaged over blocks:

$$EI = -61.1 + 2.50\,X_1 + 9.6\,X_2 - 0.17\,X_3 + 0.315\,X_4 + 0.0122\,{X_1}^2 + 2.02\,{X_2}^2 + 0.0012\,{X_3}^2 - 0.000364\,{X_4}^2 - 0.225\,X_1\,X_2 - 0.0142\,X_1\,X_3 - 0.00357\,X_1\,X_4 - 0.095\,X_2\,X_3 - 0.0252\,X_2\,X_4 + 0.00069\,X_3\,X_4$$

where X_1 is M/O, X_2 is %KOH, X_3 is T and X_4 is S.

The F-test and p-value evaluated the significance of the model and its factors in the ANOVA (Table 7).

Table 7. Analysis of Variance for energy intensity as response.

Source	DF	Adj SS	Adj MS	F-Value	p-Value
Model	15	26.0914	1.73943	1.32	0.318
Blocks	1	1.9411	1.94110	1.47	0.248
Linear	4	5.7165	1.42912	1.08	0.407
M/O	1	4.5401	4.54009	3.44	0.088
%KOH	1	1.1603	1.16027	0.88	0.367
T (°C)	1	0.0022	0.00222	0.00	0.968
S	1	0.0139	0.01389	0.01	0.920
Square	4	2.2881	0.57202	0.43	0.782
M/O*M/O	1	0.0298	0.02976	0.02	0.883
%KOH*%KOH	1	0.6252	0.62521	0.47	0.504
T (°C)*T (°C)	1	0.0022	0.00224	0.00	0.968
S*S	1	2.0272	2.02719	1.54	0.239
2-Way Interaction	6	14.8614	2.47691	1.88	0.166
M/O*%KOH	1	1.8293	1.82926	1.39	0.262
M/O*T (°C)	1	0.7268	0.72676	0.55	0.472
M/O*S	1	4.5903	4.59031	3.48	0.087
%KOH*T (°C)	1	0.8978	0.89776	0.68	0.425
%KOH*S	1	6.3378	6.33781	4.81	0.049
T (°C)*S	1	0.4796	0.47956	0.36	0.558
Error	12	15.8239	1.31866		
Lack-of-Fit	10	13.4998	1.34998	1.16	0.548
Pure Error	2	2.3241	1.16203		
Total	27	41.9153			

DF: total degrees of freedom; Adj SS: adjusted sum of squares; Adj MS: adjusted mean squares; F-Value: Fisher test statistic; p-Value: probability value.

The F-value for certain variables and their combinations is lower than that for the Lack of Fit. Consequently, a partial lack of fit is associated with the quadratic model, suggesting that a more complex model should be adopted to adequately describe the experimental behaviour of the objective function in relation to specific quadratic combinations of variables. Indeed, with a p-value higher than 0.05, the quadratic model did not adequately describe the process. Moreover,

only the combination of catalyst amount and stirring significantly affected the energy intensity at the operating conditions tested, as confirmed by the Pareto graph (Fig. 14). The energy consumption strongly depends on the duration of the reaction. After the same time of 90 minutes, the initial operating conditions did not significantly influence the energy intensity value. However, residual plots in Fig. 15 confirmed the validity of experimental tests.

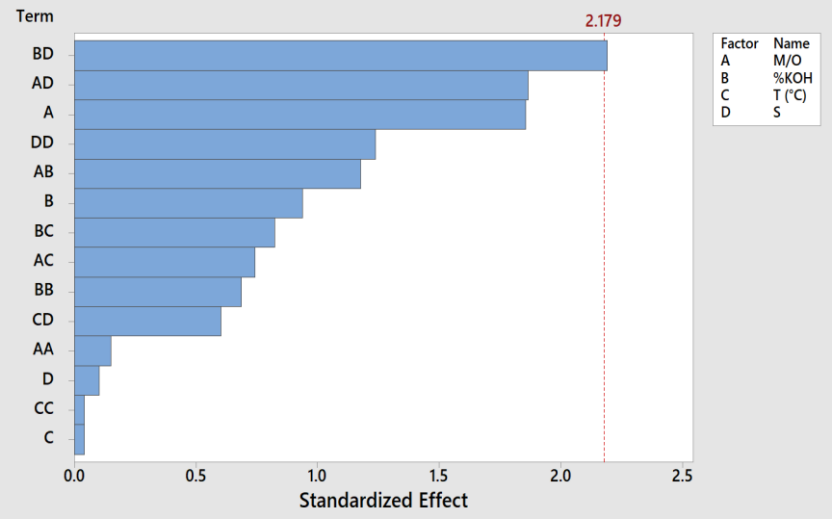

Figure 14. Pareto Chart of the standardised effects of single factors and their combinations on energy intensity (significance value: 0.05).

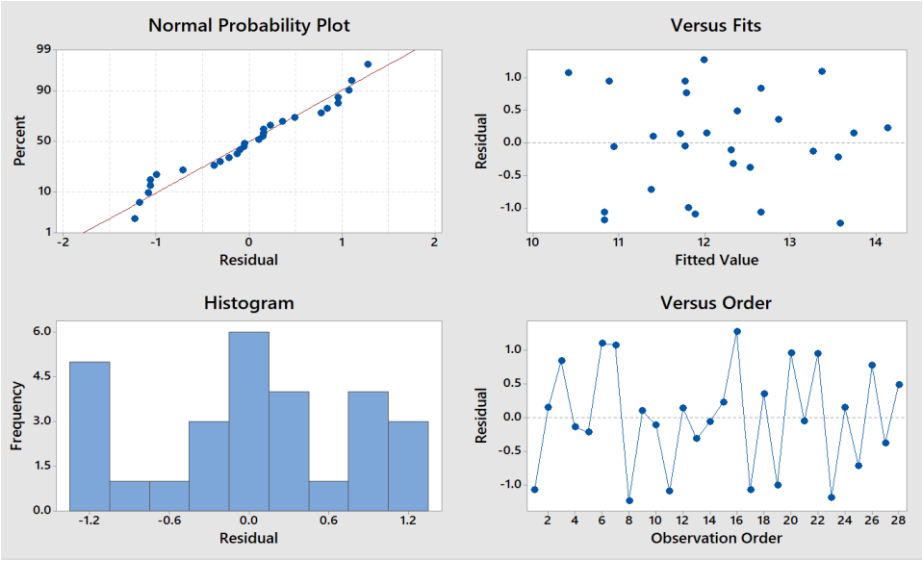

Figure 15. Residual plots for the statistical analysis with energy intensity as a response.

The influence of independent variables on EI is graphically evident in the surface plots (Fig. 16a-f) and contour plots (Fig. 17a-f). Low stirring and methanol-to-oil ratio are the best conditions

for minimising energy intensity (dark blue, Fig. 17c).

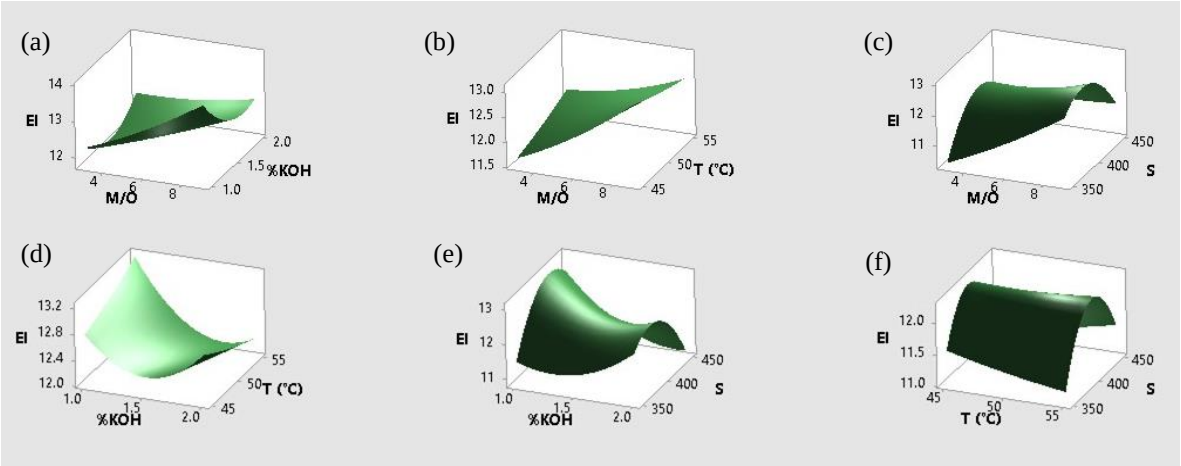

Figure 16. Surface plots of energy intensity after 90 minutes of alkaline transesterification of WCO at different combinations of operating conditions by RSM (hold values: M/O: 6; %KOH: 1.5; T: 50 °C; S: 400 rpm).

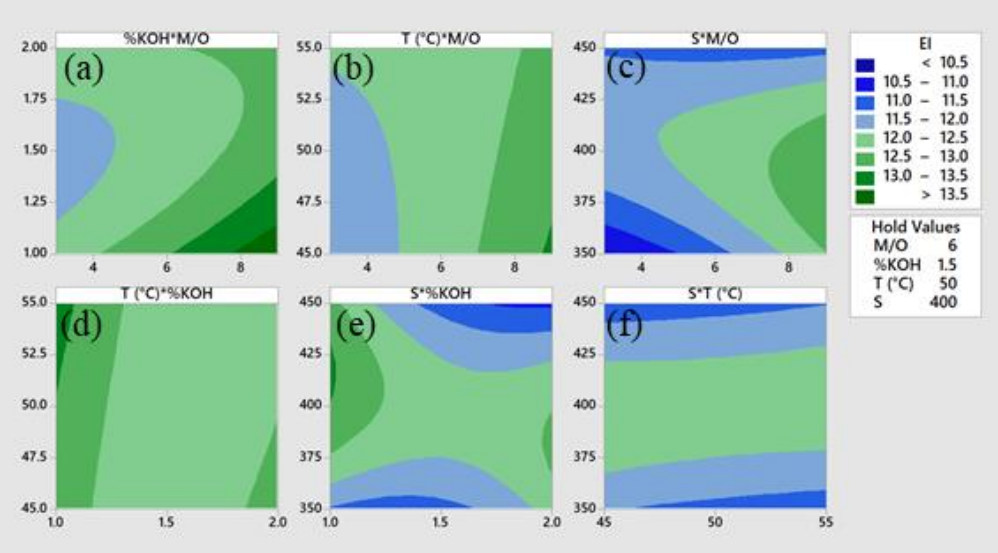

Figure 17. Contour plots of response surfaces for energy intensity as a response.

Effect on green chemistry balance. Finally, the one-way ANOVA was performed to evaluate the influence of independent variables on green chemistry balance (GCB) as a response.

The analysis of the CCD design in uncoded units generated the following quadratic model averaged over blocks:

$$GCB = 1.03 - 0.0713\,X_1 + 0.711\,X_2 + 0.161\,X_3 - 0.0236\,X_4 - 0.00287\,{X_1}^2 - 0.195\,{X_2}^2 - 0.00162\,{X_3}^2 + 0.000025\,{X_4}^2 - 0.00939\,X_1 X_2 + 0.000425\,X_1 X_3 + 0.000253\,X_1 X_4 - 0.00697\,X_2 X_3 + 0.000651\,X_2 X_4 + 0.000026\,X_3 X_4$$

where X_1 is M/O, X_2 is %KOH, X_3 is T and X_4 is S.

The F-test and p-value evaluated the significance of the model and its factors in the ANOVA (Table 8).

Table 8. Analysis of Variance for green chemistry balance as a response.

Source	DF	Adj SS	Adj MS	F-Value	p-Value
Model	15	0.067416	0.004494	1.55	0.224
Blocks	1	0.005379	0.005379	1.86	0.198
Linear	4	0.009071	0.002268	0.78	0.557
M/O	1	0.001063	0.001063	0.37	0.556
%KOH	1	0.001230	0.001230	0.42	0.527
T (°C)	1	0.002054	0.002054	0.71	0.416
S	1	0.004724	0.004724	1.63	0.226
Square	4	0.020944	0.005236	1.81	0.192
M/O*M/O	1	0.001629	0.001629	0.56	0.468
%KOH*%KOH	1	0.005794	0.005794	2.00	0.183
T (°C)*T (°C)	1	0.003995	0.003995	1.38	0.263
S*S	1	0.009679	0.009679	3.34	0.092
2-Way Interaction	6	0.036612	0.006102	2.11	0.128
M/O*%KOH	1	0.003175	0.003175	1.10	0.316
M/O*T (°C)	1	0.000650	0.000650	0.22	0.644
M/O*S	1	0.022998	0.022998	7.94	0.016
%KOH*T (°C)	1	0.004851	0.004851	1.68	0.220
%KOH*S	1	0.004238	0.004238	1.46	0.250
T (°C)*S	1	0.000700	0.000700	0.24	0.632
Error	12	0.034740	0.002895		
Lack-of-Fit	10	0.030765	0.003077	1.55	0.455
Pure Error	2	0.003975	0.001987		
Total	27	0.102157			

DF: total degrees of freedom; Adj SS: adjusted sum of squares; Adj MS: adjusted mean squares; F-Value: Fisher test statistic; p-Value: probability value.

The F-value for certain variables and their combinations is lower than that for the Lack of Fit. Consequently, a partial lack of fit is associated with the quadratic model, suggesting that a more complex model should be adopted to adequately describe the experimental behaviour of the objective function in relation to specific quadratic combinations of variables. Indeed, with a p-value higher than 0.05, the quadratic model did not adequately describe the process. Moreover, only the combination of M/O and stirring significantly affected the green chemistry balance, as confirmed by the Pareto graph (Fig. 18). Residual plots (Fig. 19) confirmed the validity of the

experimental tests.

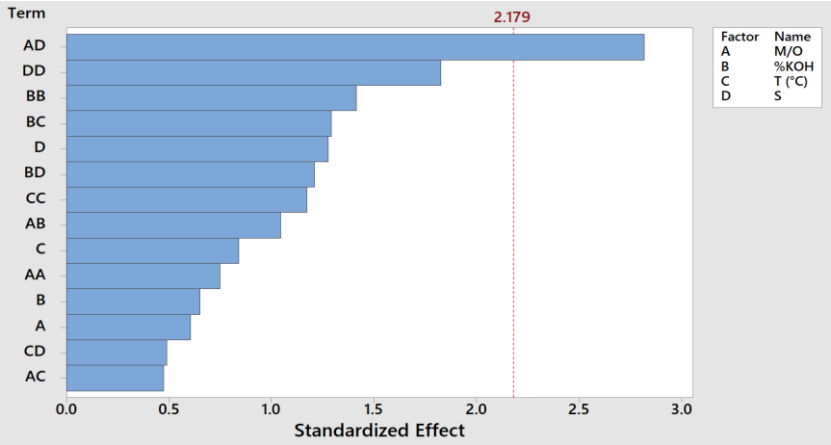

Figure 18. Pareto Chart of the standardised effects of single factors and their combinations on green chemistry balance (significance value: 0.05).

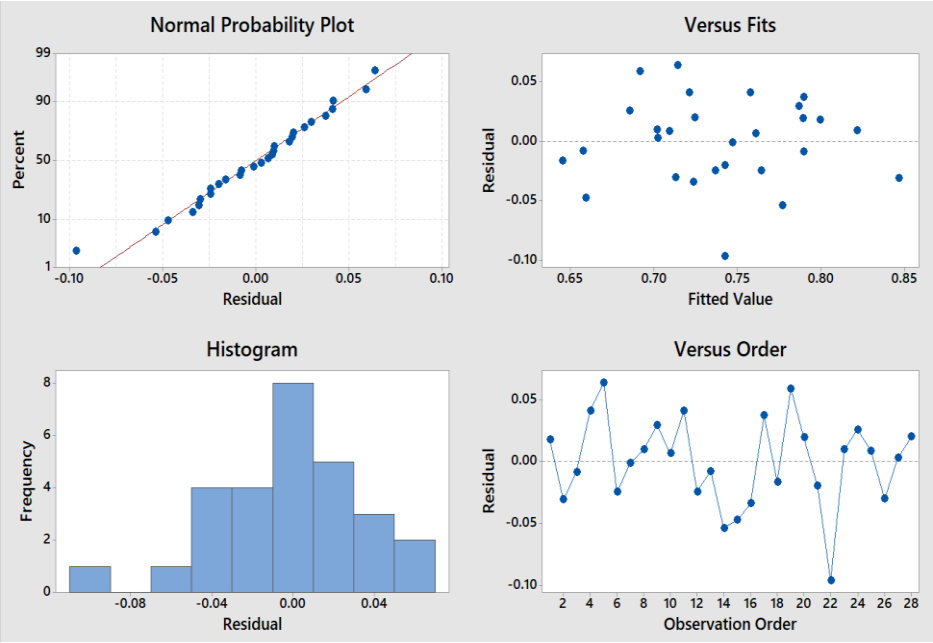

Figure 19. Residual plots for the statistical analysis with green chemistry balance as a response.

The influence of independent variables on GCB is graphically evident in the surface plots (Fig. 20a-f) and contour plots (Fig. 21a-f), showing that the best conditions are high stirring and M/O (dark green, Fig. 21c).

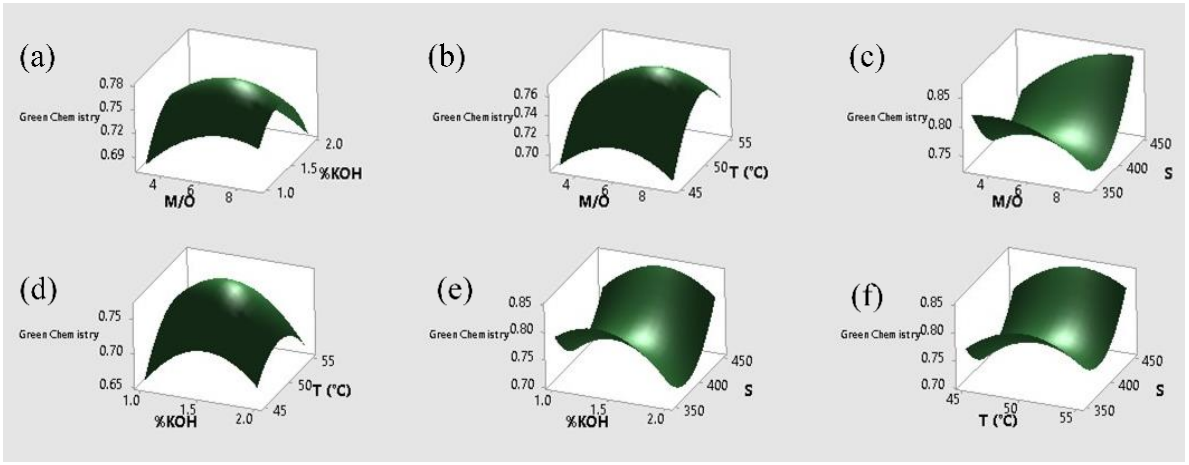

674

675 **Figure 20**. Surface plots of green chemistry balance of alkaline transesterification of WCO at
676 different combinations of operating conditions by RSM (hold values: M/O: 6; %KOH: 1.5; T:
677 50 °C; S: 400 rpm).

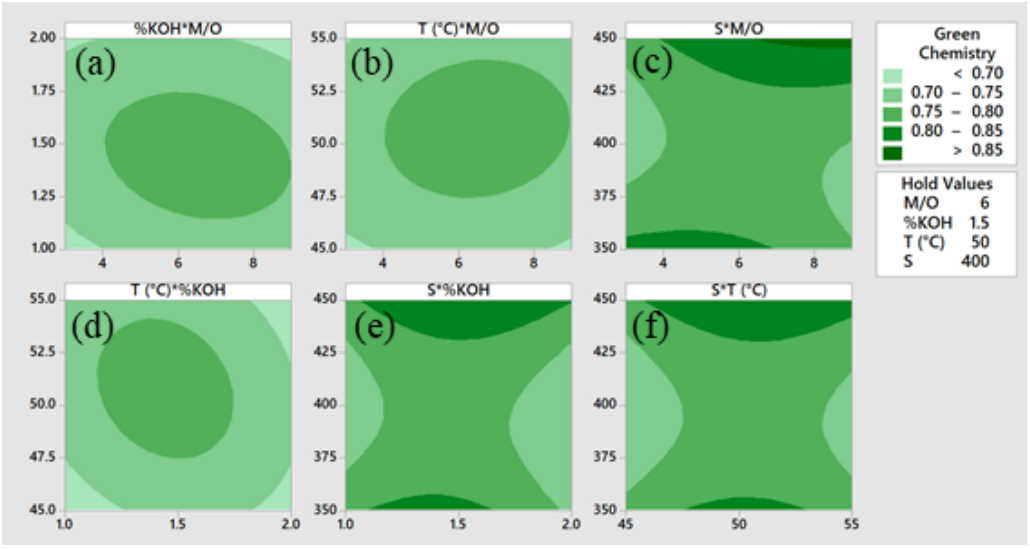

678

679 **Figure 21**. Contour plots of response surfaces for green chemistry balance as a response.

680 **Multi-objective optimisation of operating conditions**. A multi-objective optimisation is
681 necessary to consider the transesterification's yield, energy consumption, and green chemistry
682 balance. The yield and green chemistry balance should be maximised, whereas the energy
683 intensity should be minimised. Therefore, the results of multi-objective optimisation (Fig. 23)
684 differ from single-response optimisation (Fig. 22). Indeed, the optimal conditions vary
685 significantly when each response is used as a single performance criterion. As an example, M/O
686 and S should be maximum to optimise the yield and green chemistry balance (Fig. 22a,c) but

minimum to optimise the energy intensity (Fig. 22b). Or else, %KOH and T should have similar intermediate values to optimise, but minimum to optimise the energy intensity. Multi-objective optimisation overcomes the drawback of single-objective optimisation by simultaneously optimising all three responses in this process. The optimal conditions are M/O of 3, 1.3 wt% of KOH, temperature of 50.7 °C, and stirring of 350 rpm. These results differ from the few previous works in the literature about the multi-objective optimisation of WCO transesterification, but this may be due to the different conditions tested. Indeed, Outili et al. (Outili et al., 2020) tested the methanol-to-oil ratio, catalyst concentration, and temperature in the ranges 4-8, 0.5-2 wt%, and 45-60 °C for 30 minutes of reaction, whereas in this work, stirring was also considered, and the reaction lasted 90 minutes; moreover, they considered other green metrics to calculate the green chemistry balance and measured theoretical energy consumption instead of experimental energy intensity.

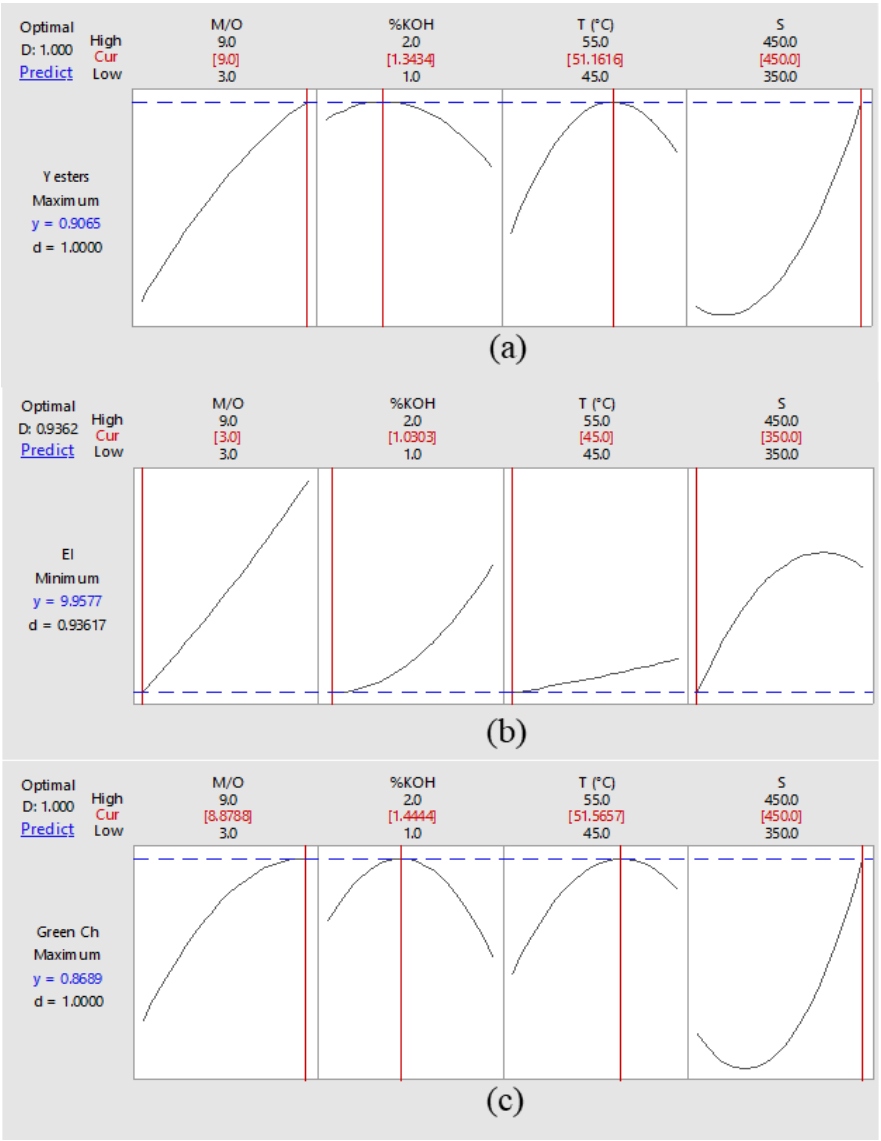

699

700 **Figure 22**. Single-objective optimisation for each response: (a) yield of esters, (b) energy
701 intensity, (c) green chemistry balance.

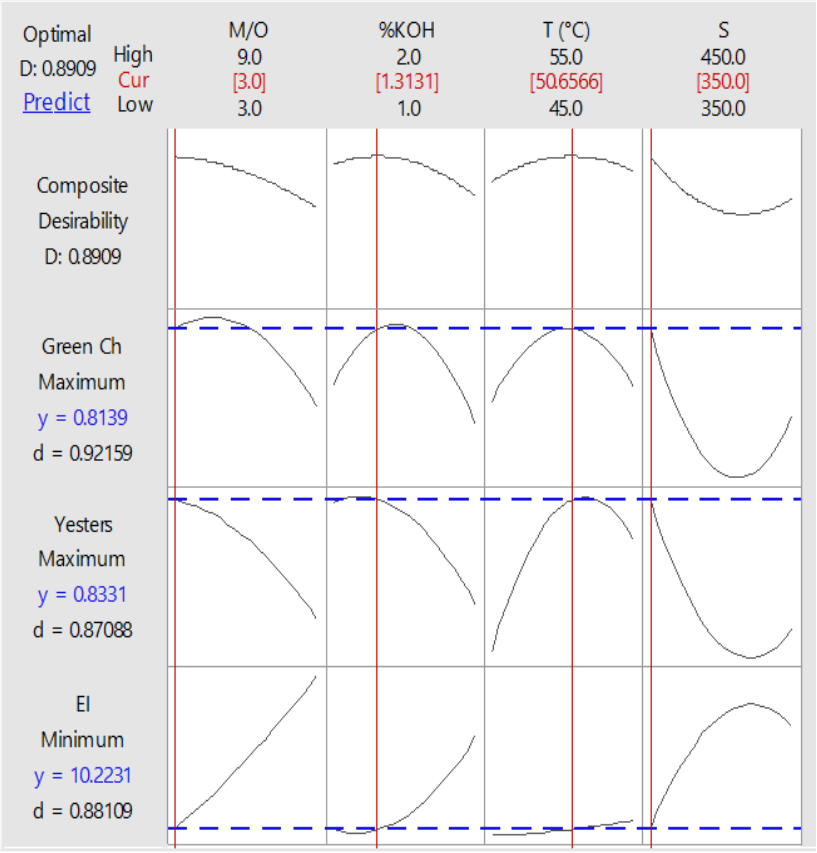

Figure 23. Multi-objective optimisation results of WCO transesterification to biodiesel.

4. Future challenges and perspectives

Although biodiesel production from WCO has been extensively studied, the reported results in the literature vary significantly due to the heterogeneity of raw materials. A global appoach provides insights into developing efficient and cost-effective biodiesel production methods. Using waste cooking oil significantly reduces the process cost and addresses the problem concerning its disposal. Therefore, focusing on the barrier of feedstock supply and management, innovation in process, reactor configuration, and development of cost-effective catalysts, would be required. The biodiesel production by homogeneous alkaline catalysis is simple and effective. However, very high-quality feedstock is needed, requiring pre-treatments which make the biodiesel production expensive and non-competitive. The integrated two-step homogeneous acid-base processes can handle low-quality feedstocks but with more catalyst and processing

steps. Replacement of homogeneous catalysts with heterogeneous catalysts could enhance the efficiency and sustainability of biodiesel synthesis while reducing costs and environmental impacts. However, more research is required to increase their activity, stability, and reusability in mild operating conditions, fast reaction rates, and reasonable costs for industrial applications. Finally, considering glycerol as a co-product of transesterification with high value lowers the biodiesel costs significantly and the glycerol purification should be optimised.

5. Conclusions

Recent attention has focused on energy consumption and the principles of green chemistry in biodiesel production. This study optimised the operating conditions for converting household WCO into biodiesel using RSM applied to a CCD-based experimental plan to analyse the energy consumption and sustainability through a green chemistry approach, optimising the reaction within a single reactor under diverse conditions. Crude biodiesel was characterised using refractometry and multiple light scattering after product separation. Compared to more labour-intensive chromatographic techniques, these methods are simple and rapid and provide reliable conversion and separation data. The reaction was optimised for yield, energy use, and environmental impact through RSM, by evaluating the effects of methanol-to-oil ratio (M/O), percentage of potassium hydroxide (%KOH), temperature (T), and stirring speed (S) as independent variables. The peak yield of esters was measured at 89.43%, attained at a temperature of 55 °C, a stirring speed of 350 rpm, with a M/O of 9 and a catalyst concentration of 1%. Gas chromatography analysis indicated that the total fraction of oil eligible for esterification was 96.7%. Consequently, the actual yield of esters, in relation to the oil that can be effectively converted, was recorded at 92.5%. The optimal conditions for achieving the highest yields of crude biodiesel and esters were characterised by significant energy intensity. The energy intensity values associated with the transesterification reaction are deemed acceptable within a laboratory setting and align with the estimated value of 37.13 MJ/kg reported

by numerous industrial processes for biodiesel production. The optimum condition regarding yield does not align with the optimum condition concerning the E factor and, more broadly, with eco-sustainability. The maximum value for the balance of green chemistry, quantified at 83.11%, corresponds to the minimum energy intensity value, resulting in a suboptimal ester yield. Conversely, the lowest balance of green chemistry, quantified at 61.21%, was observed when the minimum ester yield reached 42% alongside a high energy intensity (EI) of 14.36 MJ/kg. Then, the optimal conditions fluctuated when evaluating individual performance criteria. Nonetheless, a multi-objective approach was demonstrated to be critical for overall optimisation by concurrently optimising all three responses within this process. Results showed that the multi-objective optimisation varied from single-response optimisation when each response was treated as an independent performance criterion. In particular, the optimal conditions were M/O of 3, a KOH concentration of 1.3 wt%, a temperature of 50.7 °C, and a stirring speed of 350 rpm.

In conclusion, while reaction time, type of alcohol, alcohol-to-oil molar ratio, reaction temperature, quantity of catalyst, and mixing intensity were typically optimised by RSM to achieve maximum biodiesel yield from Waste Cooking Oil, it is essential to note that the highest yield does not inherently ensure an environmentally sustainable process. The application of green chemistry principles is essential for guaranteeing sustainability in such processes. Therefore, addressing a more comprehensive optimisation approach involving green chemistry principles is necessary and contributes significantly to a broader vision of the process.

List of abbreviations

a_o: intercept term in the statistical model

a_i: linear coefficients in the statistical model

a_{ii}: quadratic coefficients in the statistical model

a_{ij}: interactive coefficients in the statistical model

A: acidity

765 Adj MS: Adjusted Mean Squares

766 Adj SS: Adjusted Sum of Squares

767 AE: Atom Economy

768 AEff: Atom Efficiency

769 ANOVA: Analysis Of Variance

770 ASTM: American Society for Testing and Materials

771 BBD: Box-Behnken Design

772 C: Concentration

773 CCD: Central Composite Design

774 CFPP: Cold Filter Plugging Point

775 DF: total Degrees of Freedom

776 E factor: Environmental factor

777 E': normalised environmental factor

778 EI: Energy Intensity

779 FFA: Free Fatty Acid

780 FAME: Fatty Acid Methyl Esters

781 FSt: Stoichiometric Factor

782 FSt': normalised stoichiometric factor

783 F-Value: Fisher test statistic

784 HPLC: High-Performance Liquid Chromatography

785 GC: Gas Chromatography

786 M/O: Methanol-to-Oil molar ratio

787 MW: Molecular Weight

788 OA: Oleic Acid

789 PMI: Process Mass Intensity

PMP: Process Mass Productivity

p-Value: probability value

R: response in the statistical model

RME: Reaction Mass Efficiency

RSM: Response Surface Methodology

S: Stirring

T: Temperature

V: Volume

WCO: Waste Cooking Oil

x: mass fraction

X_1: methanol-to-oil ratio in the statistical model

X_2: catalyst concentration in the statistical model

X_3: temperature in the statistical model

X_4: stirring in the statistical model

Y: Yield

References

Abbah, E.C., Nwandikom, G.I., Egwuonwu, C.C., Nwakuba, N.R., 2016. Effect of Reaction Temperature on the Yield of Biodiesel From Neem Seed Oil, American Journal of Energy Science.

Abbaszaadeh, A., Ghobadian, B., Omidkhah, M.R., Najafi, G., 2012. Current biodiesel production technologies: A comparative review, in: Energy Conversion and Management. pp. 138–148. https://doi.org/10.1016/j.enconman.2012.02.027

Adekoya, O.A., Giwa, A., Yusuff, A.S., Giwa C, A., 2015. D-Optimal-Experimental-Design-of-Biodiesel-Production-from-Waste-Cooking-Oil-of-ABUAD-Cafeterias.docx. Int J Sci Eng Res 6.

Ahmad, G., Imran, S., Farooq, M., Shah, A.N., Anwar, Z., Rehman, A.U., Imran, M., 2023. Biodiesel Production from Waste Cooking Oil Using Extracted Catalyst from Plantain Banana Stem via RSM and ANN Optimization for Sustainable Development. Sustainability (Switzerland) 15. https://doi.org/10.3390/su151813599

Ali Ijaz Malik, M., Zeeshan, S., Khubaib, M., Ikram, A., Hussain, F., Yassin, H., Qazi, A., 2024. A review of major trends, opportunities, and technical challenges in biodiesel production from waste sources. Energy Conversion and Management: X. https://doi.org/10.1016/j.ecmx.2024.100675

All statistics for Create Response Surface Design (Central Composite) [WWW Document],

2023. . Minitab . URL https://support.minitab.com/en-us/minitab/21/help-and-how-to/statistical-modeling/doe/how-to/response-surface/create-response-surface-design/create-central-composite-design/examine-the-design/all-statistics/ (accessed 1.18.24).
Anastas, P.T., Warner, J.C., 1998. Green Chemistry: Theory and Practice. Oxford University Press, New York.
Atapour, M., Kariminia, H.R., Moslehabadi, P.M., 2014. Optimization of biodiesel production by alkali-catalyzed transesterification of used frying oil. Process Safety and Environmental Protection 92, 179–185. https://doi.org/10.1016/j.psep.2012.12.005
Ayoola, A.A., Hymore, K.F., Omonhinmin, C.A., 2016. Optimization of biodiesel production from selected waste oils using response surface methodology. Biotechnology. https://doi.org/10.3923/biotech.2016
Babadi, A.A., Rahmati, S., Fakhlaei, R., Barati, B., Wang, S., Doherty, W., Ostrikov, K., 2022. Emerging technologies for biodiesel production: Processes, challenges, and opportunities. Biomass Bioenergy. https://doi.org/10.1016/j.biombioe.2022.106521
Bai, H., Tian, J., Talifu, D., Okitsu, K., Abulizi, A., 2022. Process optimization of esterification for deacidification in waste cooking oil: RSM approach and for biodiesel production assisted with ultrasonic and solvent. Fuel 318. https://doi.org/10.1016/j.fuel.2022.123697
Bajwa, W., Ikram, A., Malik, M.A.I., Razzaq, L., Khan, A.R., Latif, A., Hussain, F., Qazi, A., 2024. Optimization of biodiesel yield from waste cooking oil and sesame oil using RSM and ANN techniques. Heliyon 10. https://doi.org/10.1016/j.heliyon.2024.e34804
Bashir, M.A., Wu, S., Zhu, J., Krosuri, A., Khan, M.U., Ndeddy Aka, R.J., 2022. Recent development of advanced processing technologies for biodiesel production: A critical review. Fuel Processing Technology 227. https://doi.org/10.1016/j.fuproc.2021.107120
Bhonsle, A.K., Yusuff, A.S., Trivedi, J., Singh, J., Singh, R.K., Atray, N., 2022. Transesterification of used cooking oil at ambient temperature using novel solvent: experimental investigations and optimisation by response surface methodology. International Journal of Ambient Energy 43, 4801–4811. https://doi.org/10.1080/01430750.2021.1919925
Blekas, G., Tsimidou, M., Boskou, D., 2006. Olive Oil Composition, in: Olive Oil. AOCS Publishing, pp. 41–72. https://doi.org/10.1201/9781439832028.pt2
Bobadilla, M.C., Lorza, R.L., Escribano-Garcia, R., Gómez, F.S., González, E.P.V., 2017. An improvement in biodiesel production from waste cooking oil by applying thought multi-response surface methodology using desirability functions. Energies (Basel) 10. https://doi.org/10.3390/en10010130
Bohlouli, A., Mahdavian, L., 2021. Catalysts used in biodiesel production: a review. Biofuels 12, 885–898. https://doi.org/10.1080/17597269.2018.1558836
Calvo-Flores, F.G., 2009. Sustainable chemistry metrics. ChemSusChem 2, 905–919. https://doi.org/10.1002/cssc.200900128
Darnoko, D., Cheryan, M., 2000. Kinetics of palm oil transesterification in a batch reactor. JAOCS 77, 1263–1267.
De Paola, Maria Gabriela, Arcuri, N., Calabrò, V., De Simone, M., 2017. Thermal and stability investigation of phase change material dispersions for thermal energy storage by T-history and optical methods. Energies (Basel) 10, 354. https://doi.org/10.3390/en10030354
De Paola, M. G., Calabrò, V., De Simone, M., 2017. Light scattering methods to test inorganic PCMs for application in buildings. IOP Conf Ser Mater Sci Eng 251. https://doi.org/10.1088/1757-899X/251/1/012122
De Paola, M.G., De Simone, M., Arcuri, N., Calabrò, V., 2016. Crossed analysis by T-history and Turbiscan for the characterization of PCM with Glauber salt, in: INNOSTORAGE Conference. Ben-Gurion University of the Negev.
De Paola, M.G., Lopresto, C.G., 2021. Waste oils and their transesterification products as novel bio-based phase change materials. Journal of Phase Change Materials 1. https://doi.org/https://doi.org/10.6084/jpcm.v1i1.6
De Paola, M.G., Mazza, I., Paletta, R., Lopresto, C.G., Calabrò, V., 2021a. Small-Scale Biodiesel Production Plants — An Overview. Energies (Basel) 14, 1901.
De Paola, M.G., Paletta, R., Lopresto, C.G., Calabrò, V., Paola, D., 2021b. Multiple light

879 scattering as a preliminary tool for starch-based film formulation. Journal of Phase Change
880 Material 1. https://doi.org/10.6084/jpcm.v1i2.15
881 De, R., Bhartiya, S., Shastri, Y., 2019. Multi-objective optimization of integrated biodiesel
882 production and separation system. Fuel 243, 519–532.
883 https://doi.org/10.1016/j.fuel.2019.01.132
884 Dicks, A.P., Hent, A., 2015. Green Chemistry Metrics - A Guide to Determining and Evaluating
885 Process Greenness. Springer, London.
886 Dorado, M.P., Ballesteros, E., López, F.J., Mittelbach, M., 2004. Optimization of alkali-
887 catalyzed transesterification of Brassica Carinata oil for biodiesel production. Energy and
888 Fuels 18, 77–83. https://doi.org/10.1021/ef0340110
889 Dubey, A., Prasad, R.S., Singh, J.K., 2020. An Analytical and Economical Assessment of the
890 Waste Cooking Oil based Biodiesel using Optimized Conditions on the Process Variables.
891 Energy Sources, Part A: Recovery, Utilization and Environmental Effects.
892 https://doi.org/10.1080/15567036.2020.1839600
893 Dwivedi, G., Jain, S., Shukla, A.K., Verma, P., Verma, T.N., Saini, G., 2022. Impact analysis of
894 biodiesel production parameters for different catalyst. Environ Dev Sustain.
895 https://doi.org/10.1007/s10668-021-02073-w
896 El-Gendy, N.S., El-Gharabawy, A.A.S.A., Amr, S.S., Ashour, F.H., 2015. Response surface
897 optimization of an alkaline transesterification of waste cooking oil. Int. J. ChemTech Res 8,
898 385–398.
899 Encinar, J.M., González, J.F., Rodríguez-Reinares, A., 2005. Biodiesel from Used Frying Oil.
900 Variables Affecting the Yields and Characteristics of the Biodiesel. Ind. Eng. Chem. Res.
901 44, 5491–5499.
902 Farouk, S.M., Tayeb, A.M., Abdel-Hamid, S.M.S., Osman, R.M., 2024. Recent advances in
903 transesterification for sustainable biodiesel production, challenges, and prospects: a
904 comprehensive review. Environmental Science and Pollution Research.
905 https://doi.org/10.1007/s11356-024-32027-4
906 Felizardo, P., Neiva Correia, M.J., Raposo, I., Mendes, J.F., Berkemeier, R., Bordado, J.M.,
907 2006. Production of biodiesel from waste frying oils. Waste Management 26, 487–494.
908 https://doi.org/10.1016/j.wasman.2005.02.025
909 Foon Cheng, S., Hock Chuah, C., 2004. Kinetics study on transesterification of palm oil.
910 García-Moreno, P.J., Khanum, M., Guadix, A., Guadix, E.M., 2014. Optimization of biodiesel
911 production from waste fish oil. Renew Energy 68, 618–624.
912 https://doi.org/10.1016/j.renene.2014.03.014
913 Gumahin, A.C., Galamiton, J.M., Allerite, M.J., Valmorida, R.S., Laranang, J.R.L., Mabayo,
914 V.I.F., Arazo, R.O., Ido, A.L., 2019. Response surface optimization of biodiesel yield from
915 pre-treated waste oil of rendered pork from a food processing industry. Bioresour
916 Bioprocess 6. https://doi.org/10.1186/s40643-019-0284-2
917 Gupta, V., Pal Singh, K., 2023. The impact of heterogeneous catalyst on biodiesel production; a
918 review, in: Materials Today: Proceedings. Elsevier Ltd, pp. 364–371.
919 https://doi.org/10.1016/j.matpr.2022.10.175
920 Halwe, A.D., Deshmukh, S.J., Kanu, N.J., Gupta, E., Tale, R.B., 2021. Optimization of the novel
921 hydrodynamic cavitation based waste cooking oil biodiesel production process parameters
922 using integrated L9Taguchi and RSM approach, in: Materials Today: Proceedings. Elsevier
923 Ltd, pp. 5934–5941. https://doi.org/10.1016/j.matpr.2021.04.484
924 Hamze, H., Akia, M., Yazdani, F., 2015. Optimization of biodiesel production from the waste
925 cooking oil using response surface methodology. Process Safety and Environmental
926 Protection 94, 1–10. https://doi.org/10.1016/j.psep.2014.12.005
927 Hoque, M.E., Singh, A., Chuan, Y.L., 2011. Biodiesel from low cost feedstocks: The effects of
928 process parameters on the biodiesel yield. Biomass Bioenergy 35, 1582–1587.
929 https://doi.org/10.1016/j.biombioe.2010.12.024
930 Issariyakul, T., Dalai, A.K., 2012. Comparative kinetics of transesterification for biodiesel
931 production from palm oil and mustard oil. Canadian Journal of Chemical Engineering 90,
932 342–350. https://doi.org/10.1002/cjce.20679
933 Jeyakumar, N., Narayanasamy, B., Balasubramaniam, V., 2019. Optimization of used cooking

oil methyl ester production using response surface methodology. Energy Sources, Part A: Recovery, Utilization and Environmental Effects 41, 2313–2325. https://doi.org/10.1080/15567036.2018.1555633
Karmee, S.K., Chadha, A., 2005. Preparation of biodiesel from crude oil of Pongamia pinnata. Bioresour Technol 96, 1425–1429. https://doi.org/10.1016/j.biortech.2004.12.011
Kerras, H., Merouani, R., Nekkab, C., Outili, N., Meniai, AH., 2018. Optimization of the frying oil waste transesterification reaction time to biodiesel. Algerian Journal of Engineering Research AJER 4, 65–70.
Kiran, K., Hebbar, G.S., 2021. Optimization of Biodiesel Production from Waste Cooking Oil by Box Behnken Design Using Response Surface Methodology. INTERNATIONAL JOURNAL of RENEWABLE ENERGY RESEARCH 11.
Knothe, G., Razon, L.F., 2017. Biodiesel fuels. Prog Energy Combust Sci 58, 36–59. https://doi.org/10.1016/j.pecs.2016.08.001
Kolakoti, A., Setiyo, M., Waluyo, B., 2021. Biodiesel Production from Waste Cooking Oil: Characterization, Modeling and Optimization. Mechanical Engineering for Society and Industry 1, 22–30. https://doi.org/10.31603/mesi.5320
Lapkin, A., Constable, D.J.C., 2009. Green Chemistry Metrics: Measuring and Monitoring Sustainable Processes, Green Chemistry Metrics: Measuring and Monitoring Sustainable Processes. John Wiley & Sons, Ltd. https://doi.org/10.1002/9781444305432
Leung, D.Y.C., Guo, Y., 2006. Transesterification of neat and used frying oil: Optimization for biodiesel production. Fuel Processing Technology 87, 883–890. https://doi.org/10.1016/j.fuproc.2006.06.003
Lopresto, C.G., 2024. Sustainable biodiesel production from waste cooking oils for energetically independent small communities: an overview. International Journal of Environmental Science and Technology. https://doi.org/10.1007/s13762-024-05779-2
Lopresto, C.G., De Paola, M.G., Albo, L., Policicchio, M.F., Chakraborty, S., Calabro, V., 2019. Comparative analysis of immobilized biocatalyst: study of process variables in trans-esterification reaction. 3 Biotech 9. https://doi.org/10.1007/s13205-019-1985-0
Lopresto, C.G., De Paola, M.G., Calabrò, V., 2024. Importance of the properties, collection, and storage of waste cooking oils to produce high-quality biodiesel – An overview. Biomass Bioenergy. https://doi.org/10.1016/j.biombioe.2024.107363
Lopresto, C.G., Gentile, M., Caravella, A., Candamano, S., Calabrò, V., 2025. De-acidification of waste cooking oils by adsorption on industrial waste: Kinetic analysis of a green pretreatment for biodiesel production. Chemosphere 380. https://doi.org/10.1016/j.chemosphere.2025.144460
Lopresto, C.G., Naccarato, S., Albo, L., De Paola, M.G., Chakraborty, S., Curcio, S., Calabrò, V., 2015. Enzymatic transesterification of waste vegetable oil to produce biodiesel. Ecotoxicol Environ Saf 121, 229–235. https://doi.org/10.1016/j.ecoenv.2015.03.028
Mandari, V., Devarai, S.K., 2022. Biodiesel Production Using Homogeneous, Heterogeneous, and Enzyme Catalysts via Transesterification and Esterification Reactions: a Critical Review. Bioenergy Res. https://doi.org/10.1007/s12155-021-10333-w
Marchetti, J.M., Miguel, V.U., Errazu, a. F., 2007. Possible methods for biodiesel production. Renewable and Sustainable Energy Reviews 11, 1300–1311. https://doi.org/10.1016/j.rser.2005.08.006
Mathiyazhagan, M., Ganapathi, a, 2011. Factors Affecting Biodiesel Production. Res Plant Biol 1, 1–5.
Meher, L.C., Kulkarni, M.G., Dalai, A.K., Naik, S.N., 2006. Transesterification of karanja (Pongamia pinnata) oil by solid basic catalysts, in: European Journal of Lipid Science and Technology. pp. 389–397. https://doi.org/10.1002/ejlt.200500307
Milano, J., Ong, H.C., Masjuki, H.H., Silitonga, A.S., Chen, W.H., Kusumo, F., Dharma, S., Sebayang, A.H., 2018a. Optimization of biodiesel production by microwave irradiation-assisted transesterification for waste cooking oil-Calophyllum inophyllum oil via response surface methodology. Energy Convers Manag 158, 400–415. https://doi.org/10.1016/j.enconman.2017.12.027
Milano, J., Ong, H.C., Masjuki, H.H., Silitonga, A.S., Kusumo, F., Dharma, S., Sebayang, A.H.,

Cheah, M.Y., Wang, C.T., 2018b. Physicochemical property enhancement of biodiesel synthesis from hybrid feedstocks of waste cooking vegetable oil and Beauty leaf oil through optimized alkaline-catalysed transesterification. Waste Management 80, 435–449. https://doi.org/10.1016/j.wasman.2018.09.005

Mukhtar, A., Saqib, S., Lin, H., Hassan Shah, M.U., Ullah, S., Younas, M., Rezakazemi, M., Ibrahim, M., Mahmood, A., Asif, S., Bokhari, A., 2022. Current status and challenges in the heterogeneous catalysis for biodiesel production. Renewable and Sustainable Energy Reviews. https://doi.org/10.1016/j.rser.2021.112012

Mulvihill, M.J., Beach, E.S., Zimmerman, J.B., Anastas, P.T., 2011. Green chemistry and green engineering: A framework for sustainable technology development. Annu Rev Environ Resour 36, 271–293. https://doi.org/10.1146/annurev-environ-032009-095500

Myers, R.H., Montgomery, D.C., Anderson-Cook, C.M., 2016. Response surface methodology: process and product optimization using designed experiments. John Wiley & Sons.

Najafi, B., Faizollahzadeh Ardabili, S., Shamshirband, S., Chau, K.W., Rabczuk, T., 2018. Application of ANNS, ANFIS and RSM to estimating and optimizing the parameters that affect the yield and cost of biodiesel production. Engineering Applications of Computational Fluid Mechanics 12, 611–624. https://doi.org/10.1080/19942060.2018.1502688

Naveenkumar, R., Baskar, G., 2021. Process optimization, green chemistry balance and technoeconomic analysis of biodiesel production from castor oil using heterogeneous nanocatalyst. Bioresour Technol 320, 124347. https://doi.org/10.1016/j.biortech.2020.124347

Okechukwu, O.D., Joseph, E., Nonso, U.C., Kenechi, N.-O., 2022. Improving heterogeneous catalysis for biodiesel production process. Cleaner Chemical Engineering 3, 100038. https://doi.org/10.1016/j.clce.2022.100038

Oliveira, D. DE, Luccio, M. DI, Faccio, C., Dalla Rosa, C., Paulo Bender, A.O., Lipke, N., Amroginski, C., Dariva, C., Vladimir Oliveira, J. DE, 2005. Optimization of Alkaline Transesterification of Soybean Oil and Castor Oil for Biodiesel Production.

Outili, N., Kerras, H., Nekkab, C., Merouani, R., Meniai, A.H., 2020. Biodiesel production optimization from waste cooking oil using green chemistry metrics. Renew Energy 145, 2575–2586. https://doi.org/10.1016/j.renene.2019.07.152

Oza, S., Kodgire, P., Kachhwaha, S.S., 2021a. Analysis of RSM Method for Optimization of Ultrasound-Assisted KOH Catalyzed Biodiesel Production from Waste Cotton-Seed Cooking Oil, in: Applied Mathematical Modeling and Analysis in Renewable Energy. CRC Press, pp. 133–148. https://doi.org/10.1201/9781003159124-9

Oza, S., Prajapati, N., Kodgire, P., Kachhwaha, S.S., 2021b. An ultrasound-assisted process for the optimization of biodiesel production from waste cottonseed cooking oil using response surface methodology. Water-Energy Nexus 4, 187–198. https://doi.org/10.1016/j.wen.2021.11.001

Özbay, N., Oktar, N., Tapan, N.A., 2008. Esterification of free fatty acids in waste cooking oils (WCO): Role of ion-exchange resins. Fuel 87, 1789–1798. https://doi.org/10.1016/j.fuel.2007.12.010

Özgür, C., 2021. Optimization of biodiesel yield and diesel engine performance from waste cooking oil by response surface method (RSM). Pet Sci Technol 39, 683–703. https://doi.org/10.1080/10916466.2021.1954019

Pathak, S., 2015. Acid catalyzed transesterification. J Chem Pharm Res 7, 1780–1786.

Patle, D.S., Sharma, S., Ahmad, Z., Rangaiah, G.P., 2014. Multi-objective optimization of two alkali catalyzed processes for biodiesel from waste cooking oil. Energy Convers Manag 85, 361–372. https://doi.org/10.1016/j.enconman.2014.05.034

Pisarello, M.L., Maquirriain, M., Sacripanti Olalla, P., Rossi, V., Querini, C.A., 2018. Biodiesel production by transesterification in two steps: Kinetic effect or shift in the equilibrium conversion? Fuel Processing Technology 181, 244–251. https://doi.org/10.1016/j.fuproc.2018.09.028

Razzaq, L., Imran, S., Anwar, Z., Farooq, M., Abbas, M.M., Khan, H.M., Asif, T., Amjad, M., Soudagar, M.E.M., Shaukat, N., Fattah, I.M.R., Rahman, S.M.A., 2020. Maximising yield

and engine efficiency using Optimised waste cooking oil biodiesel. Energies (Basel) 13. https://doi.org/10.3390/en13225941
Ruhul, A.M., Kalam, M.A., Masjuki, H.H., Fattah, I.M.R., Reham, S.S., Rashed, M.M., 2015. State of the art of biodiesel production processes: A review of the heterogeneous catalyst. RSC Adv. https://doi.org/10.1039/c5ra09862a
Selvaraj, R., Moorthy, I.G., Kumar, R.V., Sivasubramanian, V., 2019. Microwave mediated production of FAME from waste cooking oil: Modelling and optimization of process parameters by RSM and ANN approach. Fuel 237, 40–49. https://doi.org/10.1016/j.fuel.2018.09.147
Sharma, A., Kodgire, P., Kachhwaha, S.S., 2019. Biodiesel production from waste cotton-seed cooking oil using microwave-assisted transesterification: Optimization and kinetic modeling. Renewable and Sustainable Energy Reviews 116. https://doi.org/10.1016/j.rser.2019.109394
Sheldon, R.A., 2018. Metrics of Green Chemistry and Sustainability: Past, Present, and Future. ACS Sustain Chem Eng 6, 32–48. https://doi.org/10.1021/acssuschemeng.7b03505
Singh, D., Sharma, D., Soni, S.L., Sharma, S., Kumar Sharma, P., Jhalani, A., 2020. A review on feedstocks, production processes, and yield for different generations of biodiesel. Fuel 262, 116553. https://doi.org/10.1016/j.fuel.2019.116553
Stoytcheva, M., Montero, G., 2011. Biodiesel - Feedstocks and Processing Technologies. InTech, Janeza Trdine, Croatia.
Suhara, A., Karyadi, Herawan, S.G., Tirta, A., Idris, M., Roslan, M.F., Putra, N.R., Hananto, A.L., Veza, I., 2024. Biodiesel Sustainability: Review of Progress and Challenges of Biodiesel as Sustainable Biofuel. Clean Technologies 6, 886–906. https://doi.org/10.3390/cleantechnol6030045
Sun, S., Guo, J., Chen, X., 2021. Biodiesel preparation from Semen Abutili (Abutilon theophrasti Medic.) seed oil using low-cost liquid lipase Eversa® transform 2.0 as a catalyst. Ind Crops Prod 169. https://doi.org/10.1016/j.indcrop.2021.113643
Sun, S., Li, K., 2020. Biodiesel production from phoenix tree seed oil catalyzed by liquid lipozyme TL100L. Renew Energy 151, 152–160. https://doi.org/10.1016/j.renene.2019.11.006
Tacias-Pascacio, V.G., Torrestiana-Sánchez, B., Dal Magro, L., Virgen-Ortíz, J.J., Suárez-Ruíz, F.J., Rodrigues, R.C., Fernandez-Lafuente, R., 2019. Comparison of acid, basic and enzymatic catalysis on the production of biodiesel after RSM optimization. Renew Energy 135, 1–9. https://doi.org/10.1016/j.renene.2018.11.107
Tan, Y.H., Abdullah, M.O., Nolasco Hipolito, C., 2016. Comparison of Biodiesel Production between Homogeneous and Heterogeneous Base Catalysts. Applied Mechanics and Materials 833, 71–77. https://doi.org/10.4028/www.scientific.net/amm.833.71
Thirugnanasambandham, K., Shine, K., Aziz, H.A., Gimenes, M.L., 2017. Biodiesel synthesis from waste oil using novel microwave technique: Response surface modeling and optimization. Energy Sources, Part A: Recovery, Utilization and Environmental Effects 39, 636–642. https://doi.org/10.1080/15567036.2016.1196270
Tubino, M., Junior, J.G.R., Bauerfeldt, G.F., 2014. Biodiesel synthesis with alkaline catalysts: A new refractometric monitoring and kinetic study. Fuel 125, 164–172. https://doi.org/10.1016/j.fuel.2014.01.096
Ugheoke, B.I., Onoja Patrick, D., Kefas, H.M., Onche, E.O., 2007. Determination of Optimal Catalyst Concentration for Maximum Biodiesel Yield from Tigernut (Cyperus Esculentus) Oil.
Verma, P., Sharma, M.P., 2016. Review of process parameters for biodiesel production from different feedstocks. Renewable and Sustainable Energy Reviews. https://doi.org/10.1016/j.rser.2016.04.054
Vicente, G., Martínez, M., Aracil, J., 2004. Integrated biodiesel production: A comparison of different homogeneous catalysts systems. Bioresour Technol 92, 297–305. https://doi.org/10.1016/j.biortech.2003.08.014
Yatish, K. V., Lalithamba, H.S., Suresh, R., Arun, S.B., Kumar, P.V., 2016. Optimization of scum oil biodiesel production by using response surface methodology. Process Safety and

Environmental Protection 102, 667–672. https://doi.org/10.1016/j.psep.2016.05.026
Yıldızhan, Ş., Uludamar, E., Çalık, A., Dede, G., Özcanlı, M., 2017. Fuel properties, performance and emission characterization of waste cooking oil (WCO) in a variable compression ratio (VCR) diesel engine. European Mechanical Science 1, 56–62.
Zabala, S., Arzamendi, G., Reyero, I., Gandía, L.M., 2014. Monitoring of the methanolysis reaction for biodiesel production by off-line and on-line refractive index and speed of sound measurements. Fuel 121, 157–164. https://doi.org/10.1016/j.fuel.2013.12.056
Zhang, Y., Li, Y., Sun, S., 2024a. Unveiling the innovation: Optimized biodiesel production from emerging Acer truncatum Bunge seed oil using novel and highly effective alkaline ionic liquid catalyst. Chemical Engineering Journal 487. https://doi.org/10.1016/j.cej.2024.150603
Zhang, Y., Li, Z., Li, Y., Sun, S., 2024b. Biodiesel preparation from tiger nut oil utilizing a novel hydroxy-functionalized basic ionic liquid catalytic transesterification procedure: optimization, kinetics, and thermodynamic studies. Energy Convers Manag 303. https://doi.org/10.1016/j.enconman.2024.118182
Zhang, Y., Sun, S., 2023. A review on biodiesel production using basic ionic liquids as catalysts. Ind Crops Prod. https://doi.org/10.1016/j.indcrop.2023.117099
Zulqarnain, Ayoub, M., Yusoff, M.H.M., Nazir, M.H., Zahid, I., Ameen, M., Sher, F., Floresyona, D., Budi Nursanto, E., 2021. A comprehensive review on oil extraction and biodiesel production technologies. Sustainability (Switzerland) 13, 1–28. https://doi.org/10.3390/su13020788

Biodiesel production from waste cooking oils – Application of green chemistry principles to the multi-objective optimisation of alkaline transesterification

Abstract

In the present work, alkaline transesterification converted waste household cooking oil into biodiesel, a renewable alternative to fossil fuels. After characterising oil and choosing the independent variables of the reaction (methanol-to-oil molar ratio, catalyst concentration, temperature, and stirring), three dependent variables were selected to analyse biodiesel production globally, considering technical, energetic and environmental aspects. Therefore, biodiesel yield, energy intensity, and green chemistry balance were chosen as responses. This work considered four normalised green metrics with the best values close to 100% to calculate the green chemistry balance and the "greenness" of the reaction, providing a comprehensive view of the sustainability of biodiesel production. After obtaining an experimental plan using a central composite design, the process responses under different operating conditions were assessed. The optimal conditions were obtained by response surface methodology and optimisation tools in both a single-criterion approach for each response and a multi-objective approach. Moreover, the analysis of variance was performed to determine the significance of quadratic models and the effects of independent factors on each response. When the three responses were simultaneously optimised, the results showed a maximum ester yield of 83.3%, minimum energy intensity of 10.2 MJ/kg, and maximum green chemistry balance of 81.4% at methanol to oil molar ratio of 3, KOH catalyst concentration of 1.3 wt%, temperature of 50.7 °C and stirring of 350 rpm. Nevertheless, different results were obtained when a single performance criterion was used, indicating the importance of a global multi-objective approach to the process involving green chemistry principles and process performance optimisation.

Keywords: biodiesel, multi-objective optimisation, green chemistry, transesterification, waste

cooking oils, response surface methodology.

1. Introduction

The ASTM (American Society for Testing and Materials) standard defines biodiesel as an apolar mixture of alkyl esters (usually Fatty Acid Methyl Esters, FAME) with long chains of fatty acids. Over the past few decades, biodiesel has gained significant attention for its versatility in applications such as a phase change material (De Paola and Lopresto, 2021) and a green solvent (Knot he and Razon, 2017), as well as innovative uses like plasticiser and lubricant. However, its most prominent application is as a green alternative to conventional petrodiesel. Biodiesel offers several advantages, including reduced pollutant emissions and particulate matter, mitigation of global warming impacts, enhanced countries' energy independence, and positive effects on agriculture (De Paola et al., 2021a). Despite these benefits, the widespread adoption of biodiesel is limited by its high production price, low feedstock availability, fluctuating oil prices, and inconsistent policy support (Suhara et al., 2024). Moreover, biodiesel production from waste sources has gained attention as a sustainable alternative to avoid the environmental consequences of dedicated feedstock cultivation, such as deforestation and biodiversity loss, often associated with expanding plantations like palm oil in tropical regions (Ali Ijaz Malik et al., 2024). Given their established collection and processing infrastructure, this highlights the potential of waste materials like waste cooking oil (WCO) and animal fats as economically viable feedstocks.

Oil can be diluted, micro-emulsified or chemically converted by many technologies from more traditional pyrolysis and transesterification to less conventional methods such as reactive distillation and supercritical conditions, microwaves, ultrasound, membrane, plasma, etc. The advantages and disadvantages of each technique are summarised in Table 1 (Abbaszaadeh et al., 2012; Babadi et al., 2022; Bashir et al., 2022; Singh et al., 2020; Zulqarnain et al., 2021).

Table 1. Advantages and disadvantages of ~~different biodiesel production~~various ~~-~~techniques to reduce oil viscosity or produce biodiesel.

Production technologies	Advantages	Disadvantages
Dilution	Simplicity of the process.	Carbon deposit in the engine cylinder, ineffective combustion.
Microemulsion	Simplicity of the process.	Less volatile and stable fuel, higher viscosity.
Pyrolysis	Simplicity of the process and low emissions.	High installation cost, high carbon residue, lower purity, high temperature clinker requirement.
Transesterification	Biodiesel properties comparable to fossil diesel, ease of scale-up for industrial scale.	Low conversion efficiency, non-reusability of the catalyst.
Catalytic distillation	Simple separation of products.	The use of solvents and reaction rate are dependent on catalyst recovery.
Reactive distillation	The possibility of processing raw materials with a high content of free fatty acids, simplicity of the process, lower requirement for methanol, and simple separation of products.	High energy demand and process conversion are influenced by catalyst efficiency.
Microwave-assisted transesterification	High reaction speeds, low heat losses, high yield, higher biodiesel purity, and simple product separation.	Process conversion is strongly influenced by catalyst activity, and it is difficult to scale up commercially due to uncontrolled heating.
Ultrasound-assisted transesterification	High reaction speeds and yields; reduced energy consumption, quantity of catalyst, production cost, separation time, reaction temperature and alcohol/oil ratio.	Higher catalyst demand, soap formation, high cost, difficult scale-up.
Plasma-assisted transesterification	Very low reaction times, non-dependency on the catalyst, and absence of soaps.	Difficult control of the reaction mechanism. High cost.
Electrolysis-assisted transesterification	Low temperature, short reaction times, and the presence of water increase the yield. The presence of free fatty acids and water does not cause problems, and it is low-cost.	Sensitivity to high pH. Need to monitor the conductivity of the electrolyte constantly.
Magnetic particle-assisted transesterification	Not limited by the disadvantages of filtration, lower pressure heat, efficient separation	Agglomeration of magnetic catalysts, preliminary coating of organic catalysts.
Transesterification with supercritical fluids	High reaction speed, high conversion efficiency, absence of catalysts, no problems in free fatty acids and water presence, and no pre-treatment required.	High energy, high cost, high temperatures (250-400 °C), and high pressure (40 MPa) are required. It is not easy to scale up to an industrial scale.
Transesterification with ionic liquids	High chemical and thermal stability, high catalytic activity, low or negligible vapour pressure and flammability, lower toxicity than organic solvents, a wide range of applications, liquids at room temperature, and possible recyclability.	High synthesis costs, limitations in large-scale applications, non-biodegradability, high viscosity, and inconvenient separation.
Transesterification with eutectic solvents	Simplicity of preparation, high purity, low cost, absence of reactivity with water and toxicity, biodegradability.	Formation of a complex liquid-liquid interface, uncertainty about stability after prolonged uses and over the entire life cycle of the process.
Biocatalytic transesterification	Eco-friendly process, simplified product separation, recyclability of biocatalysts, high product quality.	High initial cost, inhibition by glycerol, complex immobilisation techniques, lower reaction rates.

Various researchers have given more attention to transesterification for producing biodiesel, as it has several advantages, such as the employment of various feedstocks, production of biodiesel with good fuel properties, reduction of fuel viscosity, miscibility of the biodiesel with any

proportion of fossil fuel, cost-effectiveness, and high conversion efficiency (Dwivedi et al., 2022; Mandari and Devarai, 2022). Transesterification is the conversion of triglycerides into biodiesel using alcohols (typically methanol or ethanol), as shown in Figure 1.

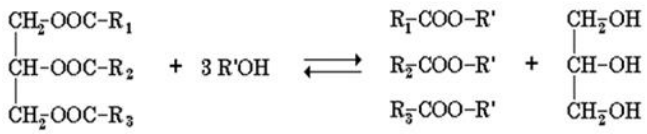

Figure 1. Transesterification of triglycerides with alcohol to produce biodiesel (methyl or ethyl–esters mixture) and glycerol (R1, R2, R3: long-chain fatty acids; R': short-chain carbon group).

Catalysts play a significant role in the transesterification process (Bohlouli and Mahdavian, 2021) and are classified as chemical (acid or alkali) and biological (enzymes) (Lopresto et al., 2019, 2015). The selection of any catalyst depends on the oil quality, quantity of FFA content in oil, operating conditions, catalyst activity required, cost, and availability (Mandari and Devarai, 2022). The chemical catalytic transesterification is industrially adopted and includes homogeneous or heterogeneous catalysis (Okechukwu et al., 2022). Homogeneous catalysts, distinguished in alkaline (such as potassium or sodium hydroxide) or acid (mainly sulfuric or phosphoric acid), are commonly used in commercialised biodiesel production as they possess high catalytic activity (Dwivedi et al., 2022). The alkaline reaction mechanism encompasses three distinct stages (refer to Figure 2). The initial stage involves an attack by the alcohol anion (alkoxide ion) on the carbonyl carbon atom of the triglyceride molecule, forming a tetrahedral intermediate. In the subsequent stage, the tetrahedral intermediate reacts with an alcohol, thereby regenerating the anion of the alcohol. The third and final stage entails the rearrangement of the tetrahedral intermediate produced during the second stage, which yields the fatty acid ester and a diglyceride.

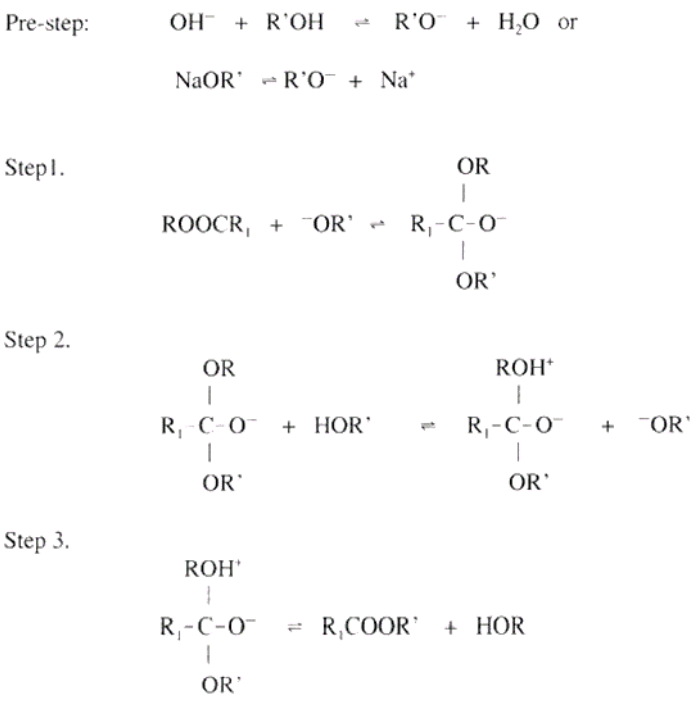

Figure 2. Alkaline transesterification mechanism of triglycerides.

Alkaline catalysts are usually used in the reaction due to their high availability, cost-effectiveness and lower corrosivity than acids. Moreover, they require moderate operating conditions, and the rate of base-catalysed reaction is about 4000 times higher than that of acid catalysis, with the same amount of catalyst used, which is why it is used more for industrial applications. Still, alkaline catalysis has technological limits related to the process's sensitivity to the reagents' purity and the presence of water in the starting oil, causing undesired hydrolysis and saponification reactions with consequent lower biodiesel yield and more difficult and expensive process downstream (Lopresto et al., 2025; Marchetti et al., 2007).

Acid-catalysed transesterification (Fig. 3) involves the protonation of the ester's carbonyl group, forming the carbocation (II). Following a nucleophilic attack by the alcohol, this produces the tetrahedral intermediate (III), which eliminates the alcohol to form the new ester (IV) and regenerate the catalyst H^+ (Pathak, 2015).

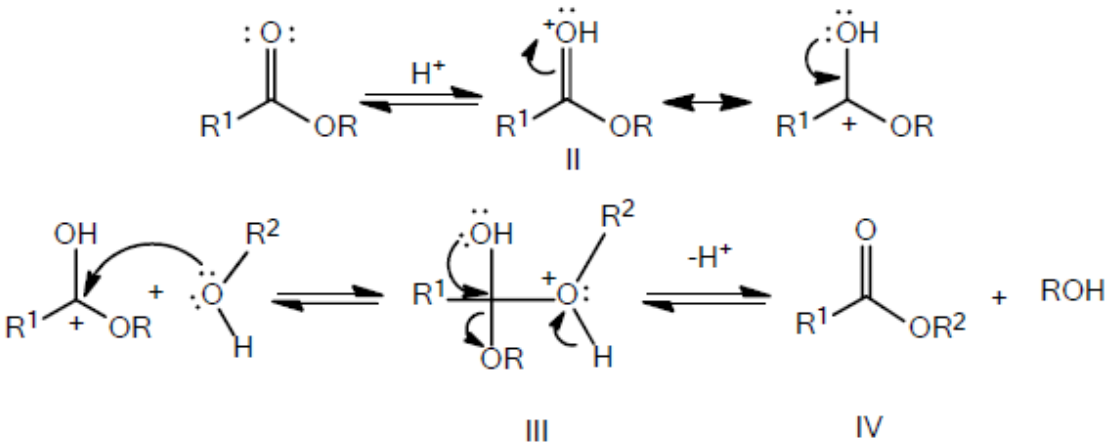

Figure 3. Acid transesterification mechanism of triglycerides.

Due to the low reaction rate, the higher temperature (55–80 °C) and the high alcohol/oil molar ratio required of 30:1, acid-catalysed transesterification has not gained the same attention as the alkaline process. Among the negative aspects, the corrosion of equipment, valves, and pipes in contact with the reaction mixture is added, resulting in a request for more constructive measures. However, acid catalysts do not give rise to the unwanted saponification reaction in the presence of free fatty acid (FFA) and water in the starting oil. Therefore, it is advisable to use acid catalysis with oils containing a high FFA content, possibly at a preliminary reaction stage (Lopresto, 2024). Although conventional alkaline homogeneous transesterification quickly leads to high triglyceride conversions at fast reaction rates, energy demand is high for the post-treatments, and product purification and catalyst recovery processes are complex, aqueous quenching, wastewater and loss of catalysts (Tan et al., 2016). Such critical issues can be overcome with heterogeneous catalysis, both basic (basic zeolites, alkaline earth metal oxides, hydrotalcites) and acidic (ZrO_2, cation-exchange resins, solid heteropoly acids, zeolites). They have high activity, high selectivity, reusability, easy separation from the products, and water tolerance properties (Ruhul et al., 2015). Moreover, they avoid soaps forming during the reaction and make the catalyst easily recoverable, but with possible leaching of active sites of the medium during the reaction and product contamination, catalyst deactivation, mass transfer limitation, lower yields

at higher reaction times and temperatures, low scalability, and high total costs (Gupta and Pal Singh, 2023; Mukhtar et al., 2022; Stoytcheva and Montero, 2011).

In order to decrease the cost of biodiesel product, some new oil feedstocks and catalysts have been developed such as basic ionic liquids (Zhang et al., 2024a, 2024b; Zhang and Sun, 2023) and low-cost liquid lipases(Sun et al., 2021; Sun and Li, 2020). Moreover, transitioning from the current technology based on homogeneous alkaline catalysis to a new approach based on heterogeneous catalysts is a fundamental challenge for lower-cost biodiesel production (Farouk et al., 2024). However, it is not mature for commercial application and is still under development. Therefore, homogenous alkaline transesterification is the most commonly employed technique in industrial biodiesel production from WCO, an economically viable feedstock derived from household, restaurant, and food-processing residues (Lopresto et al., 2024). Three catalysts are usually used for alkaline-catalysed transesterification: sodium hydroxide (NaOH), potassium hydroxide (KOH) and sodium methoxide (CH_3ONa). Most of the studies show that the best properties of biodiesel were obtained by using KOH as a catalyst (Darnoko and Cheryan, 2000; Dorado et al., 2004; Encinar et al., 2005; Karmee and Chadha, 2005; Meher et al., 2006; Ugheoke et al., 2007). Besides, some studies show the best results as fuel using NaOH (Felizardo et al., 2006; Foon Cheng and Hock Chuah, 2004; Oliveira et al., 2005; Vicente et al., 2004). In another study, they exhibited similar trends in converting triglycerides to esters, reaching a similar value of ester content in the product. Still, the amount of NaOH used was smaller than that of KOH and CH_3ONa for the same mass feedstock oil. Nevertheless, after the reaction and product separation, the product mixture was separated into two liquid layers for KOH. In contrast, a mixture of glycerol and soap in a solid state was formed for NaOH and CH_3ONa. Since the lower solid phase could not flow out directly from the bottom of the separation unit, using KOH as a catalyst is undoubtedly more convenient and straightforward since the glycerol layer in liquid state can be removed easily by directly outflowing from the bottom of the separation unit. For

this reason, KOH is commonly used to produce biodiesel using waste cooking oil (Leung and Guo, 2006).

Firstly, this study aims to optimise the operating conditions for converting household WCO into biodiesel using Response Surface Methodology (RSM) applied to a Central Composite Design (CCD)-based experimental plan. Optimising the parameters affecting the transesterification process is critical to improve biodiesel production efficiency. RSM provides the statistical framework for analysing experimental data collected using designs like CCD, by generating a response surface model. This mathematical relationship describes how input variables influence the response variable. CCD combines factorial and axial points, allowing for efficient exploration of the RSM with fewer experimental runs and helping estimate the nonlinearity of dependent variables, maximising information from experimental results. By using fewer runs, CCD helps reduce the overall cost and time associated with experimentation. The combination of CCD and RSM allows for identifying optimal conditions, leading to improved process or product outcomes. Together, they minimise experimentation time and costs, enhance process understanding, and enable prediction of responses. Although the optimisation of biodiesel production from WCO has been extensively studied, the reported results vary significantly due to the heterogeneity of raw materials, as summarised in Table 2.

155 **Table 2**. Optimisation of batch homogeneous alkaline transesterification from WCO by RSM since 2014.

Alcohol	Temperature [°C]	Alcohol-to-oil molar ratio	Amount of catalyst [% wt]	Mixing intensity [rpm]	Reaction time [min]	Yield of biodiesel [%]	Ref.
Methanol	24.44	6.52:1	0.78 (NaOH)	499.67	19.99	100	(Bobadilla et al., 2017)
	40	6:1 (v/v)	2 (NaOH)	-	180	95.71	(Adekoya et al., 2015)
	40	9:1	1 (NaOH)	300	90	83.6	(García-Moreno et al., 2014)
	52.7	7.54:1	0.875 (KOH)	266	70.2	99	(El-Gendy et al., 2015)
	55	8:1	0.6 (KOH)	-	80	92.43	(Jeyakumar et al., 2019)
	55	60 (% vol)	0.5 (KOH)	1000	90	93.3	(Milano et al., 2018b)
	57.50	8.5:1	0.25 (KOH)	600	180	93	(Razzaq et al., 2020)
	60	5:1	0.75 (KOH)	-	80	92	(Dubey et al., 2020)
	60	7.2:1	1.27 (KOH)	300	60	83.94	(Tacias-Pascacio et al., 2019)
	60-62	9.51-10.67:1	0.86-1.24 (KOH)	400	70-80	97.7-98.5	(Ayoola et al., 2016)
	62	4.5:1	1.2 (KOH)	600	75	93	(Yatish et al., 2016)
	62.75	6.05:1	0.77 (KOH)	-	72.63	93.124	(Özgür, 2021)
	65	3:1	0.55 (KOH)	-	45	95.28	(Gumahin et al., 2019)
	65	7.5:1	1.4 (KOH)	500	60	99.38	(Hamze et al., 2015)
	65	9:1	0.72 (NaOH)	-	45	92.05	(Atapour et al., 2014)
	65	15:1	5 (KOH)	700	150	95.40	(Ahmad et al., 2023)
	65	0.15:1 (v/v)	0.75 (NaOH) (%w/v)	800-900	90	97	(Kiran and Hebbar, 2021)
	73.8	6.58:1	1.13 (NaOH)	824.45	74.02	95.92	(Najafi et al., 2018)
Methanol	-	59.6 (% v/v)	0.774 (KOH)	600	7.15	97.65	(Milano et al., 2018a)
(microwave-	-	10:1	1.05 (KOH)	350	3	94	(Bajwa et al., 2024)
assisted)	50	7:1	0.65 (KOH)	8 s ON/22 s OFF (pulse time)	9.6	96.55	(Sharma et al., 2019)
	75	6:1	1 (KOH)	600	1	93	(Selvaraj et al., 2019)
Methanol (+ novel solvent)	36.83	4:1	0.5 (KOH)	1000	10	94.83	(Bhonsle et al., 2022)
Methanol (ultrasound-assisted)	50	6:1	0.5 (KOH)	-	10	98	(Oza et al., 2021a, 2021b)
Methanol (ultrasound-assisted + co-solvent)	40	6:1	2 (KOH)	7 s ON/1 s OFF (pulse time)	-	98.5	(Bai et al., 2022)

Methanol (hydrodynamic cavitation)	55	12:1	14 (KOH) [g]	-	42.5	100	(Halwe et al., 2021)
Ethanol	60	6:1	1 (Na ethoxide)	600	180	96.5 (%FAEE in biodiesel)	(Ortega et al., 2021)
	60	12.9:1	1.62 (KOH)	200	60	89.75	(Danane et al., 2022)
	64.96	7.005:1	1.25 (NaOH)	592.18	88.02	95.53	(Najafi et al., 2018)
Ethanol (microwave-assisted)	70	-	1 (KOH)	-	200 s	97	(Thirugnanasambandham et al., 2017)

156

In literature, reaction time, alcohol type, alcohol-to-oil molar ratio, reaction temperature, catalyst amount, and mixing intensity were usually optimised by RSM to obtain the maximum biodiesel yield from WCO. Nevertheless, the highest yield does not guarantee the greenest process. Indeed, to ensure the sustainability of a process or product and promote the transition from a linear economy to a circular economy, it becomes essential to use the principles of so-called green chemistry and green engineering, which have been established in the last decades (Mulvihill et al., 2011). Therefore, addressing a more comprehensive optimisation approach involving green chemistry principles is necessary, considering consumed reagents, non-recovered solvents, and energy consumption. Despite this, very little attention has been paid to a broader vision of the process, which considers the biodiesel yield, energy aspects, and environmental sustainability (De et al., 2019; Outili et al., 2020; Patle et al., 2014). Therefore, we chose a multi-objective approach to investigate the alkali-catalysed transesterification from WCO. The effect of the temperature, the methanol-to-oil molar ratio, the catalyst amount, and the stirring on the WCO transesterification was investigated. Yields, energy consumption, and green metrics were experimentally obtained, and quadratic models related each studied response to the four factors. The significance of the factors and models was determined by analysis of variance (ANOVA) with the Minitab 18 software tool. Finally, the operating conditions were analysed by RSM, and the multi-objective optimisation was compared with single-objective optimisation.

2. Experimental

2.1 Chemicals

Honeywell provided acetone (>99.8%), acetonitrile (>99.9%), diethyl ether (99.8%), ethanol (>98%), and methanol (99.8%). VWR Chemicals supplied sodium hydroxide (99.2%) and potassium hydroxide (85.5%), and Fluka Chemika provided phenolphthalein (>99%).

2.2 Waste cooking oils

WCO is a very heterogeneous feedstock with various properties depending on the type of virgin

oil and frying procedure. The WCO used in this experiment was waste oil from domestic cooking operations with a mixture of olive oil, sunflower seed oil, and peanut oil, used for frying once or twice. Firstly, solid residues of foods in frying oil were removed by a first gross filtration with a steel cooking filter and a subsequent vacuum filtration. Then, the acidity and moisture were measured by titration. Specifically, the content of FFA was determined by acid-base titration according to EN 14104 (Özbay et al., 2008), with a titrant solution of NaOH 0.01 M, a 50:50 solution by volume of diethyl ether and ethanol (to which oil is added), and phenolphthalein as an indicator. In detail, 2 g of oil and 1 g of phenolphthalein per 100 ml of solvent were solubilised, and the titrant solution was added to the point of toning with the appearance of a pink colour. Acidity (A), the amount of sodium hydroxide neutralising the fatty acids contained in one gram of sample, was obtained by Equation 1 or 2.

$$A\ (\%) = \frac{C_{NaOH} * V_{NaOH} * MW_{OA}}{1000 * m_{sample}} * 100 \quad (1)$$

$$A\ (\frac{\text{mg KOH}}{\text{g sample}}) = \frac{C_{KOH} * V_{KOH} * MW_{KOH}}{m_{sample}} \quad (2)$$

where C [mmol/mL] was the concentration of NaOH or KOH in the titrant solution, V [mL] was the volume of the titrant solution added up to the point of colour change, MW_{OA} was the molecular weight [mg/mmol] of oleic acid (OA) used as a reference, MW_{KOH} was the molecular weight [mg/mmol] of potassium hydroxide (KOH) equal to 56.1, and m [g] was the mass of the oil sample used for the titration.

The presence of water was measured by a coulometric titration in the MKC-501 Karl Fischer Moisture Titrator (Coulometric) from Kyoto Electronics (KEM). After a pre-titration (injecting 5 mL of catholyte into the inner burette and 150 mL of anolyte into the titration cell), a sample of oil is injected into the titration cell. Then, electrolysis begins, and titration is carried out. In the Karl Fisher titration, the iodine is generated by electrolysis of an iodide contained in the solvent loaded into the titration cell, to which the sample for analysis is added after weighing.

The electrolytic process and the subsequent quantitative measurement of iodine, generated stoichiometrically as a function of the water content in the sample, are made possible by an electrolytic cell and a double electrode of Pt. Finally, the detected moisture and titrated water amounts are displayed.

The fatty acid composition of the WCO determines the characteristics of the oils and, therefore, of the obtained biodiesel. The fatty acids of the glycerides present in the oil were converted into the respective methyl esters by esterification. A Clarus 500 gas chromatograph (GC) with the N9316354 Elite-FFAP Capillary Column (30 m x 0.32 mm I.D. x 0.25 µm) from PerkinElmer was used to evaluate the content of the esters and methyl esters of fatty acids using the UNI EN 14103 method. The mean molecular weight of the oil (MW_{oil}) was calculated according to the fatty acid analysis by Equation 3 (Atapour et al., 2014):

$$MW_{oil} = 3 \cdot \sum(MW_i \cdot x_i) \quad (3)$$

where MW_i and x_i are molecular weight and mass fraction of the i^{th} fatty acid, respectively.

2.3 Experimental plan

Based on the literature (De Paola et al., 2021a; Issariyakul and Dalai, 2012; Pisarello et al., 2018), four operating parameters were chosen to vary to evaluate the effect on biodiesel yield, energy consumption, and process greenness. The four independent variables were methanol/oil molar ratio M/O (3; 6; 9), KOH content (1%; 1.5%; 2%), temperature T (45 °C; 50 °C; 55 °C) and stirring S (350 rpm; 400 rpm; 450 rpm). An experimental plan (Table 3) has been developed based on a Central Composite Design (CCD) through the Minitab 18 software tool.

Table 3. An experimental plan was developed using the Minitab® software tool.

Run Order	M/O	%KOH	T (°C)	S (rpm)
1	9	2	55	450
2	9	1	55	450
3	6	1.5	50	400
4	9	1	55	350
5	3	1	55	450
6	9	1	45	450
7	3	1	45	350
8	9	1	45	350

9	9	2	45	450
10	3	2	45	350
11	3	2	55	350
12	3	2	45	450
13	3	1	45	450
14	3	1	55	350
15	9	2	45	350
16	3	2	55	450
17	6	1.5	50	400
18	9	2	55	350
19	6	1.5	45	400
20	6	1.5	50	350
21	6	1.5	50	400
22	6	1.5	50	400
23	6	1.5	50	450
24	6	2	50	400
25	3	1.5	50	400
26	6	1.5	55	400
27	6	1	50	400
28	9	1.5	50	400

2.4 Reaction

The reaction tests were carried out in batch mode in a system consisting of a magnetic heating plate, a glass three-necked round-bottom flask, and a condensation column connected to a Crioterm thermostat bath set to a cooling water temperature of 20 °C for the refrigerant action of the condenser in a closed loop. The flask acted as a reactor and was equipped with three necks: a side neck was intended for the insertion of a thermocouple for measuring the temperature; the other lateral neck was used for the insertion of reagents and the sampling of the reaction mixture to be analysed; the third, finally, was the upper one, used for connection with a six-bubble condenser for the recovery of methanol evaporated during the reaction, which was then condensed and made to fall back into the reaction mixture (Fig. 4). The stirring was guaranteed by a magnet placed in rotation by the magnetic action of the heating plate on which the flask was placed.

Figure 4. Batch reaction system.

The oil was preheated inside the flask until the reaction temperature was reached. According to Table 3, the stirring speed (350-450 rpm) and temperature (45-55 °C) values varied in each test. Then, the solution formed by methanol and potassium hydroxide, previously prepared, was added to the oil. Each reaction test was conducted for 90 minutes. Samples of the reaction mixture were taken at predefined times and stored in the freezer at -20 °C until analysis. The concentrations of triglycerides and esters in reaction mixture were analysed by High-Performance Liquid Chromatography (HPLC), model Jasco 4000, column Adsorbosphere HS C18 (Alltech, 250 mm x 4.6 mm x 5 μm), mobile phase acetone/acetonitrile 70:30 v/v, flux 1 mL/min, injection loop 20 μL, pump mode Single Pressure Gradient, detector RI, analysis time 40 min. This is a common method for separating esters, monoglycerides, diglycerides, and triglycerides, which have different retention times. Chromatograms were ~~studied~~ analysed using the ChromNav 2.0 software, and the peaks of esters, monoglycerides, diglycerides, and triglycerides were identified using methyl oleate, monoolein, diolein, and triolein as standards, respectively.

2.5 Product separation and biodiesel washing

After the reaction, each reaction mixture was transferred for 24 h to a separating funnel to separate esters and glycerol into two distinct layers due to their different densities. After the separation, the masses of the biodiesel and glycerol phases were measured. Then, crude biodiesel was repeatedly washed with 30%v/v of distilled water. This step was crucial to removing excess glycerol, methanol or potassium hydroxide. Initial washing caused the water to turn murky; thus, it was left to settle for an hour and was centrifuged at 4000 rpm for 10 minutes. The washed biodiesel was then extracted from the biodiesel–water mixture. The washing process was repeated until the water became clear. The pure biodiesel was extracted and stored in a conical flask.

The yield of crude biodiesel is defined in Equation 4 (Kerras et al., 2018):

$$Y_{\text{crude biodiesel}} = \frac{\text{mass of crude biodiesel (g)}}{\text{mass of oil (g)}} \quad (4)$$

where "mass of crude biodiesel" is the mass of the ester phase after the separation from the glycerol phase; "mass of oil" is the mass of oil used as a reagent.

The yield of esters after 90 minutes considers the mass percentage of esters in crude biodiesel based on HPLC analyses (Equation 5).

$$Y_{\text{esters}} = Y_{\text{crude biodiesel}} \cdot \%\text{esters}_{\text{HPLC}}/100 \quad (5)$$

where $Y_{\text{crude biodiesel}}$ is defined in Equation 4.

2.6 Analysis of crude biodiesel

The progress of the reaction mixture's refractive index was found to be correlated with the oil's conversion into biodiesel (Zabala et al., 2014). This analysis, carried out on biodiesel after its separation from glycerol by a portable digital refractometer (Hanna Instruments), allows for the online monitoring of the reaction progress and data acquisition in a relatively simple, reliable, and cost-effective manner (Tubino et al., 2014).

Moreover, crude biodiesel was analysed using the Turbiscan® instrument for 15 minutes at 25

°C, with scans every minute to assess its stability and the possible phenomena of phase separation and destabilisation. Turbiscan® is based on multiple light scattering and used to detect up to 200 times more rapidly than the human eye destabilisation phenomena, such as sedimentation, coalescence, flocculation, and creaming, providing guidance on the stability of the solution analysed (De Paola et al., 2021b, 2016; Maria Gabriela De Paola et al., 2017; M. G. De Paola et al., 2017). Graphs show the trends of backscattering and transmission in ordinate and the cell's height in abscissa. The first profile is displayed in blue, and the last one is in red. Graphs are usually in reference mode, so the first profile is subtracted from all other profiles to optimise variations.

Finally, biodiesel was characterised as follows. The presence of water was measured by MKC-501 Karl Fischer Moisture Titrator (Coulometric) from Kyoto Electronics (KEM). The iodine value (IV) is the mass of iodine absorbed by the sample under the conditions specified in international standard EN 14111. The iodine value of biodiesel was evaluated by dissolving a biodiesel sample in the solvent (50:50 by weight of cyclohexane and acetic acid) and adding the Wijs reagent containing iodine mono-chlorinate to acetic acid. After a certain period, a solution of potassium iodide and water was added, proceeding with the titration of the iodine released with a sodium thiosulphate solution until the blue stain appeared in the titrated solution. The impact of sulphur and phosphorus on engine integrity and catalyst life is crucial to our research. We measured this using the optical emission spectrometer Optima 7000 DV (PerkinElmer), equipped with a Polyscience NO772035 chiller and a FIAC EwispireVS204 compressor, to provide valuable insights for the field of renewable energy. The cold filter plugging point (CFPP) serves as a crucial index, indicating the temperature at which a standard test filter starts clogging due to the formation of a gel or crystal under specified test conditions. This measurement, determined with dedicated equipment (New Lab 200), is a key factor in assessing biodiesel quality. Esters and methyl esters of fatty acids were measured using the UNI EN 14103 method

by Clarus 500 gas chromatograph (GC) with the N9316354 Elite-FFAP Capillary Column (30 m x 0.32 mm I.D. x 0.25 µm) from PerkinElmer.

2.7 Energy consumption measurement

As part of our comprehensive study, we measured the reaction system's energy consumption. The magnetic heating plate and the cooling system were connected to a power meter (branded Maxcio, model PM01, maximum power 3680 W) to assess the energy absorbed by the reaction system, recorded at 15-minute intervals. These data were crucial in determining the energy intensity (EI) and the energy consumed after 90 minutes per mass of the desired product, biodiesel (Equation 6) (Calvo-Flores, 2009).

$$\text{EI}\ [\text{MJ/kg}] = \frac{\text{total energy}}{\text{mass of desired product}} \quad (6)$$

2.8 Green metrics evaluation

Green chemistry is the design of chemical products and processes that reduce or eliminate the use and generation of hazardous substances throughout their lifecycles (design, manufacture, use, and end of life) according to 12 principles (Anastas and Warner, 1998). To apply and evaluate these principles objectively, several crucial parameters – known as green metrics – have been defined to determine biodiesel production's sustainability and environmental impact and assess the best solution between alternatives. Six green mass-based metrics were evaluated in this work: environmental factor (E factor, Eq. 7), atom economy (AE, Eq. 8), atom efficiency (AEff, Eq. 9), process mass intensity (PMI, Eq. 10), process mass productivity (PMP, Eq. 11), reaction mass efficiency (RME, Eq. 12), stoichiometric factor (FSt, Eq. 13) (Calvo-Flores, 2009; Dicks and Hent, 2015; Lapkin and Constable, 2009; Sheldon, 2018).

$$\text{E factor} = \frac{\sum m_{\text{waste}}}{m_{\text{desired product}}} \quad (7)$$

$$AE = \frac{n_{desired\ product} MW_{desired\ product}}{\sum n_{reagents} MW_{reagents}} \quad (8)$$

$$AEff = AE \cdot Y_{reaction} \quad (9)$$

$$PMI = \frac{\sum m_{reagents}}{m_{desired\ product}} = E\ factor + 1 \quad (10)$$

$$PMP = \frac{1}{PMI} \cdot 100 \quad (11)$$

$$RME = \frac{m_{desired\ product}}{\sum m_{reagents}} = \frac{1}{1+E\ factor} \quad (12)$$

$$FSt = 1 + \frac{\sum m_{reagents\ in\ excess}}{\sum m_{stoichiometric\ reagents}} \quad (13)$$

In our case, the desired product is biodiesel. The waste comprises by-products (glycerol) and non-reacted reagents, oil and methanol. The reagent in excess is methanol.

All green metrics are normalised to have a value between 0 and 1, corresponding to the worst and ideal situations. The E factor is the only parameter for which the optimal situation is 0 and the worst situation is 1. Therefore, to unify the impact of all the used parameters, a new environmental factor is defined by complementing 1 as in Equation 14 (Naveenkumar and Baskar, 2021).

$$E' = 1 - E\ factor \quad (14)$$

Moreover, the stoichiometric factor is 1 when reagents are in stoichiometric proportions; otherwise, it is higher than 1. A new stoichiometric factor is defined as

$$FSt' = \frac{1}{FSt} \quad (15)$$

The green chemistry balance estimates the reaction's greenness, which is the mean value of four normalised green metrics (E', AEff, PMP, FSt'). The best value is close to 1 (or 100%).

A graphical representation of the results in an Excel radar chart evidenced the reaction's green

346 character.

347 ***2.9 Statistical analysis***

348 Statistical analysis was performed by the Minitab 18 software tool.

349 The one-way analysis of variance (ANOVA) was performed with a significance level of 0.05 to
350 assess which parameters and combinations of these most affect each response (yield of reaction,
351 energy consumption, green chemistry balance). A full quadratic model (Equation 16) was
352 generated by setting the following parameters: factors = 4, replicates = 1, α = 1, cube points =
353 16, centre points in cube = 2; axial points = 8, centre points in axial = 2 ("All statistics for Create
354 Response Surface Design (Central Composite)," 2023). It correlated each studied response with
355 the four factors as follows:

356 $$R = a_0 + \sum_{i=1}^{4} a_i X_i + \sum_{i=1}^{4} a_{ii} {X_i}^2 + \sum_{i=1}^{4} \sum_{j=1}^{4} a_{ij} X_i X_j \quad (16)$$

357 where R is the response, a_o is the intercept term, a_i are the linear coefficients, a_{ii} are the quadratic
358 coefficients, a_{ij} are the interactive coefficients, X_1 is M/O, X_2 is %KOH, X_3 is T and X_4 is S.

359 A probability (p-test) [50] confirmed the significant condition with a Pareto graph, together with
360 a Fisher test (F-test) evaluating the significance of the model and its factors in the ANOVA. The
361 Pareto Chart of the standardised effects allows identifying the most statistically significant
362 factors and their combination with each response. The red line indicates which effects are
363 statistically significant.

364 The values of p-test, F-test, total degrees of freedom (DF), adjusted sum of squares (Adj SS) and
365 adjusted mean squares (Adj MS) were provided by the Minitab 18 software.

366 Then, residual plots confirm the validity of the experimental tests, as described below. *Normal*
367 *Probability Plot* identifies deviations from normality and any anomaly in the values from the
368 experimental tests. *Versus Fits* shows an analysis of the residuals, i.e., the difference between the

value obtained from the experimental values and the estimate through a regression analysis. The *histogram* is the diagram of the residual values *vs* the frequency and evaluates whether the variance follows the normal distribution. *Versus Order* presents the values of the residuals on the ordinates and the order in which the data were collected on the abscissas.

In addition, the factors or combinations of them that most influence the process and their optimal values were obtained by RSM (Myers et al., 2016) and contour diagrams, two-dimensional diagrams in which different colours indicate the response to different factors.

Finally, a multi-objective optimisation was performed considering the effects of temperature, molar alcohol to oil ratio, stirring, and catalyst amount on biodiesel yield, green chemistry balance, and energy consumption.

3. Results and discussion

3.1 Waste cooking oils

Homogeneous alkaline transesterification is usually recommended for WCO with free fatty acid content below 0.5% in anhydrous conditions. Based on the measured low free fatty acid content of the WCO (<0.5%) and not detected water, a homogeneous alkaline transesterification was pursued for biodiesel synthesis without any pre-treatment. The GC results are given in Table 4.

Table 4. Fatty acid composition and esters produced of waste cooking oil (GC analysis).

Fatty acid	%
Myristic (C14:0)	0.1
Palmitic (C16:0)	10.4
Palmitoleic (C16:1)	0.7
Stearic (C18:0)	3.0
Oleic (C18:1)	57.7
Linoleic (C18:2)	25.0
Linolenic (C18:3)	0.6
Arachidic (C20:0)	0.5
Eicosenic (C20:1)	0.5
Behenic (C22:0)	0.8
Erucic (C22:1)	0.1
Lignoceric (C24:0)	0.4
Nervonic (C24:1)	0.1

Esters C14-C24	95.4
Total esters	96.7
Total saturated fatty acids	15.2

The primary fatty acids are oleic, linoleic, and palmitic, with prevalent oleic acid as expected in olive oil (Blekas et al., 2006). The amount of esterifiable fatty acids exceeds 95%, consistent with domestic WCO characterisation. Domestic frying is usually carried out for a few minutes and a maximum of 2-3 reuses, so oil degradation is limited. The molecular weight of WCO was estimated at 838 g/mol.

3.2 Reaction

The 28 experiments proposed by the CCD (Table 3) were performed following the above experimental protocol. The percentage of esters and triglycerides in relation to the total mass of glycerides and esters after 90 minutes of reaction is given in Table 5. The lowest percentage of esters was obtained in test 15 at the lowest values of stirring (350 rpm) and temperature (45 °C) but at the highest value of catalyst quantity (2%) and molar methanol/oil ratio (9). The highest percentage of esters was obtained in test 4 with the lowest values of stirring (350 rpm) and catalyst quantity (1%) and the highest values of temperature (55 °C) and methanol/oil ratio (9). The effect of each variable on biodiesel yield is well-known and optimised in literature. Although the stoichiometric methanol-to-oil ratio (M/O) is 3:1, the reversible transesterification requires methanol excess to be effective towards the ester production by shifting the equilibrium to the expected product. A M/O value below 5:1 is insufficient and gives low yields. Most literature finds the optimum molar ratio between 5:1 and 7:1. A further increase of the molar ratio to 9:1 or 12:1 is often associated with a decrease in the biodiesel yield, probably because of the catalyst deactivation by the excess methanol. Moreover, an unnecessary excess of methanol complicates the separation between biodiesel and glycerol after the reaction (Hoque et al., 2011). In contrast, some researchers (see Table 2) considered an optimal M/O ratio higher than 6:1, up to 15:1. This depends on the interactions with other operating conditions. As regards the catalyst concentration, its increase leads to higher biodiesel production. Still, the biodiesel yield declines

significantly when the catalyst concentration becomes higher than a particular value due to the formation of fatty acid salts (soap) (Hoque et al., 2011; Leung and Guo, 2006). As evident in Table 2, most optimal values are in the range 0.5-1.5%wt when KOH is used as an alkaline catalyst, but lower (e.g. 0.25%) (Razzaq et al., 2020) and higher (e.g. 5%) (Ahmad et al., 2023) values were found as optimal. Transesterification can occur at different temperatures ranging from ambient temperature to a temperature close to the boiling point of methanol (68 °C at atmospheric pressure). A higher reaction temperature generally speeds up the reaction and increases the biodiesel yield in a shorter reaction period due to the reduction in the viscosity of oils (Hoque et al., 2011). However, some studies observed that an increase in reaction temperature beyond the optimal level of 55-60 °C led to decreased biodiesel yield: higher reaction temperature accelerated the saponification of the triglycerides and increased volatility and miscibility (Abbah et al., 2016; Leung and Guo, 2006). Finally, the reaction rate of transesterification increases with increasing mixing degree (Leung and Guo, 2006). On the other hand, a higher stirring speed favours the formation of soap (Mathiyazhagan and Ganapathi, 2011).

Therefore, each operating condition influences the biodiesel yield in different ways. The different results found in this manuscript and the literature depend on how the levels of the investigated variables interact.

3.3 Separation of biodiesel and glycerol

After a few minutes, the separation between the upper phase, consisting essentially of biodiesel (golden coloured), and the lower phase, composed mainly of glycerol (dark brown), was already evident (Fig. 5).

Figure 5. The reaction mixture is separated in a funnel. The yellow upper phase consists of crude esters, and the brownish lower phase consists of crude glycerol.

After the separation, the crude biodiesel was extracted and transferred to another conical flask. Then, the yields of crude biodiesel and esters were calculated and shown in Table 5. The highest yield was reached in test 4 at 55 °C, 350 rpm, with a M/O of 9 and 1% of catalyst. The maximum yield in esters was 89.43% (compared to the initial oil mass) in Test 4. As reported in Table 2, this value is lower than some reported data in the literature (Ayoola et al., 2016; El-Gendy et al., 2015; Hamze et al., 2015), but it is higher than other optimised results (García-Moreno et al., 2014; Tacias-Pascacio et al., 2019). The GC analysis revealed that the total fraction of oil that could be esterified is 96.7%. Then, the actual yield of esters compared to the effectively convertible oil is 92.5%. This value is in accordance with most previous findings, with optimised yields typically in the range of 92-95% (see Table 2). The variation in biodiesel yield for different fat/oil sources could be mainly due to the variation of FFA and water contents in various types of oils. This difference in FFA content causes the catalyst to react differently towards the oils (Verma and Sharma, 2016).

3.4 Analysis of biodiesel

Biodiesel was characterised by refractometry. Fig. 6 shows the Brix degrees of crude esters, measured by a digital refractometer, for all experimental tests.

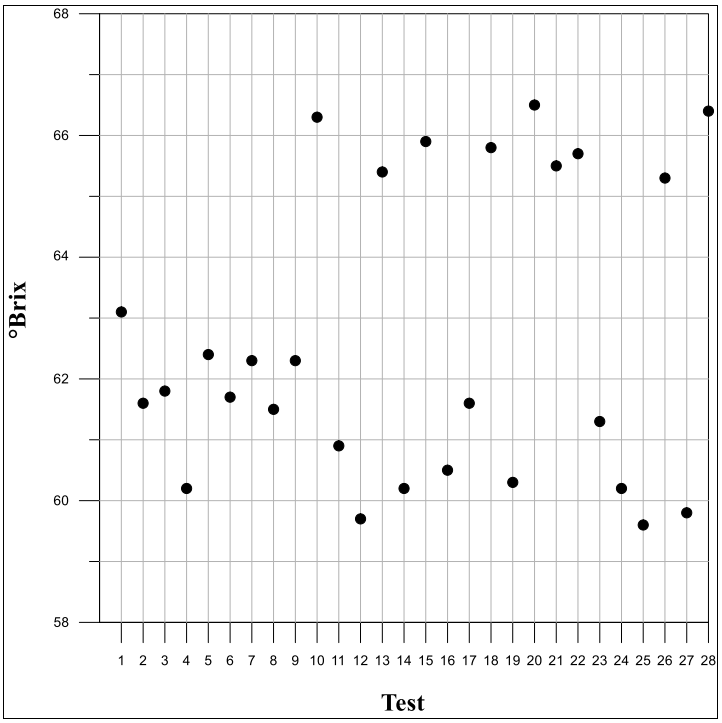

Figure 6. Brix degrees of crude esters after a 90-minute reaction and separation in a funnel.

The minimum value of °Brix of esters is about 60, corresponding to a refractive index (nD) of 1.44, corresponding to conversion values of waste oil greater or equal to 85% (Zabala et al., 2014). This result is following previous literature (Kerras et al., 2018). In addition, when the Brix value was higher than 65 (tests 10, 13, 15, 18, 20, 21, 22, 26, 28), the corresponding refractive index was 1.45, in turn corresponding to low conversions and yields (<85%).

Moreover, Turbiscan analysis was functional in analysing the product stability and comparing sedimentation and centrifugation to separate reaction products.

Centrifugation leads to a clear separation between the phases, and the biodiesel phase is clear and relatively stable, as evident from the analyses by Turbiscan (Fig. 7a).

After product separation by decanting in a separating funnel, the biodiesel sample was unstable and turbid after 60 minutes (Fig. 7b) but clear and stable after 24 hours (Fig. 7c), with a transmittance profile comparable to that obtained after centrifugation. This confirms the literature on waiting about a day for efficient decantation.

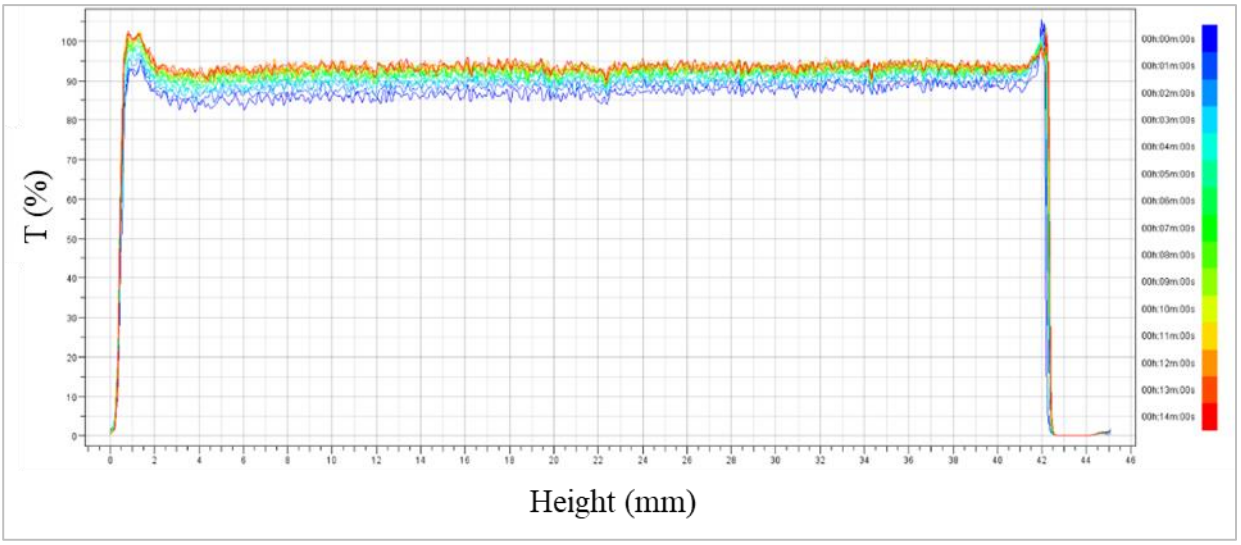

(a)

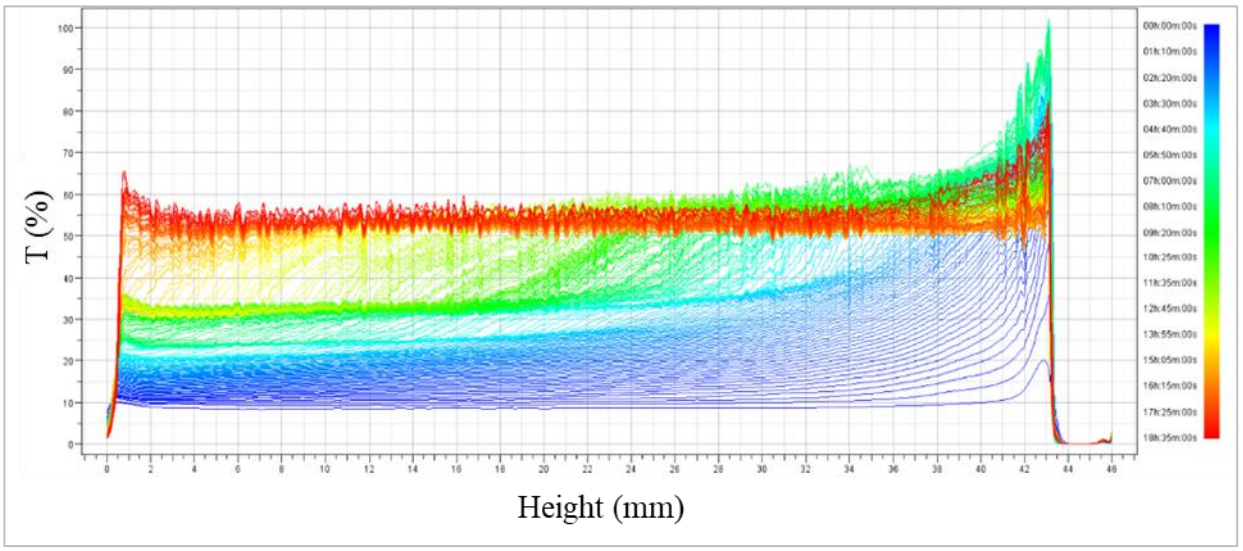

(b)

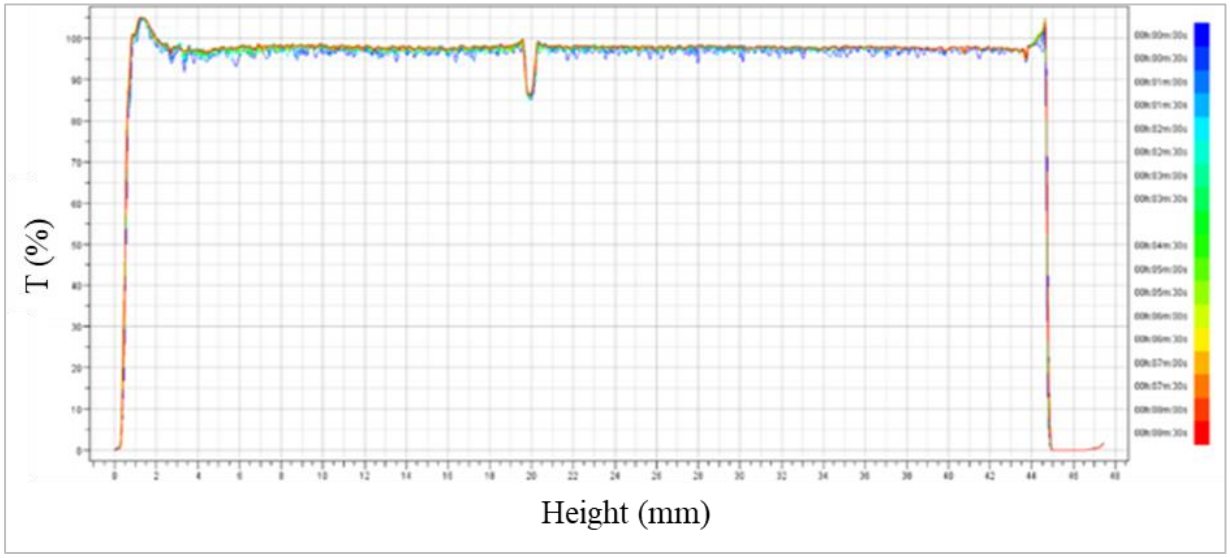

(c)

Figure 7. Transmittance profiles by Turbiscan for a biodiesel sample after separation from glycerol by centrifugation (a); after 60 minutes of separation from glycerol by sedimentation in a separating funnel (b); after 24 hours of separation from glycerol by sedimentation in a separating funnel (c).

Finally, biodiesel was characterised for water content, iodine value, sulphur and phosphorus content, cold filter plugging point, and fatty acid composition.

The sulphur content of a fuel affects engine wear and deposit formation. It must not exceed 10 ppm for EN 14214, with two standard values, S15 and S500, for ASTM D6751. The S15 sulphur content standard allows a maximum of 15 ppm, whereas the S500 sulphur content standard permits a maximum of 500 ppm. When animal fats and waste vegetable oils are utilised for biodiesel production, the sulphur content is likely higher due to sulphur-containing compounds such as proteins (Alptekin et al., 2014). Nevertheless, no sulphur traces were detected in this study.

Furthermore, no soaps, water, or traces of phosphorus were found in the biodiesel samples.

As the iodine value depends solely on the source of the vegetable oil, the biodiesel esters derived from the same oil should exhibit similar iodine values. Conversely, the iodine value ought to remain unaffected by the conversion process and, therefore, should not vary with the yield of esters. The iodine value of the produced methyl esters was approximately 96, consistent with literature that shows values ranging from 73.2 to 99.4 for WCO-derived biodiesel. It aligns with the biodiesel fuel standard within the limits set by legislation, which stipulates a maximum permissible iodine value of 120. Therefore, the biodiesel produced exhibited a low tendency for oxidation.

The CFPP characterises a fuel's cold-flow operability, as it directly influences its utility, particularly in cold climate conditions. Biodiesel has a CFPP value of -4 °C, rendering it suitable for temperate winter climates, in line with existing literature and compliant with standard EN 14214, which sets limits at 4 °C in summer and 1 °C in winter (Yıldızhan et al., 2017).

The composition of fatty acids in biodiesel can indicate significant fuel properties, particularly the cetane number, which is determined by the fatty acids' structure, chain length, and bonding (Kolakoti et al., 2021). Since the transesterification reaction does not affect the fatty acid composition (Alptekin et al., 2014), the fatty acid profile of biodiesel was the same as that of the oil (Table 4) and other biodiesel derived from WCO. For instance, Park et al. produced biodiesel containing 64.9% methyl oleate and 20.1% methyl palmitate, values that are very close to those obtained in this study, which were 57.7% and 25.0%, respectively (Park et al., 2019). The low amount of saturated esters (15.1%) confirms the good low-temperature characteristic of biodiesel, which does not tend to solidify during the winter in temperate climate regions.

3.5 Energy consumption

Figure 8a shows the cumulative power and energy the reaction system consumed after 90 minutes. It is immediately clear that the condition at which the highest yields of crude biodiesel and esters are obtained (test 4) is also the most energy-consuming. Nevertheless, it is not necessary to wait for all tests for 90 minutes to consider the achievement of the reaction equilibrium. Therefore, the power and energy values consumed until the moment the concentration of esters can be regarded as constant (an increase of less than 2 percentage points after 15 minutes) are reported in Fig. 8b.

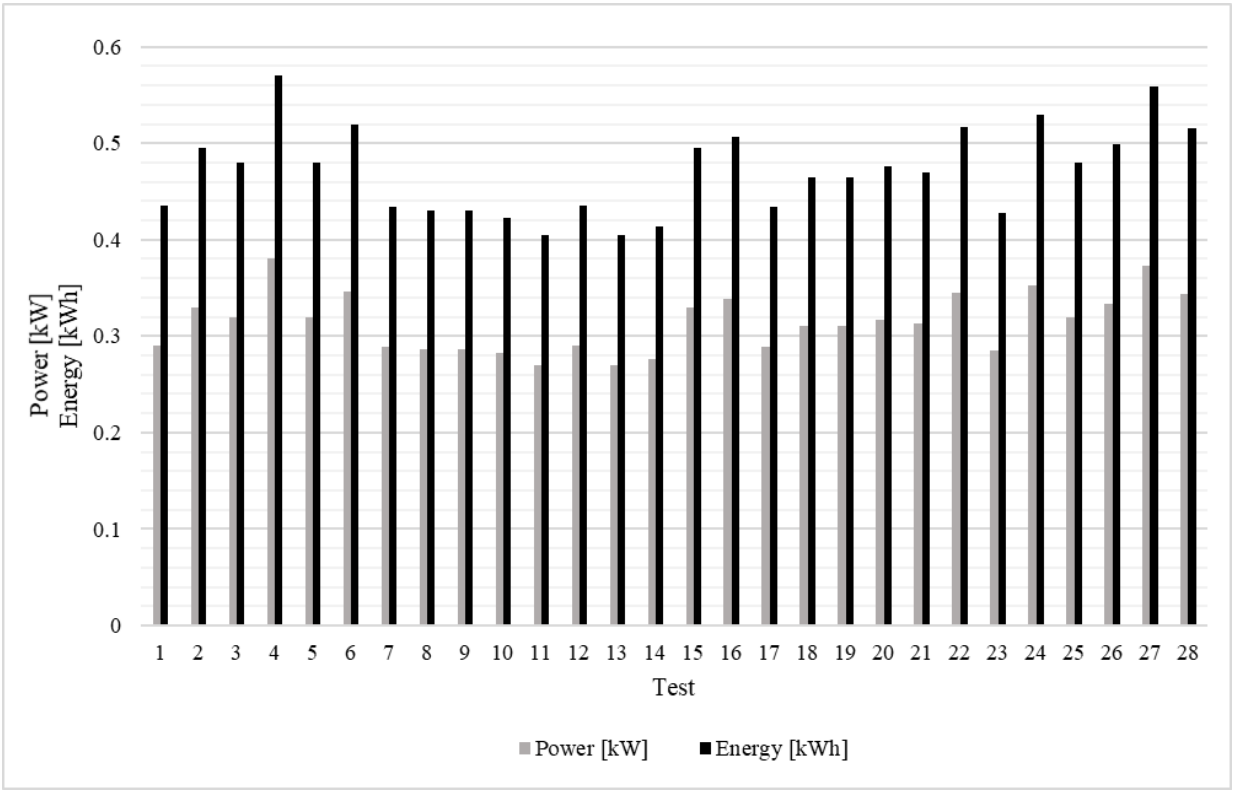

515

516 **(a)**

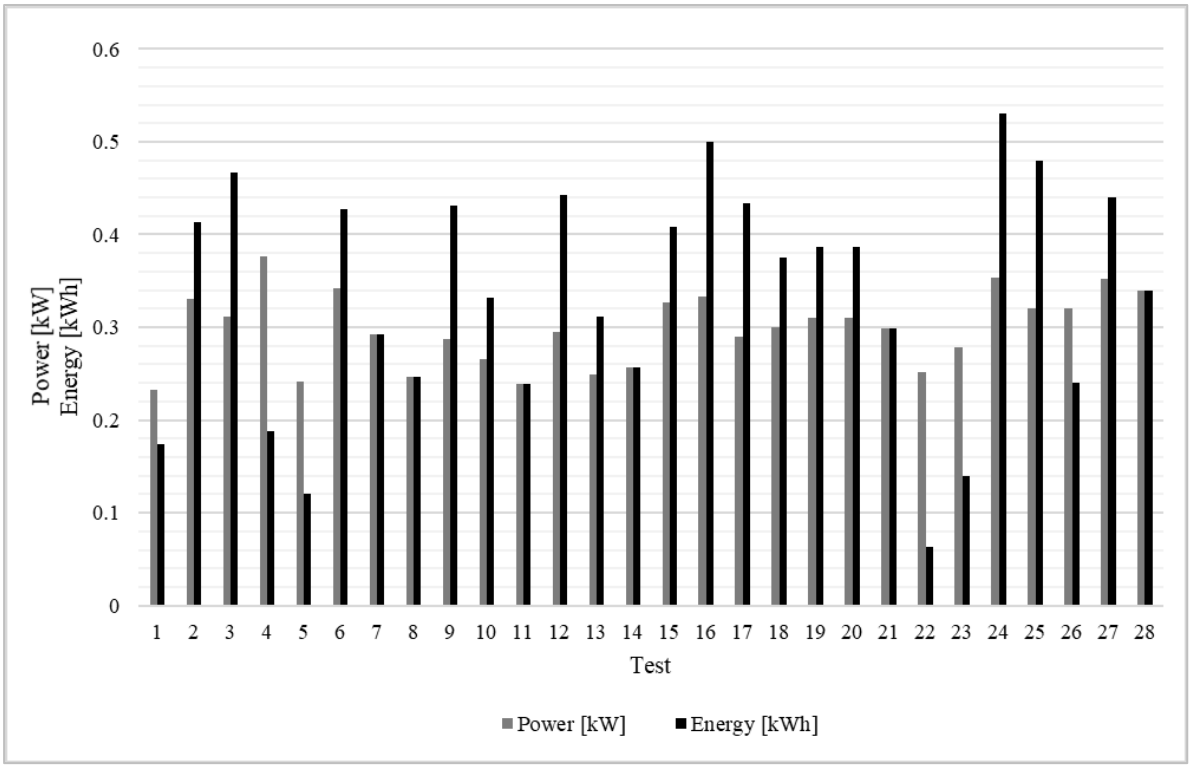

517

518 **(b)**

519 **Figure 8**. Power and energy consumed by the reaction equipment after 90 minutes (a); after
520 achieving reaction equilibrium (increase in ester concentration of less than 2 percentage points

after 15 minutes) (b).

Table 5 reports the energy intensity values for all tests. The EI values of the transesterification reaction are acceptable for a laboratory scale and are also consistent with the 37.13 MJ/kg value estimated by several industrial processes to obtain biodiesel (Marchetti et al., 2007).

3.6 Green metrics evaluation

Green metrics and green chemistry balance are summarised in Table 5 for each test.

The values of RME and PMI (and PMP, in turn) are closely related to the E factor. At the same time, atom efficiency and atom economy depend on the molecular weights of reagents, products, and yield. Energy intensity depends on the mass of biodiesel obtained and the energy absorbed.

The closer the E factor is to 0, the more virtuous the process will be, with fewer undesired products. Although it has an average value of 0.36, the parameter varies from a minimum of 0.21 in Test 23 to a maximum of 0.57 in Test 15, with a value of 0.27 in Test 4, where optimal process conditions were demonstrated. It can be observed that the optimal condition from the point of view of the yield does not correspond to the optimal condition from the point of view of the E factor and, in general, of the eco-sustainability.

The atom economy is 0.92 for all tests because the molecular weights of products and reagents are always the same when using the same reaction.

The atom efficiency considers the actual reaction yield. Therefore, the minimum atom efficiency is calculated in the test where the minimum yield of esters was observed (Test 15). At the same time, its maximum value corresponds to Test 4, which shows the optimal conditions of the reaction and the maximum yield of crude biodiesel and esters.

The PMI value varies between a minimum of 1.21 in test 23 and a maximum of 1.57 in test 15, while the PMP value (which is the reciprocal of PMI·100 and the percentage form of RME) follows a reverse trend, with a minimum of 63.58% in test 15 and a maximum of 82.63% in test

545 23.

546 The stoichiometric factor is 1 with the stoichiometric M/O ratio and higher than 1 with excess
547 alcohol, as expected.

548 The highest green chemistry balance value, 83.11%, in test 23 corresponds to the minimum
549 energy intensity value, so test 23 has the most favourable conditions for green chemistry and
550 energy consumption. However, a non-optimal ester yield was achieved in test 23. The lowest
551 green chemistry balance, 61.21%, was achieved in test 15, where the minimum ester yield of
552 42% and high EI of 14.36 MJ/kg were also reached.

553 **Table 5**. Yield values, energy intensity, some green metrics (E factor, atom efficiency AEff,
554 process mass intensity PMI, reaction mass efficiency RME, stoichiometric factor FSt), and green
555 chemistry balance.

Test	$Y_{crude\ biodiesel}$ (%)	Y_{esters} (%)	*EI (MJ/kg)*	E factor (/)	AEff (/)	PMI (/)	RME (/)	FSt (/)	*Green chemistry balance (%)*
1	89.83	*85.57*	*9.76*	0.24	0.79	1.24	0.80	1.08	*81.73*
2	90.53	*87.04*	*13.89*	0.26	0.80	1.26	0.80	1.08	*81.56*
3	83.01	*78.18*	*13.50*	0.29	0.72	1.29	0.77	1.08	*78.09*
4	**91.98** ↑	***89.43*** ↑	*13.13*	0.27	0.82	1.27	0.79	1.16	*79.86*
5	85.99	*78.00*	*13.34*	0.30	0.72	1.30	0.77	1.08	*77.82*
6	85.98	*71.37*	***14.47*** ↑	0.36	0.66	1.36	0.74	1.08	*73.96*
7	90.10	*72.22*	*11.48*	0.35	0.66	1.35	0.74	1.08	*74.56*
8	83.73	*68.99*	*12.35*	0.42	0.63	1.42	0.71	1.08	*71.14*
9	89.97	*86.61*	*11.50*	0.25	0.80	1.25	0.80	1.08	*81.64*
10	83.13	*67.69*	*12.20*	0.31	0.62	1.31	0.76	1	*76.72*
11	90.89	*82.95*	*10.80*	0.33	0.76	1.33	0.75	1.16	*76.26*
12	89.41	*74.84*	*11.86*	0.41	0.69	1.41	0.71	1.16	*71.22*
13	**75.01** ↓	*50.43*	*12.02*	0.52	0.46	1.52	0.66	1	*64.97*
14	91.53	*75.42*	*10.88*	0.38	0.69	1.38	0.72	1.16	*72.32*
15	81.79	***42.01*** ↓	*14.36*	0.57	0.39	1.57	0.64	1	***61.21*** ↓
16	90.30	*66.79*	*13.27*	0.42	0.61	1.42	0.70	1.16	*68.97*
17	89.26	*85.47*	*11.59*	0.22	0.78	1.22	0.82	1.08	*82.67*
18	84.53	*45.08*	*13.22*	0.54	0.41	1.54	0.65	1	*62.90*
19	87.37	*78.18*	*10.81*	0.33	0.72	1.33	0.75	1.16	*75.04*
20	80.22	*73.81*	*11.84*	0.25	0.68	1.25	0.80	1	*80.85*
21	79.88	*61.29*	11.72	0.39	0.56	1.39	0.72	1	*72.26*
22	82.13	*48.06*	12.72	0.52	0.44	1.52	0.66	1	64.61
23	88.73	*85.25*	**9.65** ↓	0.21	0.78	1.21	0.83	1.08	**83.11** ↑
24	87.14	*67.99*	12.17	0.37	0.62	1.37	0.73	1.16	71.16
25	90.80	*73.26*	10.66	0.39	0.67	1.39	0.72	1.16	71.78
26	78.66	*53.94*	12.56	0.45	0.50	1.45	0.69	1	68.27
27	87.55	*72.73*	12.15	0.42	0.67	1.42	0.71	1.16	70.50
28	79.84	*70.42*	12.87	0.39	0.65	1.39	0.72	1	74.45

Fig. 9 below reports a global representation of the main green metrics calculated in this work and reported in percentage scale (E', Aeff, PMP, FSt'), energy intensity (EI, MJ/kg), and crude biodiesel yield (Y, %) for tests 4 and 15.

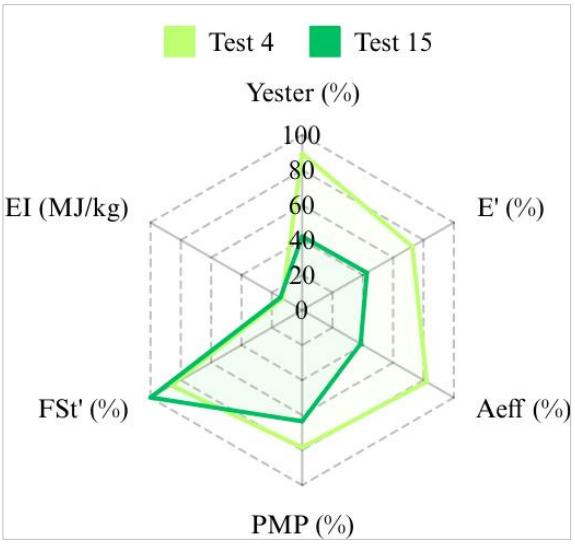

Figure 9. Radar chart of green metrics, energy intensity, and yield in tests 4 and 15.

3.7 Statistical analysis

Experimental results were analysed using the response surface model, a quadratic polynomial equation, and the Minitab 18 software tool for CCD data treatment. Analysis of variance (ANOVA) and regression were performed to evaluate the fitting model, the primary factors and interactions, and the significance of each studied response.

Effect on ester yield. The Minitab 18 software tool performed the one-way ANOVA to evaluate the influence of independent variables (M/O, %KOH, T, S) on ester yield as a response.

The analysis of the CCD design in uncoded units generated the following quadratic model averaged over blocks:

$$Y_{esters} = -2.62 - 0.117\,X_1 + 0.30\,X_2 + 0.341\,X_3 - 0.0265\,X_4 - 0.00207\,{X_1}^2 - 0.134\,{X_2}^2$$
$$- 0.00306\,{X_3}^2 + 0.000027\,{X_4}^2 - 0.037\,X_1\,X_2 + 0.00001\,X_1\,X_3$$
$$+ 0.000472\,X_1\,X_4 - 0.0144\,X_2\,X_3 + 0.00238\,X_2\,X_4 - 0.00002\,X_3\,X_4$$

where X_1 is M/O, X_2 is %KOH, X_3 is T and X_4 is S.

The F-test and p-value evaluated the significance of the model and its factors in the ANOVA (Table 6).

Table 6. Analysis of Variance for a yield of esters as a response.

Source	DF	Adj SS	Adj MS	F-Value	p-Value
Model	15	0.285589	0.019039	1.20	0.380
Blocks	1	0.016163	0.016163	1.02	0.333
Linear	4	0.054350	0.013588	0.86	0.517
M/O	1	0.000134	0.000134	0.01	0.928
%KOH	1	0.011807	0.011807	0.74	0.405
T (°C)	1	0.014953	0.014953	0.94	0.351
S	1	0.027456	0.027456	1.73	0.213
Square	4	0.028918	0.007229	0.46	0.767
M/O*M/O	1	0.000849	0.000849	0.05	0.821
%KOH*%KOH	1	0.002735	0.002735	0.17	0.685
T (°C)*T (°C)	1	0.014302	0.014302	0.90	0.361
S*S	1	0.011420	0.011420	0.72	0.413
2-Way Interaction	6	0.192144	0.032024	2.02	0.142
M/O*%KOH	1	0.034003	0.034003	2.14	0.169
M/O*T (°C)	1	0.000000	0.000000	0.00	0.998
M/O*S	1	0.080231	0.080231	5.05	0.044
%KOH*T (°C)	1	0.020765	0.020765	1.31	0.275
%KOH*S	1	0.056763	0.056763	3.58	0.083
T (°C)*S	1	0.000382	0.000382	0.02	0.879
Error	12	0.190459	0.015872		
Lack-of-Fit	10	0.179050	0.017905	3.14	0.266
Pure Error	2	0.011409	0.005704		
Total	27	0.476048			

DF: total degrees of freedom; Adj SS: adjusted sum of squares; Adj MS: adjusted mean squares; F-Value: Fisher test statistic; p-Value: probability value.

The F-value for certain variables and their combinations is lower than that for the Lack of Fit. Consequently, a partial lack of fit is associated with the quadratic model, suggesting that a more complex model should be adopted to adequately describe the experimental behaviour of the objective function in relation to specific quadratic combinations of variables. Indeed, at the 95% confidence level, the p-value of the quadratic model was higher than 0.05, indicating that it is not adequate to describe the process. With a p-value lower than 0.05, only the combination of M/O and stirring had a significant effect at the operating conditions tested, as confirmed by the Pareto graph (Fig. 10). Equilibrium conditions were probably reached after 90 minutes, and the impact of different initial operating conditions was not significant.

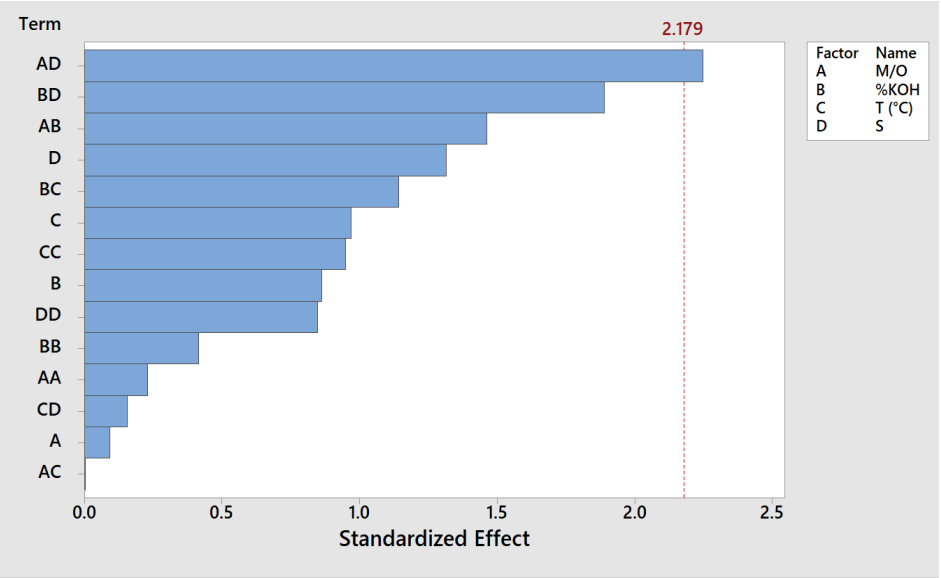

588

589 **Figure 10**. Pareto Chart of the standardised effects of single factors and their combinations on
590 esters yield (significance value: 0.05).

591 Fig. 11 shows a set of graphs confirming the validity of the experimental tests. Since the points

592 fluctuate around zero, there is no relation.

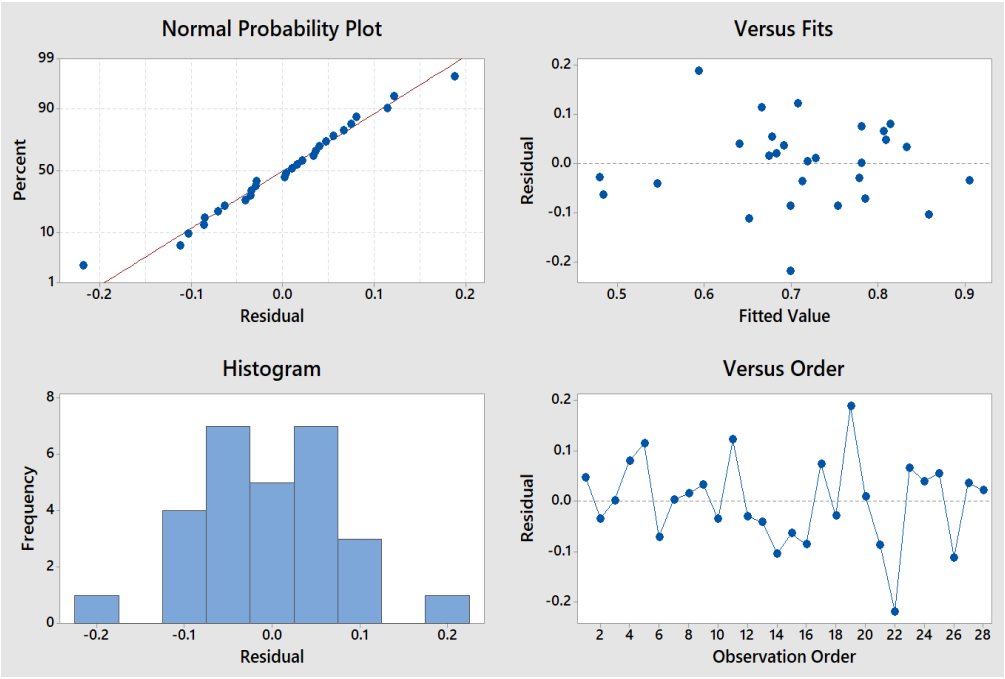

593

594 **Figure 11**. Residual plots for the statistical analysis with a yield of esters as a response.

595 The surface plots (Fig. 12a-f) show the influence of independent variables on the yield of esters

596 Y_{esters}. Combining M/O and stirring (Fig. 12c) allows obtaining higher yield values than other

combinations. In particular, a yield higher than 90% was attained with the combination of M/O=9 and S=450 rpm. Fig. 13a-f shows the contour diagrams of the different factors, confirming that the combination of the highest stirring and methanol/oil ratio gave the highest yield (dark green, Fig. 13c).

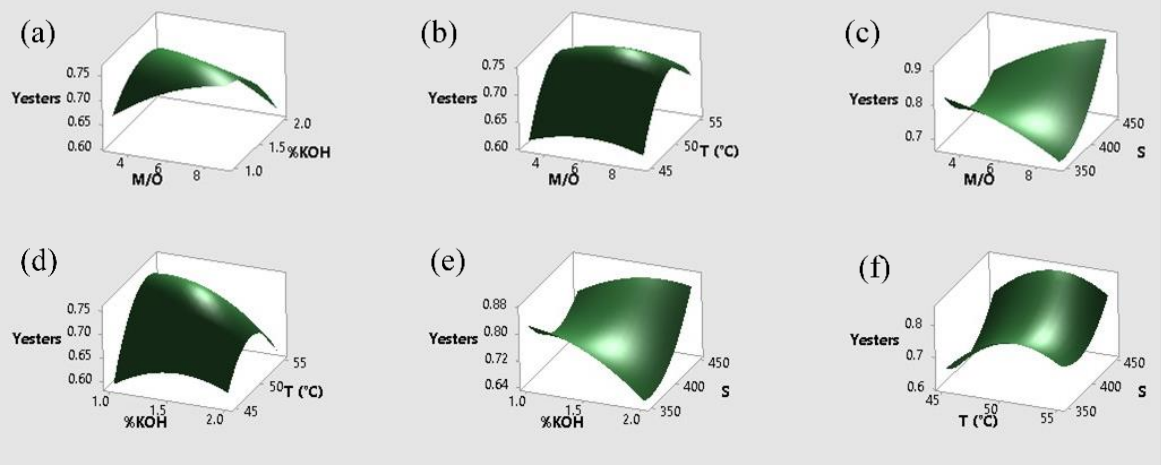

Figure 12. Surface plots of esters yields from alkaline transesterification of WCO at different combinations of operating conditions by RSM (hold values: M/O: 6; %KOH: 1.5; T: 50 °C; S: 400 rpm).

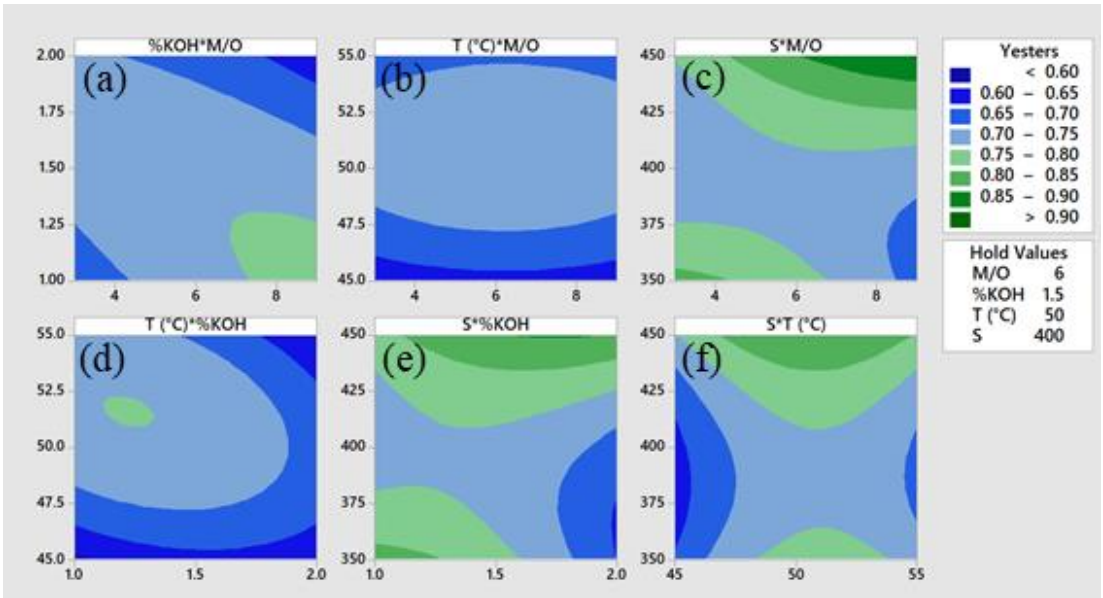

Figure 13. Contour plots of response surfaces for a yield of esters as a response.

Effect on energy intensity. The one-way ANOVA was performed to evaluate the influence of independent variables on energy intensity (EI) as a response.

The analysis of the CCD design in uncoded units generated the following quadratic model averaged over blocks:

$$EI = -61.1 + 2.50\,X_1 + 9.6\,X_2 - 0.17\,X_3 + 0.315\,X_4 + 0.0122\,{X_1}^2 + 2.02\,{X_2}^2 + 0.0012\,{X_3}^2 - 0.000364\,{X_4}^2 - 0.225\,X_1\,X_2 - 0.0142\,X_1\,X_3 - 0.00357\,X_1\,X_4 - 0.095\,X_2\,X_3 - 0.0252\,X_2\,X_4 + 0.00069\,X_3\,X_4$$

where X_1 is M/O, X_2 is %KOH, X_3 is T and X_4 is S.

The F-test and p-value evaluated the significance of the model and its factors in the ANOVA (Table 7).

Table 7. Analysis of Variance for energy intensity as response.

Source	DF	Adj SS	Adj MS	F-Value	p-Value
Model	15	26.0914	1.73943	1.32	0.318
Blocks	1	1.9411	1.94110	1.47	0.248
Linear	4	5.7165	1.42912	1.08	0.407
M/O	1	4.5401	4.54009	3.44	0.088
%KOH	1	1.1603	1.16027	0.88	0.367
T (°C)	1	0.0022	0.00222	0.00	0.968
S	1	0.0139	0.01389	0.01	0.920
Square	4	2.2881	0.57202	0.43	0.782
M/O*M/O	1	0.0298	0.02976	0.02	0.883
%KOH*%KOH	1	0.6252	0.62521	0.47	0.504
T (°C)*T (°C)	1	0.0022	0.00224	0.00	0.968
S*S	1	2.0272	2.02719	1.54	0.239
2-Way Interaction	6	14.8614	2.47691	1.88	0.166
M/O*%KOH	1	1.8293	1.82926	1.39	0.262
M/O*T (°C)	1	0.7268	0.72676	0.55	0.472
M/O*S	1	4.5903	4.59031	3.48	0.087
%KOH*T (°C)	1	0.8978	0.89776	0.68	0.425
%KOH*S	1	6.3378	6.33781	4.81	0.049
T (°C)*S	1	0.4796	0.47956	0.36	0.558
Error	12	15.8239	1.31866		
Lack-of-Fit	10	13.4998	1.34998	1.16	0.548
Pure Error	2	2.3241	1.16203		
Total	27	41.9153			

DF: total degrees of freedom; Adj SS: adjusted sum of squares; Adj MS: adjusted mean squares; F-Value: Fisher test statistic; p-Value: probability value.

The F-value for certain variables and their combinations is lower than that for the Lack of Fit. Consequently, a partial lack of fit is associated with the quadratic model, suggesting that a more complex model should be adopted to adequately describe the experimental behaviour of the objective function in relation to specific quadratic combinations of variables. Indeed, with a p-value higher than 0.05, the quadratic model did not adequately describe the process. Moreover,

only the combination of catalyst amount and stirring significantly affected the energy intensity at the operating conditions tested, as confirmed by the Pareto graph (Fig. 14). The energy consumption strongly depends on the duration of the reaction. After the same time of 90 minutes, the initial operating conditions did not significantly influence the energy intensity value. However, residual plots in Fig. 15 confirmed the validity of experimental tests.

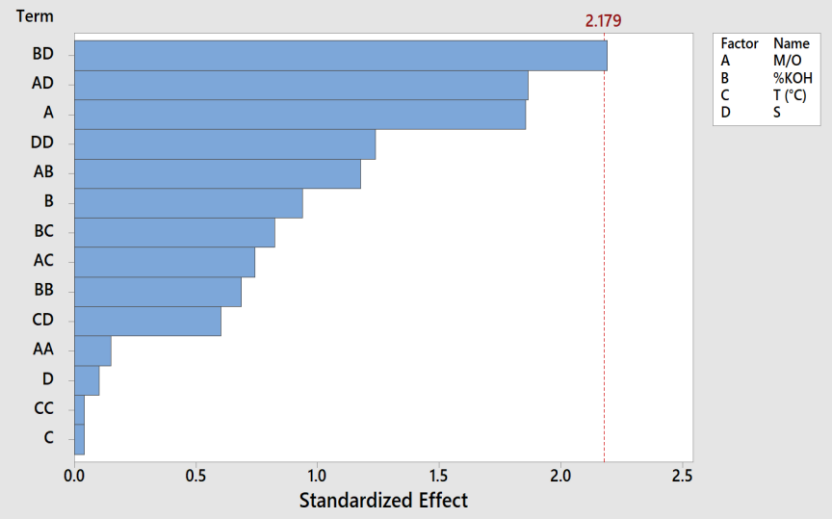

Figure 14. Pareto Chart of the standardised effects of single factors and their combinations on energy intensity (significance value: 0.05).

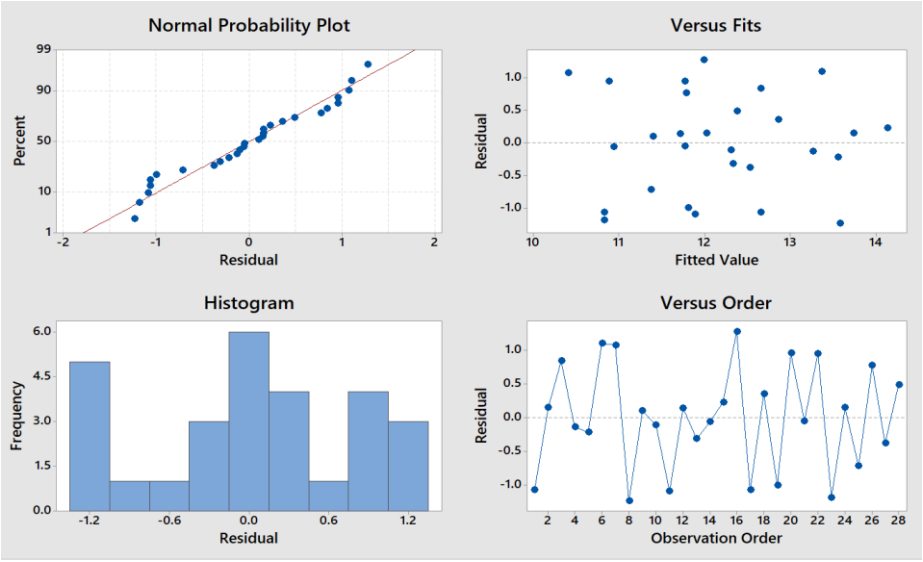

Figure 15. Residual plots for the statistical analysis with energy intensity as a response.

The influence of independent variables on EI is graphically evident in the surface plots (Fig. 16a-f) and contour plots (Fig. 17a-f). Low stirring and methanol-to-oil ratio are the best conditions

for minimising energy intensity (dark blue, Fig. 17c).

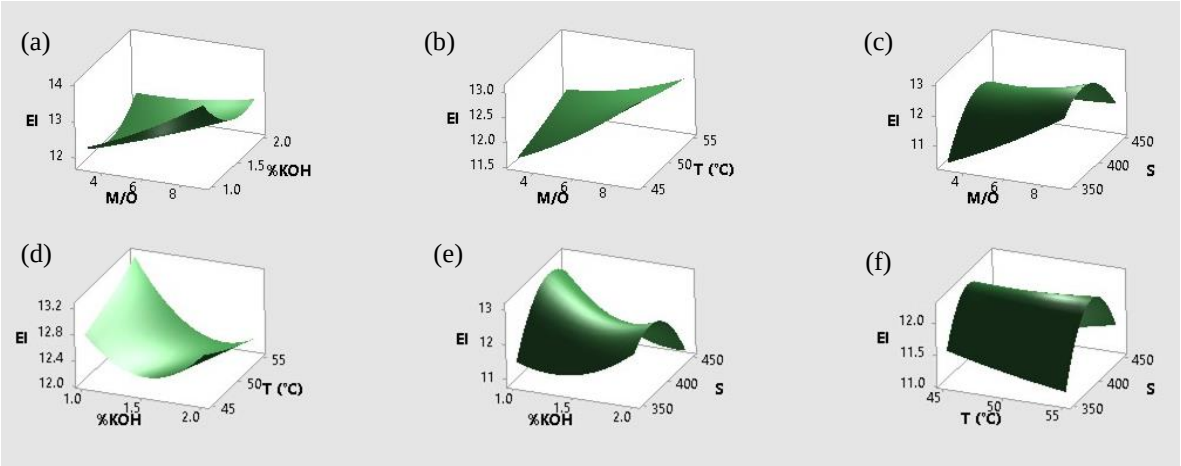

Figure 16. Surface plots of energy intensity after 90 minutes of alkaline transesterification of WCO at different combinations of operating conditions by RSM (hold values: M/O: 6; %KOH: 1.5; T: 50 °C; S: 400 rpm).

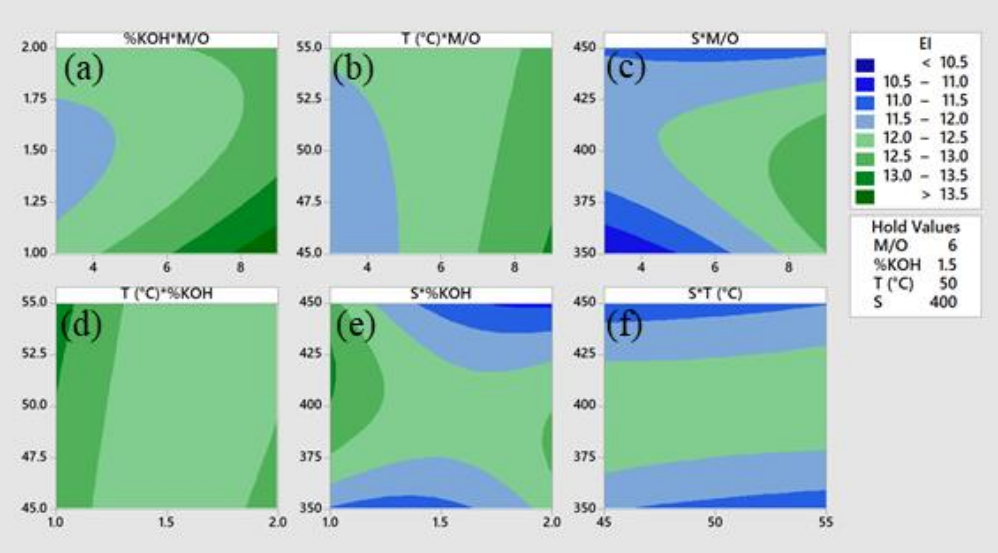

Figure 17. Contour plots of response surfaces for energy intensity as a response.

Effect on green chemistry balance. Finally, the one-way ANOVA was performed to evaluate the influence of independent variables on green chemistry balance (GCB) as a response.

The analysis of the CCD design in uncoded units generated the following quadratic model averaged over blocks:

$$GCB = 1.03 - 0.0713\,X_1 + 0.711\,X_2 + 0.161\,X_3 - 0.0236\,X_4 - 0.00287\,{X_1}^2 - 0.195\,{X_2}^2 - 0.00162\,{X_3}^2 + 0.000025\,{X_4}^2 - 0.00939\,X_1 X_2 + 0.000425\,X_1 X_3 + 0.000253\,X_1 X_4 - 0.00697\,X_2 X_3 + 0.000651\,X_2 X_4 + 0.000026\,X_3 X_4$$

where X_1 is M/O, X_2 is %KOH, X_3 is T and X_4 is S.

The F-test and p-value evaluated the significance of the model and its factors in the ANOVA (Table 8).

Table 8. Analysis of Variance for green chemistry balance as a response.

Source	DF	Adj SS	Adj MS	F-Value	p-Value
Model	15	0.067416	0.004494	1.55	0.224
Blocks	1	0.005379	0.005379	1.86	0.198
Linear	4	0.009071	0.002268	0.78	0.557
M/O	1	0.001063	0.001063	0.37	0.556
%KOH	1	0.001230	0.001230	0.42	0.527
T (°C)	1	0.002054	0.002054	0.71	0.416
S	1	0.004724	0.004724	1.63	0.226
Square	4	0.020944	0.005236	1.81	0.192
M/O*M/O	1	0.001629	0.001629	0.56	0.468
%KOH*%KOH	1	0.005794	0.005794	2.00	0.183
T (°C)*T (°C)	1	0.003995	0.003995	1.38	0.263
S*S	1	0.009679	0.009679	3.34	0.092
2-Way Interaction	6	0.036612	0.006102	2.11	0.128
M/O*%KOH	1	0.003175	0.003175	1.10	0.316
M/O*T (°C)	1	0.000650	0.000650	0.22	0.644
M/O*S	1	0.022998	0.022998	7.94	0.016
%KOH*T (°C)	1	0.004851	0.004851	1.68	0.220
%KOH*S	1	0.004238	0.004238	1.46	0.250
T (°C)*S	1	0.000700	0.000700	0.24	0.632
Error	12	0.034740	0.002895		
Lack-of-Fit	10	0.030765	0.003077	1.55	0.455
Pure Error	2	0.003975	0.001987		
Total	27	0.102157			

DF: total degrees of freedom; Adj SS: adjusted sum of squares; Adj MS: adjusted mean squares; F-Value: Fisher test statistic; p-Value: probability value.

The F-value for certain variables and their combinations is lower than that for the Lack of Fit. Consequently, a partial lack of fit is associated with the quadratic model, suggesting that a more complex model should be adopted to adequately describe the experimental behaviour of the objective function in relation to specific quadratic combinations of variables. Indeed, with a p-value higher than 0.05, the quadratic model did not adequately describe the process. Moreover, only the combination of M/O and stirring significantly affected the green chemistry balance, as confirmed by the Pareto graph (Fig. 18). Residual plots (Fig. 19) confirmed the validity of the

experimental tests.

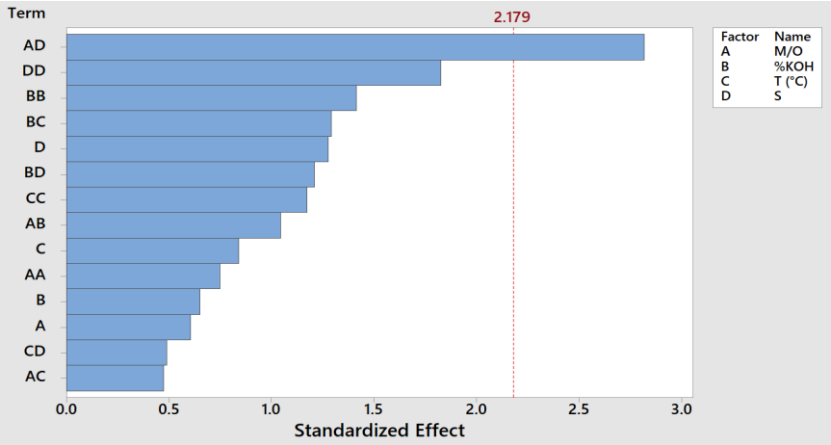

Figure 18. Pareto Chart of the standardised effects of single factors and their combinations on green chemistry balance (significance value: 0.05).

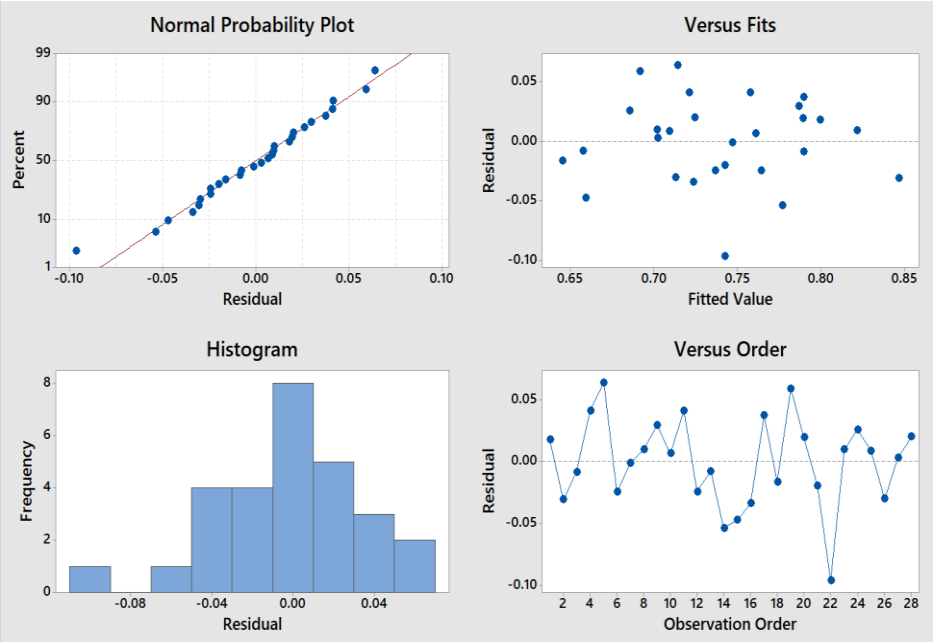

Figure 19. Residual plots for the statistical analysis with green chemistry balance as a response.

The influence of independent variables on GCB is graphically evident in the surface plots (Fig. 20a-f) and contour plots (Fig. 21a-f), showing that the best conditions are high stirring and M/O (dark green, Fig. 21c).

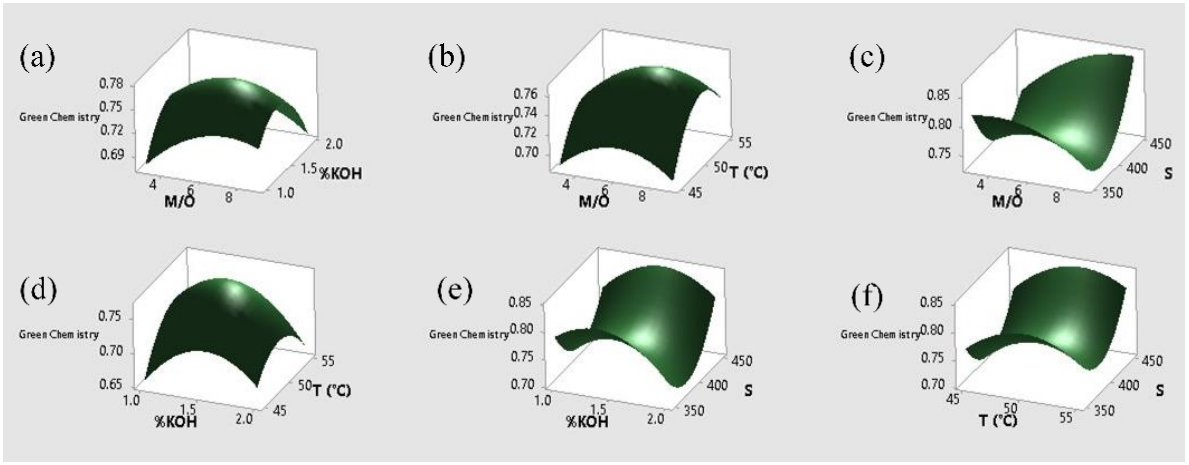

674

675 **Figure 20**. Surface plots of green chemistry balance of alkaline transesterification of WCO at
676 different combinations of operating conditions by RSM (hold values: M/O: 6; %KOH: 1.5; T:
677 50 °C; S: 400 rpm).

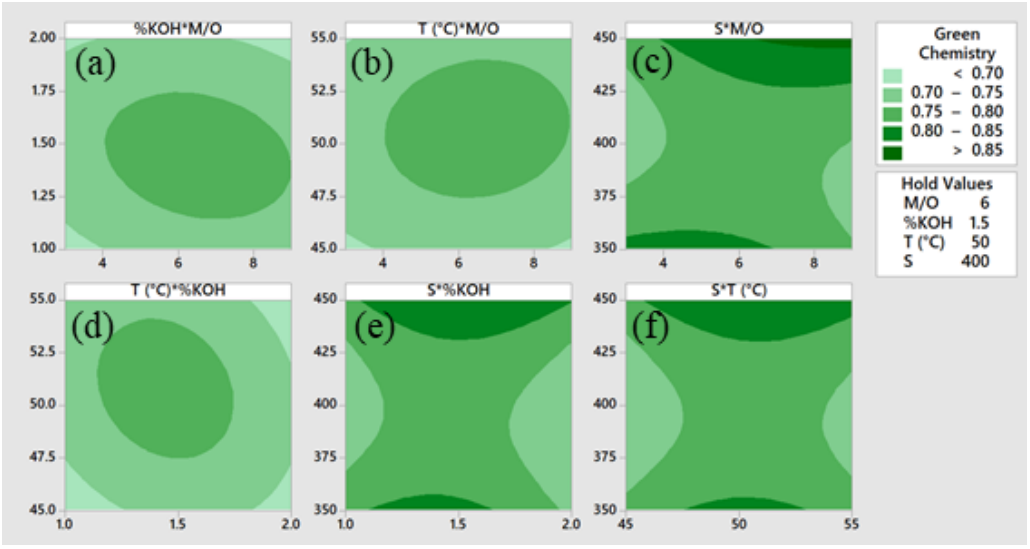

678

679 **Figure 21**. Contour plots of response surfaces for green chemistry balance as a response.

680 **Multi-objective optimisation of operating conditions**. A multi-objective optimisation is
681 necessary to consider the transesterification's yield, energy consumption, and green chemistry
682 balance. The yield and green chemistry balance should be maximised, whereas the energy
683 intensity should be minimised. Therefore, the results of multi-objective optimisation (Fig. 23)
684 differ from single-response optimisation (Fig. 22). Indeed, the optimal conditions vary
685 significantly when each response is used as a single performance criterion. As an example, M/O
686 and S should be maximum to optimise the yield and green chemistry balance (Fig. 22a,c) but

minimum to optimise the energy intensity (Fig. 22b). Or else, %KOH and T should have similar intermediate values to optimise, but minimum to optimise the energy intensity. Multi-objective optimisation overcomes the drawback of single-objective optimisation by simultaneously optimising all three responses in this process. The optimal conditions are M/O of 3, 1.3 wt% of KOH, temperature of 50.7 °C, and stirring of 350 rpm. These results differ from the few previous works in the literature about the multi-objective optimisation of WCO transesterification, but this may be due to the different conditions tested. Indeed, Outili et al. (Outili et al., 2020) tested the methanol-to-oil ratio, catalyst concentration, and temperature in the ranges 4-8, 0.5-2 wt%, and 45-60 °C for 30 minutes of reaction, whereas in this work, stirring was also considered, and the reaction lasted 90 minutes; moreover, they considered other green metrics to calculate the green chemistry balance and measured theoretical energy consumption instead of experimental energy intensity.

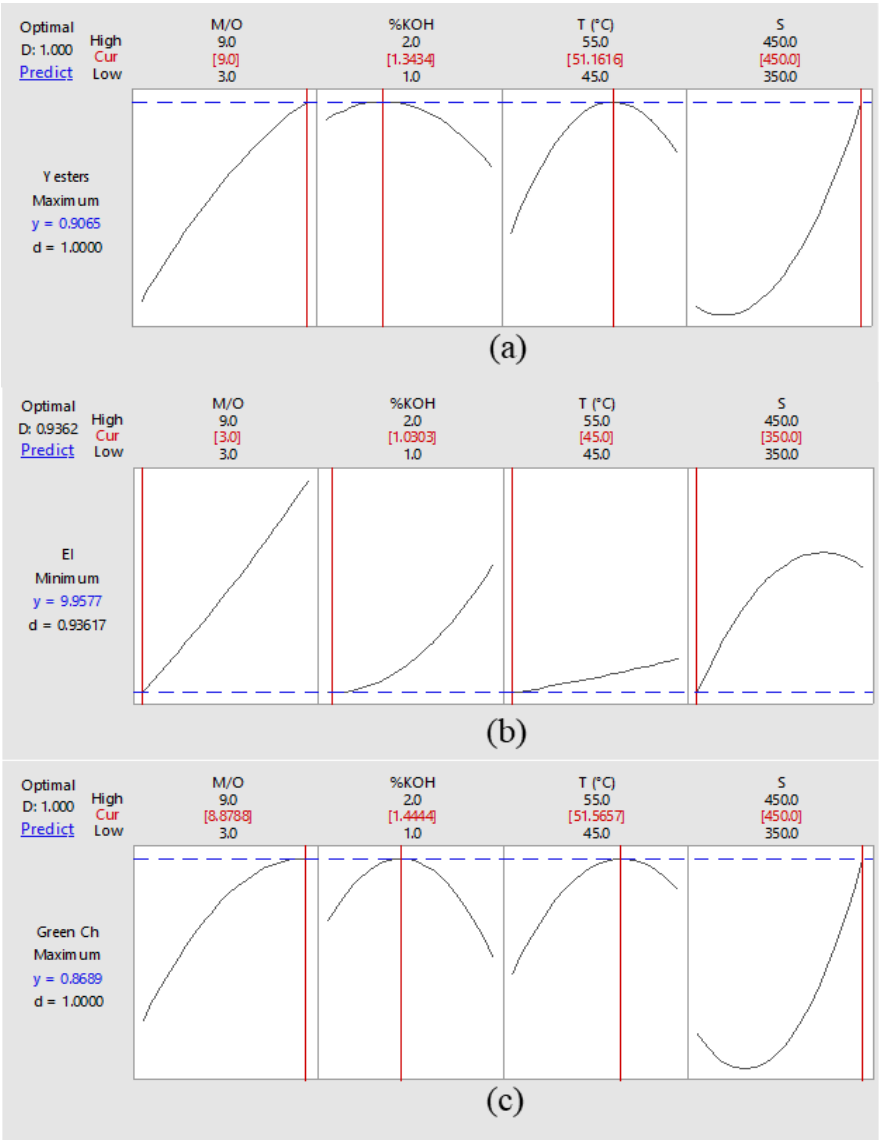

699

700 **Figure 22**. Single-objective optimisation for each response: (a) yield of esters, (b) energy
701 intensity, (c) green chemistry balance.

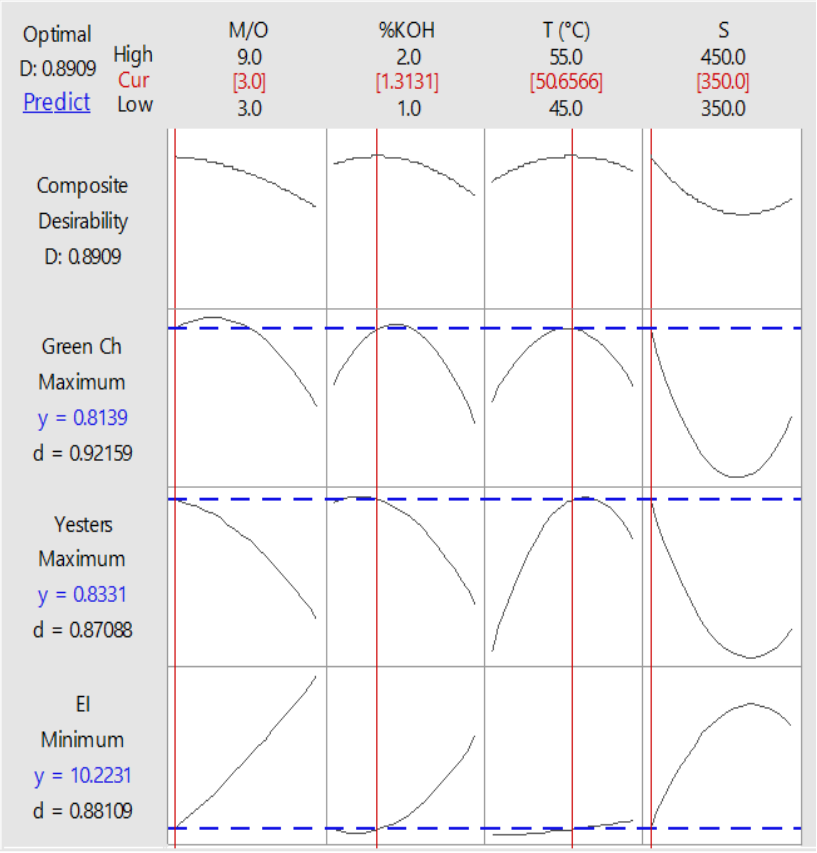

Figure 23. Multi-objective optimisation results of WCO transesterification to biodiesel.

4. Future challenges and perspectives

Although biodiesel production from WCO has been extensively studied, the reported results in the literature vary significantly due to the heterogeneity of raw materials. A global appoach provides insights into developing efficient and cost-effective biodiesel production methods. Using waste cooking oil significantly reduces the process cost and addresses the problem concerning its disposal. Therefore, focusing on the barrier of feedstock supply and management, innovation in process, reactor configuration, and development of cost-effective catalysts, would be required. The biodiesel production by homogeneous alkaline catalysis is simple and effective. However, very high-quality feedstock is needed, requiring pre-treatments which make the biodiesel production expensive and non-competitive. The integrated two-step homogeneous acid-base processes can handle low-quality feedstocks but with more catalyst and processing

steps. Replacement of homogeneous catalysts with heterogeneous catalysts could enhance the efficiency and sustainability of biodiesel synthesis while reducing costs and environmental impacts. However, more research is required to increase their activity, stability, and reusability in mild operating conditions, fast reaction rates, and reasonable costs for industrial applications. Finally, considering glycerol as a co-product of transesterification with high value lowers the biodiesel costs significantly and the glycerol purification should be optimised.

5. Conclusions

Recent attention has focused on energy consumption and the principles of green chemistry in biodiesel production. This study optimised the operating conditions for converting household WCO into biodiesel using RSM applied to a CCD-based experimental plan to analyse the energy consumption and sustainability through a green chemistry approach, optimising the reaction within a single reactor under diverse conditions. Crude biodiesel was characterised using refractometry and multiple light scattering after product separation. Compared to more labour-intensive chromatographic techniques, these methods are simple and rapid and provide reliable conversion and separation data. The reaction was optimised for yield, energy use, and environmental impact through RSM, by evaluating the effects of methanol-to-oil ratio (M/O), percentage of potassium hydroxide (%KOH), temperature (T), and stirring speed (S) as independent variables. The peak yield of esters was measured at 89.43%, attained at a temperature of 55 °C, a stirring speed of 350 rpm, with a M/O of 9 and a catalyst concentration of 1%. Gas chromatography analysis indicated that the total fraction of oil eligible for esterification was 96.7%. Consequently, the actual yield of esters, in relation to the oil that can be effectively converted, was recorded at 92.5%. The optimal conditions for achieving the highest yields of crude biodiesel and esters were characterised by significant energy intensity. The energy intensity values associated with the transesterification reaction are deemed acceptable within a laboratory setting and align with the estimated value of 37.13 MJ/kg reported

by numerous industrial processes for biodiesel production. The optimum condition regarding yield does not align with the optimum condition concerning the E factor and, more broadly, with eco-sustainability. The maximum value for the balance of green chemistry, quantified at 83.11%, corresponds to the minimum energy intensity value, resulting in a suboptimal ester yield. Conversely, the lowest balance of green chemistry, quantified at 61.21%, was observed when the minimum ester yield reached 42% alongside a high energy intensity (EI) of 14.36 MJ/kg. Then, the optimal conditions fluctuated when evaluating individual performance criteria. Nonetheless, a multi-objective approach was demonstrated to be critical for overall optimisation by concurrently optimising all three responses within this process. Results showed that the multi-objective optimisation varied from single-response optimisation when each response was treated as an independent performance criterion. In particular, the optimal conditions were M/O of 3, a KOH concentration of 1.3 wt%, a temperature of 50.7 °C, and a stirring speed of 350 rpm.

In conclusion, while reaction time, type of alcohol, alcohol-to-oil molar ratio, reaction temperature, quantity of catalyst, and mixing intensity were typically optimised by RSM to achieve maximum biodiesel yield from Waste Cooking Oil, it is essential to note that the highest yield does not inherently ensure an environmentally sustainable process. The application of green chemistry principles is essential for guaranteeing sustainability in such processes. Therefore, addressing a more comprehensive optimisation approach involving green chemistry principles is necessary and contributes significantly to a broader vision of the process.

List of abbreviations

a_o: intercept term in the statistical model

a_i: linear coefficients in the statistical model

a_{ii}: quadratic coefficients in the statistical model

a_{ij}: interactive coefficients in the statistical model

A: acidity

765 Adj MS: Adjusted Mean Squares

766 Adj SS: Adjusted Sum of Squares

767 AE: Atom Economy

768 AEff: Atom Efficiency

769 ANOVA: Analysis Of Variance

770 ASTM: American Society for Testing and Materials

771 BBD: Box-Behnken Design

772 C: Concentration

773 CCD: Central Composite Design

774 CFPP: Cold Filter Plugging Point

775 DF: total Degrees of Freedom

776 E factor: Environmental factor

777 E': normalised environmental factor

778 EI: Energy Intensity

779 FFA: Free Fatty Acid

780 FAME: Fatty Acid Methyl Esters

781 FSt: Stoichiometric Factor

782 FSt': normalised stoichiometric factor

783 F-Value: Fisher test statistic

784 HPLC: High-Performance Liquid Chromatography

785 GC: Gas Chromatography

786 M/O: Methanol-to-Oil molar ratio

787 MW: Molecular Weight

788 OA: Oleic Acid

789 PMI: Process Mass Intensity

PMP: Process Mass Productivity

p-Value: probability value

R: response in the statistical model

RME: Reaction Mass Efficiency

RSM: Response Surface Methodology

S: Stirring

T: Temperature

V: Volume

WCO: Waste Cooking Oil

x: mass fraction

X_1: methanol-to-oil ratio in the statistical model

X_2: catalyst concentration in the statistical model

X_3: temperature in the statistical model

X_4: stirring in the statistical model

Y: Yield

References

Abbah, E.C., Nwandikom, G.I., Egwuonwu, C.C., Nwakuba, N.R., 2016. Effect of Reaction Temperature on the Yield of Biodiesel From Neem Seed Oil, American Journal of Energy Science.

Abbaszaadeh, A., Ghobadian, B., Omidkhah, M.R., Najafi, G., 2012. Current biodiesel production technologies: A comparative review, in: Energy Conversion and Management. pp. 138–148. https://doi.org/10.1016/j.enconman.2012.02.027

Adekoya, O.A., Giwa, A., Yusuff, A.S., Giwa C, A., 2015. D-Optimal-Experimental-Design-of-Biodiesel-Production-from-Waste-Cooking-Oil-of-ABUAD-Cafeterias.docx. Int J Sci Eng Res 6.

Ahmad, G., Imran, S., Farooq, M., Shah, A.N., Anwar, Z., Rehman, A.U., Imran, M., 2023. Biodiesel Production from Waste Cooking Oil Using Extracted Catalyst from Plantain Banana Stem via RSM and ANN Optimization for Sustainable Development. Sustainability (Switzerland) 15. https://doi.org/10.3390/su151813599

Ali Ijaz Malik, M., Zeeshan, S., Khubaib, M., Ikram, A., Hussain, F., Yassin, H., Qazi, A., 2024. A review of major trends, opportunities, and technical challenges in biodiesel production from waste sources. Energy Conversion and Management: X. https://doi.org/10.1016/j.ecmx.2024.100675

All statistics for Create Response Surface Design (Central Composite) [WWW Document],

2023. . Minitab . URL https://support.minitab.com/en-us/minitab/21/help-and-how-to/statistical-modeling/doe/how-to/response-surface/create-response-surface-design/create-central-composite-design/examine-the-design/all-statistics/ (accessed 1.18.24).
Anastas, P.T., Warner, J.C., 1998. Green Chemistry: Theory and Practice. Oxford University Press, New York.
Atapour, M., Kariminia, H.R., Moslehabadi, P.M., 2014. Optimization of biodiesel production by alkali-catalyzed transesterification of used frying oil. Process Safety and Environmental Protection 92, 179–185. https://doi.org/10.1016/j.psep.2012.12.005
Ayoola, A.A., Hymore, K.F., Omonhinmin, C.A., 2016. Optimization of biodiesel production from selected waste oils using response surface methodology. Biotechnology. https://doi.org/10.3923/biotech.2016
Babadi, A.A., Rahmati, S., Fakhlaei, R., Barati, B., Wang, S., Doherty, W., Ostrikov, K., 2022. Emerging technologies for biodiesel production: Processes, challenges, and opportunities. Biomass Bioenergy. https://doi.org/10.1016/j.biombioe.2022.106521
Bai, H., Tian, J., Talifu, D., Okitsu, K., Abulizi, A., 2022. Process optimization of esterification for deacidification in waste cooking oil: RSM approach and for biodiesel production assisted with ultrasonic and solvent. Fuel 318. https://doi.org/10.1016/j.fuel.2022.123697
Bajwa, W., Ikram, A., Malik, M.A.I., Razzaq, L., Khan, A.R., Latif, A., Hussain, F., Qazi, A., 2024. Optimization of biodiesel yield from waste cooking oil and sesame oil using RSM and ANN techniques. Heliyon 10. https://doi.org/10.1016/j.heliyon.2024.e34804
Bashir, M.A., Wu, S., Zhu, J., Krosuri, A., Khan, M.U., Ndeddy Aka, R.J., 2022. Recent development of advanced processing technologies for biodiesel production: A critical review. Fuel Processing Technology 227. https://doi.org/10.1016/j.fuproc.2021.107120
Bhonsle, A.K., Yusuff, A.S., Trivedi, J., Singh, J., Singh, R.K., Atray, N., 2022. Transesterification of used cooking oil at ambient temperature using novel solvent: experimental investigations and optimisation by response surface methodology. International Journal of Ambient Energy 43, 4801–4811. https://doi.org/10.1080/01430750.2021.1919925
Blekas, G., Tsimidou, M., Boskou, D., 2006. Olive Oil Composition, in: Olive Oil. AOCS Publishing, pp. 41–72. https://doi.org/10.1201/9781439832028.pt2
Bobadilla, M.C., Lorza, R.L., Escribano-Garcia, R., Gómez, F.S., González, E.P.V., 2017. An improvement in biodiesel production from waste cooking oil by applying thought multi-response surface methodology using desirability functions. Energies (Basel) 10. https://doi.org/10.3390/en10010130
Bohlouli, A., Mahdavian, L., 2021. Catalysts used in biodiesel production: a review. Biofuels 12, 885–898. https://doi.org/10.1080/17597269.2018.1558836
Calvo-Flores, F.G., 2009. Sustainable chemistry metrics. ChemSusChem 2, 905–919. https://doi.org/10.1002/cssc.200900128
Darnoko, D., Cheryan, M., 2000. Kinetics of palm oil transesterification in a batch reactor. JAOCS 77, 1263–1267.
De Paola, Maria Gabriela, Arcuri, N., Calabrò, V., De Simone, M., 2017. Thermal and stability investigation of phase change material dispersions for thermal energy storage by T-history and optical methods. Energies (Basel) 10, 354. https://doi.org/10.3390/en10030354
De Paola, M. G., Calabrò, V., De Simone, M., 2017. Light scattering methods to test inorganic PCMs for application in buildings. IOP Conf Ser Mater Sci Eng 251. https://doi.org/10.1088/1757-899X/251/1/012122
De Paola, M.G., De Simone, M., Arcuri, N., Calabrò, V., 2016. Crossed analysis by T-history and Turbiscan for the characterization of PCM with Glauber salt, in: INNOSTORAGE Conference. Ben-Gurion University of the Negev.
De Paola, M.G., Lopresto, C.G., 2021. Waste oils and their transesterification products as novel bio-based phase change materials. Journal of Phase Change Materials 1. https://doi.org/https://doi.org/10.6084/jpcm.v1i1.6
De Paola, M.G., Mazza, I., Paletta, R., Lopresto, C.G., Calabrò, V., 2021a. Small-Scale Biodiesel Production Plants — An Overview. Energies (Basel) 14, 1901.
De Paola, M.G., Paletta, R., Lopresto, C.G., Calabrò, V., Paola, D., 2021b. Multiple light

879 scattering as a preliminary tool for starch-based film formulation. Journal of Phase Change
880 Material 1. https://doi.org/10.6084/jpcm.v1i2.15
881 De, R., Bhartiya, S., Shastri, Y., 2019. Multi-objective optimization of integrated biodiesel
882 production and separation system. Fuel 243, 519–532.
883 https://doi.org/10.1016/j.fuel.2019.01.132
884 Dicks, A.P., Hent, A., 2015. Green Chemistry Metrics - A Guide to Determining and Evaluating
885 Process Greenness. Springer, London.
886 Dorado, M.P., Ballesteros, E., López, F.J., Mittelbach, M., 2004. Optimization of alkali-
887 catalyzed transesterification of Brassica Carinata oil for biodiesel production. Energy and
888 Fuels 18, 77–83. https://doi.org/10.1021/ef0340110
889 Dubey, A., Prasad, R.S., Singh, J.K., 2020. An Analytical and Economical Assessment of the
890 Waste Cooking Oil based Biodiesel using Optimized Conditions on the Process Variables.
891 Energy Sources, Part A: Recovery, Utilization and Environmental Effects.
892 https://doi.org/10.1080/15567036.2020.1839600
893 Dwivedi, G., Jain, S., Shukla, A.K., Verma, P., Verma, T.N., Saini, G., 2022. Impact analysis of
894 biodiesel production parameters for different catalyst. Environ Dev Sustain.
895 https://doi.org/10.1007/s10668-021-02073-w
896 El-Gendy, N.S., El-Gharabawy, A.A.S.A., Amr, S.S., Ashour, F.H., 2015. Response surface
897 optimization of an alkaline transesterification of waste cooking oil. Int. J. ChemTech Res 8,
898 385–398.
899 Encinar, J.M., González, J.F., Rodríguez-Reinares, A., 2005. Biodiesel from Used Frying Oil.
900 Variables Affecting the Yields and Characteristics of the Biodiesel. Ind. Eng. Chem. Res.
901 44, 5491–5499.
902 Farouk, S.M., Tayeb, A.M., Abdel-Hamid, S.M.S., Osman, R.M., 2024. Recent advances in
903 transesterification for sustainable biodiesel production, challenges, and prospects: a
904 comprehensive review. Environmental Science and Pollution Research.
905 https://doi.org/10.1007/s11356-024-32027-4
906 Felizardo, P., Neiva Correia, M.J., Raposo, I., Mendes, J.F., Berkemeier, R., Bordado, J.M.,
907 2006. Production of biodiesel from waste frying oils. Waste Management 26, 487–494.
908 https://doi.org/10.1016/j.wasman.2005.02.025
909 Foon Cheng, S., Hock Chuah, C., 2004. Kinetics study on transesterification of palm oil.
910 García-Moreno, P.J., Khanum, M., Guadix, A., Guadix, E.M., 2014. Optimization of biodiesel
911 production from waste fish oil. Renew Energy 68, 618–624.
912 https://doi.org/10.1016/j.renene.2014.03.014
913 Gumahin, A.C., Galamiton, J.M., Allerite, M.J., Valmorida, R.S., Laranang, J.R.L., Mabayo,
914 V.I.F., Arazo, R.O., Ido, A.L., 2019. Response surface optimization of biodiesel yield from
915 pre-treated waste oil of rendered pork from a food processing industry. Bioresour
916 Bioprocess 6. https://doi.org/10.1186/s40643-019-0284-2
917 Gupta, V., Pal Singh, K., 2023. The impact of heterogeneous catalyst on biodiesel production; a
918 review, in: Materials Today: Proceedings. Elsevier Ltd, pp. 364–371.
919 https://doi.org/10.1016/j.matpr.2022.10.175
920 Halwe, A.D., Deshmukh, S.J., Kanu, N.J., Gupta, E., Tale, R.B., 2021. Optimization of the novel
921 hydrodynamic cavitation based waste cooking oil biodiesel production process parameters
922 using integrated L9Taguchi and RSM approach, in: Materials Today: Proceedings. Elsevier
923 Ltd, pp. 5934–5941. https://doi.org/10.1016/j.matpr.2021.04.484
924 Hamze, H., Akia, M., Yazdani, F., 2015. Optimization of biodiesel production from the waste
925 cooking oil using response surface methodology. Process Safety and Environmental
926 Protection 94, 1–10. https://doi.org/10.1016/j.psep.2014.12.005
927 Hoque, M.E., Singh, A., Chuan, Y.L., 2011. Biodiesel from low cost feedstocks: The effects of
928 process parameters on the biodiesel yield. Biomass Bioenergy 35, 1582–1587.
929 https://doi.org/10.1016/j.biombioe.2010.12.024
930 Issariyakul, T., Dalai, A.K., 2012. Comparative kinetics of transesterification for biodiesel
931 production from palm oil and mustard oil. Canadian Journal of Chemical Engineering 90,
932 342–350. https://doi.org/10.1002/cjce.20679
933 Jeyakumar, N., Narayanasamy, B., Balasubramaniam, V., 2019. Optimization of used cooking

oil methyl ester production using response surface methodology. Energy Sources, Part A: Recovery, Utilization and Environmental Effects 41, 2313–2325. https://doi.org/10.1080/15567036.2018.1555633
Karmee, S.K., Chadha, A., 2005. Preparation of biodiesel from crude oil of Pongamia pinnata. Bioresour Technol 96, 1425–1429. https://doi.org/10.1016/j.biortech.2004.12.011
Kerras, H., Merouani, R., Nekkab, C., Outili, N., Meniai, AH., 2018. Optimization of the frying oil waste transesterification reaction time to biodiesel. Algerian Journal of Engineering Research AJER 4, 65–70.
Kiran, K., Hebbar, G.S., 2021. Optimization of Biodiesel Production from Waste Cooking Oil by Box Behnken Design Using Response Surface Methodology. INTERNATIONAL JOURNAL of RENEWABLE ENERGY RESEARCH 11.
Knothe, G., Razon, L.F., 2017. Biodiesel fuels. Prog Energy Combust Sci 58, 36–59. https://doi.org/10.1016/j.pecs.2016.08.001
Kolakoti, A., Setiyo, M., Waluyo, B., 2021. Biodiesel Production from Waste Cooking Oil: Characterization, Modeling and Optimization. Mechanical Engineering for Society and Industry 1, 22–30. https://doi.org/10.31603/mesi.5320
Lapkin, A., Constable, D.J.C., 2009. Green Chemistry Metrics: Measuring and Monitoring Sustainable Processes, Green Chemistry Metrics: Measuring and Monitoring Sustainable Processes. John Wiley & Sons, Ltd. https://doi.org/10.1002/9781444305432
Leung, D.Y.C., Guo, Y., 2006. Transesterification of neat and used frying oil: Optimization for biodiesel production. Fuel Processing Technology 87, 883–890. https://doi.org/10.1016/j.fuproc.2006.06.003
Lopresto, C.G., 2024. Sustainable biodiesel production from waste cooking oils for energetically independent small communities: an overview. International Journal of Environmental Science and Technology. https://doi.org/10.1007/s13762-024-05779-2
Lopresto, C.G., De Paola, M.G., Albo, L., Policicchio, M.F., Chakraborty, S., Calabro, V., 2019. Comparative analysis of immobilized biocatalyst: study of process variables in trans-esterification reaction. 3 Biotech 9. https://doi.org/10.1007/s13205-019-1985-0
Lopresto, C.G., De Paola, M.G., Calabrò, V., 2024. Importance of the properties, collection, and storage of waste cooking oils to produce high-quality biodiesel – An overview. Biomass Bioenergy. https://doi.org/10.1016/j.biombioe.2024.107363
Lopresto, C.G., Gentile, M., Caravella, A., Candamano, S., Calabrò, V., 2025. De-acidification of waste cooking oils by adsorption on industrial waste: Kinetic analysis of a green pretreatment for biodiesel production. Chemosphere 380. https://doi.org/10.1016/j.chemosphere.2025.144460
Lopresto, C.G., Naccarato, S., Albo, L., De Paola, M.G., Chakraborty, S., Curcio, S., Calabrò, V., 2015. Enzymatic transesterification of waste vegetable oil to produce biodiesel. Ecotoxicol Environ Saf 121, 229–235. https://doi.org/10.1016/j.ecoenv.2015.03.028
Mandari, V., Devarai, S.K., 2022. Biodiesel Production Using Homogeneous, Heterogeneous, and Enzyme Catalysts via Transesterification and Esterification Reactions: a Critical Review. Bioenergy Res. https://doi.org/10.1007/s12155-021-10333-w
Marchetti, J.M., Miguel, V.U., Errazu, a. F., 2007. Possible methods for biodiesel production. Renewable and Sustainable Energy Reviews 11, 1300–1311. https://doi.org/10.1016/j.rser.2005.08.006
Mathiyazhagan, M., Ganapathi, a, 2011. Factors Affecting Biodiesel Production. Res Plant Biol 1, 1–5.
Meher, L.C., Kulkarni, M.G., Dalai, A.K., Naik, S.N., 2006. Transesterification of karanja (Pongamia pinnata) oil by solid basic catalysts, in: European Journal of Lipid Science and Technology. pp. 389–397. https://doi.org/10.1002/ejlt.200500307
Milano, J., Ong, H.C., Masjuki, H.H., Silitonga, A.S., Chen, W.H., Kusumo, F., Dharma, S., Sebayang, A.H., 2018a. Optimization of biodiesel production by microwave irradiation-assisted transesterification for waste cooking oil-Calophyllum inophyllum oil via response surface methodology. Energy Convers Manag 158, 400–415. https://doi.org/10.1016/j.enconman.2017.12.027
Milano, J., Ong, H.C., Masjuki, H.H., Silitonga, A.S., Kusumo, F., Dharma, S., Sebayang, A.H.,

Cheah, M.Y., Wang, C.T., 2018b. Physicochemical property enhancement of biodiesel synthesis from hybrid feedstocks of waste cooking vegetable oil and Beauty leaf oil through optimized alkaline-catalysed transesterification. Waste Management 80, 435–449. https://doi.org/10.1016/j.wasman.2018.09.005

Mukhtar, A., Saqib, S., Lin, H., Hassan Shah, M.U., Ullah, S., Younas, M., Rezakazemi, M., Ibrahim, M., Mahmood, A., Asif, S., Bokhari, A., 2022. Current status and challenges in the heterogeneous catalysis for biodiesel production. Renewable and Sustainable Energy Reviews. https://doi.org/10.1016/j.rser.2021.112012

Mulvihill, M.J., Beach, E.S., Zimmerman, J.B., Anastas, P.T., 2011. Green chemistry and green engineering: A framework for sustainable technology development. Annu Rev Environ Resour 36, 271–293. https://doi.org/10.1146/annurev-environ-032009-095500

Myers, R.H., Montgomery, D.C., Anderson-Cook, C.M., 2016. Response surface methodology: process and product optimization using designed experiments. John Wiley & Sons.

Najafi, B., Faizollahzadeh Ardabili, S., Shamshirband, S., Chau, K.W., Rabczuk, T., 2018. Application of ANNS, ANFIS and RSM to estimating and optimizing the parameters that affect the yield and cost of biodiesel production. Engineering Applications of Computational Fluid Mechanics 12, 611–624. https://doi.org/10.1080/19942060.2018.1502688

Naveenkumar, R., Baskar, G., 2021. Process optimization, green chemistry balance and technoeconomic analysis of biodiesel production from castor oil using heterogeneous nanocatalyst. Bioresour Technol 320, 124347. https://doi.org/10.1016/j.biortech.2020.124347

Okechukwu, O.D., Joseph, E., Nonso, U.C., Kenechi, N.-O., 2022. Improving heterogeneous catalysis for biodiesel production process. Cleaner Chemical Engineering 3, 100038. https://doi.org/10.1016/j.clce.2022.100038

Oliveira, D. DE, Luccio, M. DI, Faccio, C., Dalla Rosa, C., Paulo Bender, A.O., Lipke, N., Amroginski, C., Dariva, C., Vladimir Oliveira, J. DE, 2005. Optimization of Alkaline Transesterification of Soybean Oil and Castor Oil for Biodiesel Production.

Outili, N., Kerras, H., Nekkab, C., Merouani, R., Meniai, A.H., 2020. Biodiesel production optimization from waste cooking oil using green chemistry metrics. Renew Energy 145, 2575–2586. https://doi.org/10.1016/j.renene.2019.07.152

Oza, S., Kodgire, P., Kachhwaha, S.S., 2021a. Analysis of RSM Method for Optimization of Ultrasound-Assisted KOH Catalyzed Biodiesel Production from Waste Cotton-Seed Cooking Oil, in: Applied Mathematical Modeling and Analysis in Renewable Energy. CRC Press, pp. 133–148. https://doi.org/10.1201/9781003159124-9

Oza, S., Prajapati, N., Kodgire, P., Kachhwaha, S.S., 2021b. An ultrasound-assisted process for the optimization of biodiesel production from waste cottonseed cooking oil using response surface methodology. Water-Energy Nexus 4, 187–198. https://doi.org/10.1016/j.wen.2021.11.001

Özbay, N., Oktar, N., Tapan, N.A., 2008. Esterification of free fatty acids in waste cooking oils (WCO): Role of ion-exchange resins. Fuel 87, 1789–1798. https://doi.org/10.1016/j.fuel.2007.12.010

Özgür, C., 2021. Optimization of biodiesel yield and diesel engine performance from waste cooking oil by response surface method (RSM). Pet Sci Technol 39, 683–703. https://doi.org/10.1080/10916466.2021.1954019

Pathak, S., 2015. Acid catalyzed transesterification. J Chem Pharm Res 7, 1780–1786.

Patle, D.S., Sharma, S., Ahmad, Z., Rangaiah, G.P., 2014. Multi-objective optimization of two alkali catalyzed processes for biodiesel from waste cooking oil. Energy Convers Manag 85, 361–372. https://doi.org/10.1016/j.enconman.2014.05.034

Pisarello, M.L., Maquirriain, M., Sacripanti Olalla, P., Rossi, V., Querini, C.A., 2018. Biodiesel production by transesterification in two steps: Kinetic effect or shift in the equilibrium conversion? Fuel Processing Technology 181, 244–251. https://doi.org/10.1016/j.fuproc.2018.09.028

Razzaq, L., Imran, S., Anwar, Z., Farooq, M., Abbas, M.M., Khan, H.M., Asif, T., Amjad, M., Soudagar, M.E.M., Shaukat, N., Fattah, I.M.R., Rahman, S.M.A., 2020. Maximising yield

and engine efficiency using Optimised waste cooking oil biodiesel. Energies (Basel) 13. https://doi.org/10.3390/en13225941
Ruhul, A.M., Kalam, M.A., Masjuki, H.H., Fattah, I.M.R., Reham, S.S., Rashed, M.M., 2015. State of the art of biodiesel production processes: A review of the heterogeneous catalyst. RSC Adv. https://doi.org/10.1039/c5ra09862a
Selvaraj, R., Moorthy, I.G., Kumar, R.V., Sivasubramanian, V., 2019. Microwave mediated production of FAME from waste cooking oil: Modelling and optimization of process parameters by RSM and ANN approach. Fuel 237, 40–49. https://doi.org/10.1016/j.fuel.2018.09.147
Sharma, A., Kodgire, P., Kachhwaha, S.S., 2019. Biodiesel production from waste cotton-seed cooking oil using microwave-assisted transesterification: Optimization and kinetic modeling. Renewable and Sustainable Energy Reviews 116. https://doi.org/10.1016/j.rser.2019.109394
Sheldon, R.A., 2018. Metrics of Green Chemistry and Sustainability: Past, Present, and Future. ACS Sustain Chem Eng 6, 32–48. https://doi.org/10.1021/acssuschemeng.7b03505
Singh, D., Sharma, D., Soni, S.L., Sharma, S., Kumar Sharma, P., Jhalani, A., 2020. A review on feedstocks, production processes, and yield for different generations of biodiesel. Fuel 262, 116553. https://doi.org/10.1016/j.fuel.2019.116553
Stoytcheva, M., Montero, G., 2011. Biodiesel - Feedstocks and Processing Technologies. InTech, Janeza Trdine, Croatia.
Suhara, A., Karyadi, Herawan, S.G., Tirta, A., Idris, M., Roslan, M.F., Putra, N.R., Hananto, A.L., Veza, I., 2024. Biodiesel Sustainability: Review of Progress and Challenges of Biodiesel as Sustainable Biofuel. Clean Technologies 6, 886–906. https://doi.org/10.3390/cleantechnol6030045
Sun, S., Guo, J., Chen, X., 2021. Biodiesel preparation from Semen Abutili (Abutilon theophrasti Medic.) seed oil using low-cost liquid lipase Eversa® transform 2.0 as a catalyst. Ind Crops Prod 169. https://doi.org/10.1016/j.indcrop.2021.113643
Sun, S., Li, K., 2020. Biodiesel production from phoenix tree seed oil catalyzed by liquid lipozyme TL100L. Renew Energy 151, 152–160. https://doi.org/10.1016/j.renene.2019.11.006
Tacias-Pascacio, V.G., Torrestiana-Sánchez, B., Dal Magro, L., Virgen-Ortíz, J.J., Suárez-Ruíz, F.J., Rodrigues, R.C., Fernandez-Lafuente, R., 2019. Comparison of acid, basic and enzymatic catalysis on the production of biodiesel after RSM optimization. Renew Energy 135, 1–9. https://doi.org/10.1016/j.renene.2018.11.107
Tan, Y.H., Abdullah, M.O., Nolasco Hipolito, C., 2016. Comparison of Biodiesel Production between Homogeneous and Heterogeneous Base Catalysts. Applied Mechanics and Materials 833, 71–77. https://doi.org/10.4028/www.scientific.net/amm.833.71
Thirugnanasambandham, K., Shine, K., Aziz, H.A., Gimenes, M.L., 2017. Biodiesel synthesis from waste oil using novel microwave technique: Response surface modeling and optimization. Energy Sources, Part A: Recovery, Utilization and Environmental Effects 39, 636–642. https://doi.org/10.1080/15567036.2016.1196270
Tubino, M., Junior, J.G.R., Bauerfeldt, G.F., 2014. Biodiesel synthesis with alkaline catalysts: A new refractometric monitoring and kinetic study. Fuel 125, 164–172. https://doi.org/10.1016/j.fuel.2014.01.096
Ugheoke, B.I., Onoja Patrick, D., Kefas, H.M., Onche, E.O., 2007. Determination of Optimal Catalyst Concentration for Maximum Biodiesel Yield from Tigernut (Cyperus Esculentus) Oil.
Verma, P., Sharma, M.P., 2016. Review of process parameters for biodiesel production from different feedstocks. Renewable and Sustainable Energy Reviews. https://doi.org/10.1016/j.rser.2016.04.054
Vicente, G., Martínez, M., Aracil, J., 2004. Integrated biodiesel production: A comparison of different homogeneous catalysts systems. Bioresour Technol 92, 297–305. https://doi.org/10.1016/j.biortech.2003.08.014
Yatish, K. V., Lalithamba, H.S., Suresh, R., Arun, S.B., Kumar, P.V., 2016. Optimization of scum oil biodiesel production by using response surface methodology. Process Safety and

Environmental Protection 102, 667–672. https://doi.org/10.1016/j.psep.2016.05.026
Yıldızhan, Ş., Uludamar, E., Çalık, A., Dede, G., Özcanlı, M., 2017. Fuel properties, performance and emission characterization of waste cooking oil (WCO) in a variable compression ratio (VCR) diesel engine. European Mechanical Science 1, 56–62.
Zabala, S., Arzamendi, G., Reyero, I., Gandía, L.M., 2014. Monitoring of the methanolysis reaction for biodiesel production by off-line and on-line refractive index and speed of sound measurements. Fuel 121, 157–164. https://doi.org/10.1016/j.fuel.2013.12.056
Zhang, Y., Li, Y., Sun, S., 2024a. Unveiling the innovation: Optimized biodiesel production from emerging Acer truncatum Bunge seed oil using novel and highly effective alkaline ionic liquid catalyst. Chemical Engineering Journal 487. https://doi.org/10.1016/j.cej.2024.150603
Zhang, Y., Li, Z., Li, Y., Sun, S., 2024b. Biodiesel preparation from tiger nut oil utilizing a novel hydroxy-functionalized basic ionic liquid catalytic transesterification procedure: optimization, kinetics, and thermodynamic studies. Energy Convers Manag 303. https://doi.org/10.1016/j.enconman.2024.118182
Zhang, Y., Sun, S., 2023. A review on biodiesel production using basic ionic liquids as catalysts. Ind Crops Prod. https://doi.org/10.1016/j.indcrop.2023.117099
Zulqarnain, Ayoub, M., Yusoff, M.H.M., Nazir, M.H., Zahid, I., Ameen, M., Sher, F., Floresyona, D., Budi Nursanto, E., 2021. A comprehensive review on oil extraction and biodiesel production technologies. Sustainability (Switzerland) 13, 1–28. https://doi.org/10.3390/su13020788